This is to certify that the
thesis entitled

ANALYSIS AND SYNTHESIS OF BROADBAND TRAVELING WAVE ANTENNAS

presented by

Lanwu Zhao

has been accepted towards fulfillment
of the requirements for the

M.S. degree in Electrical and Computer Engineering

Edward J Rothwell
Major Professor's Signature

7-19-04
Date

ANALYSIS AND SYNTHESIS OF BROADBAND TRAVELING WAVE ANTENNAS

By

Lanwu Zhao

A THESIS

Submitted to
Michigan State University
In partial fulfillment of the requirements
For the degree of

MASTER OF SCIENCE

Electrical and Computer Engineering

2004

ABSTRACT

ANALYSIS AND SYNTHESIS OF BROADBAND TRAVELING WAVE ANTENNAS

By

Lanwu Zhao

GA (Genetic Algorithms) is proving to be useful for solving complex electromagnetic (EM) problems. This thesis presents one important application to wideband antenna design, a set of traveling-wave spline wire antennas. These antennas are designed to operate in the frequency band from 200 MHz to 2 GHz. These antennas are optimized based on the VSWR, the radiation efficiency and the power gain over the frequency band of interest.

Topics covered include the basic concepts of GA and its application to the spline antenna design. A brief history of the wideband antenna design is also covered. A set of spline antennas are analyzed and synthesized. The EM properties are studied and discussed. A time domain impulse response, $h_{N,TX}(t)$ is introduced to described the antenna's capability for impulse radiation. Comparisons are made between the loaded dipole, the rhombic antenna and the spline antenna for a GMC (Gaussian Modulated Cosine) input. Finally, conclusions drawn from this research are discussed.

ACKNOWLEDGMENTS

I am sincerely grateful to my academic advisor Dr. Edward Rothwell who has provided too much guidance, counsel and encouragement throughout the course of this research. This thesis couldn't be done without him. Thanks to him for being my major advisor and teacher.

I would like to thank Dr. Leo Kempel and Dr. Edward Rothwell for giving me the chance to be their research assistant; thanks to the National Science Foundation Division of Undergraduate Education Award DUE-0231312 for providing the financial support that makes the completion of thesis possible.

Many thanks to Dr John Ross, without whose technical support and guidance the completion of this thesis would be impossible. Thanks to him for letting me access to his powerful GA-NEC program to finish this research.

Thanks to Dr. Balasubraniam for serving as committee members in the defense of this thesis and giving me a deep understanding of computational electromagnetics during my study in Michigan State University.

I would also like to thank all my friends and colleagues at the EM group here at Michigan State University. They have been a constant source of friendship and support thought my many years of study and research.

Most of all, I would like to thank my wife Susan Wang and my daughter Jessie. They are the constant source of my happiness.

TABLE OF CONTENTS

LIST OF TABLES

LIST OF FIGURES

Chapter 1

INTRODUCTION

The imminent widespread commercial development of Ultra-wideband systems has sparked renewed interest in the subject of Ultra-wideband antennas [1]. Since the radiated power of the antenna over the whole particular frequency band must meet the requirements regulated by the FCC, a UWB antenna with specific properties plays a critical role in the overall UWB system. This thesis introduces a set of broadband traveling wave antennas that are suitable for the band from 200 MHz to 2 GHz. The properties of the antennas including the radiation pattern, the gain, the efficiency, the VSWR and the GMC (Gaussian modulated cosine) pulse response are investigated in this study.

Antenna performance is often the main factor which determines the overall performance of a UWB system. Many types of antennas with wideband properties had been designed and used for various UWB radio systems. In 1898, Oliver Lodge disclosed spherical dipoles, square dipoles, biconical dipoles, and bow-tie dipoles in his patent [2]. During World War Two and subsequent years additional antennas that had much wider bandwidth were introduced such as Carter's biconical antenna and conical monopole [3-4], Schelkunoff's spherical dipole [5], Lindenbald's coaxial horn spherical dipoles [6], and Brillonin's omni-directional and directional coaxial horn [7]. Later on, more manufacturable wideband antennas were pioneered, such as Stohr's ellipsoidal monopole and ellipsoidal dipole [8], R.H. DuHamel and D.E. Isbell' log periodic arrays [9], Marie's wideband slot antenna [10], Lalezari *et al's* broadband notch antenna [11], Thomas *et al's* circular element dipole [12], Harmuth's large current radiator/magnetic

antenna [13] and Barne's UWB slot antenna [14-16]. These antennas are some highlights of UWB antennas in the past century.

For some purposes, the directional and broadband properties of traveling wave antennas are desirable. The first work on traveling wave dipoles was reported by Altschuler [17] who inserted a lumped resistor at quarter wavelength from the ends of the antenna to form traveling wave propagation along the dipole antenna. Soon after there came many reports on traveling wave antennas. The most famous one was reported by T.T. Wu and R.W.P king in 1964, who studied the cylindrical antenna with variable internal impedance per unit length to form a pure outward traveling wave along the antenna at a certain frequency [18]. They derived the distributed impedance loading theoretically to form a nonreflecting traveling wave along the antenna. Based on this, they also derived the efficiency and the far zone electric field of their antenna. The efficiency of their antenna was only 50 percent due to impedance distributed along the antenna. Moreover, since the nonreflecting property only worked at the center frequency, a very wide bandwidth was not expected. For directional transmission purposes, high directivity is desired for a traveling wave antenna.

The goal of the research presented here was to develop traveling wave antennas that have higher directivity, better efficiency and wider bandwidth properties than those reported in the literature. In this study, a set of spline traveling wave wire antennas were investigated, such as the ones with close or open end, ones with symmetric and asymmetric geometry, ones that the wire radius were constant or varying, and ones with or without resistive loading at the end. With the help of GAs (Genetic Algorithms) in conjunction with NEC (Numerical Electromagnetic Code), a set of spline antennas were analyzed and synthesized using the GA-NEC program developed by John Ross [19]. The application of GA-NEC and the associated

external programs and the external Visual Basic program that called by GA-NEC are described in Chapter 2.

The GAs optimized traveling wave antennas with different geometry shapes, such as ones with geometrical symmetry and asymmetry, ones with constant wire radius and varying wire radius, and ones with open ends or with lumped resistive loading at the ends. The main features of these antennas, the far field radiation pattern, the VSWR, the input impedance and the efficiency are simulated in a free space environment over the frequency band from 200 MHz to 2GHz. The transfer function is examined and the impulse response is studied by looking at the far-zone energy distribution in time domain. This is covered in Chapter 3.

The comparison with other broadband wire antennas is carried out in Chapter 4. In this chapter, the GMC pulse response is studied. The GMC pulse energy radiation pattern is discussed and comparisons are made. The radiation efficiency simulated by NEC2 is compared.

Chapter 5 presents the conclusions as well as some future considerations on the broadband spline antenna design.

Chapter 2

THE APPLICATION OF GENETIC ALGORITHMS

Genetic algorithms (GAs) are stochastic search procedures modeled on the principle concepts of natural selection and evolution. With the advantage of computers and powerful computational techniques, nature's optimization processes can be applied in the form of genetic algorithms (GAs) to problems with high-dimension and multi-modal functions. As optimizers, GAs are effective at solving complex, combinatorial and related problems [20]. Electromagnetic (EM) optimization problems usually involve a large number of parameters. These problems are expensive to evaluate because the objective functions that arise in electromagnetics are often nonlinear, inflexible and non-differentiable. GAs are attractive for EM optimization since they can be easily applied to problems involving non-differentiable functions and discrete search spaces. It has been proven that GA is very useful for solving complex electromagnetic (EM) problems [21].

The main features that make GAs attractive to the application of this thesis, the design of broadband traveling wave antennas, are that the algorithm converges to a global extreme in a global search, its ability to optimize functions with a large number of parameters and the ability to handle complex objective functions. GAs can simultaneously operate on the global information to obtain a global extreme (desired solution) rather than a local extreme. In this application, the goal is to synthesize broadband traveling wave wire antennas with desired characteristics in terms of high directivity, good efficiency and lower Voltage Standing Wave Ratio (VSWR) over a frequency ranging from 200 MHz to 2 GHz. Since these features are

highly depended on the shape of the antennas, the radius of the wire and resistive loading of the antennas, the objective is to optimize the shapes of the antennas, the radius of the wires and the loading at the ends of the antennas to attain the optimal solutions.

The EM problems can be solved through numerical methods. The Numerical Electromagnetics Code version 2 (NEC2, available in the public domain) which is based on the Method of Moments (MoM) is applied to calculate the EM solutions to the traveling wave antennas. In GAs, by coding the parameters of the antennas into chromosomes, each individual represents one type of antenna, and the properties of the antenna are calculated through the NEC2 analysis. As the fitness-weighted functions guide the population toward to the optimal solution, NEC2 is called repetitively by the GA to solve the EM problems.

In order to take the advantage of the GA, a program is desired to have the ability to implement the GA. It must be able to generate the output file for each individual, call outside functions to perform calculations of the antenna geometry, and weight the results using fitness-weighted functions. The program GA-NEC is a perfect platform for performing the GA computation. The GA-NEC program was developed by Dr. John Ross as part of the antenna modeling and design effort at Delphi Research Labs. It is a general purpose GA based optimizer for NEC2. Dr. Ross also developed another program named AntennaCAD, which provides pre and post-processor functions that simplify the construction of the NEC2 input and output files.

2.1 Basic GA Concepts

In genetic algorithms, a set of possible solutions are generated which evolve towards an optimal global solution. An optimal solution can be achieved by a fitness-weighted selection

process. The exploration of the solution space is accomplished by crossover and mutation of the characteristics in the current population.

As powerful optimizers, GAs are effective at solving complex and combinational problems. They are especially good at finding the goal maxima in a high-dimension, multi-modal function domain. They differ from conventional algorithms in three aspects:

1. They operate on a population of trial solutions in parallel,

2. Usually, they operate on a coding of the function parameters (a chromosome) rather than the parameters themselves, and

3. They use the sample operators (selection, crossover and mutation) to search for the optimal solution in the solution domain.

In the GA procedure, successive populations of trial solutions are called generations. The generations followed are made up of children produced through the crossover and mutation operations by the selected parents with the fitness-weighted ranked selection. During the optimization, a set of individuals (populations) are chosen. They evolve toward the optimal solution as determined by the fitness function. Therefore, GA optimizers must have the ability to perform the following six tasks [20]:

1. Encode the solution parameters as genes,

2. Create a string of genes to form a chromosome (Binary-code form),

3. Initialize a starting trial solution,

4. Evaluate and assign fitness values to individuals in the population,

5. Perform reproduction through the fitness-weighted selection of individuals from the population, and

6. Perform crossover (recombination) and mutation to produce the members of the next generation.

In a simple GA, an initial population is generated with randomly assigned parameter strings or chromosomes. Each of these chromosomes represents an individual. The set of individuals form the first generation. Each of them is assigned a fitness value by evaluating the fitness function. After the individuals are sorted according to their fitness value, a ranked individual list is obtained. The ones with the higher fitness get a higher ranking. The reproduction phase produces a new generation from the current generation. During this process, a pair of individuals is selected to act as the parents. A new pair of children are generated though the crossover and mutation operation. These new children are placed in the new generation by replacing their parents. This process is repeated until there are enough children to fill the new generation. Again, the individuals in the new generation will be evaluated and assigned a fitness value in the same manner as before. The individuals in the new generation are ranked in a sorted order. The reproduction process is repeated and is terminated when the desired fitness value is met.

2.1.1 GA operations

The GA operates on a coding of parameters instead of operating on the parameters themselves. The coding is a mapping from parameter space to chromosome space. In a binary

coding, the parameters are presented by finite length of binary strings. The binary strings that represent all the parameters form a set of binary codes and are referred to as a chromosome. The binary coded parameter is called a gene. The reproduction phase involves three operations: selection, crossover and mutation.

2.1.1.1 Selection Scheme

The selection operator generates a new population from the existing one. The individuals in the new population are selected through a certain criteria. The most commonly used selection operator is known as the weighted roulette wheel selection [22]. During this selection, a roulette wheel is divided into certain number of slots to represent the individuals in the current generation. The area of each slot is proportional to the value evaluated by the fitness-weighted function. Therefore, the probability of the individual to be selected is proportional to the value of the individual itself. Highly fit individuals are more likely to be selected. This procedure is important because the convergence of the GA is strongly dependent on this choice.

2.1.1.2 Crossover Scheme

The crossover operator accepts two parents and produces two children of the next generation. It works directly on the chromosomes themselves. The purpose of the crossover operation is to combine blocks of highly fit sequences and form new sequences with even better fitness values. The simplest crossover scheme is one-point crossover, which is favored by Holland [23]. It has become the most common method of hybridizing binary chromosomes. The one-point crossover provides the simplest way to hybridize binary chromosomes without disrupting the main structure. This process is controlled by the crossover probability. In one-point crossover, if the value of a random variable is less than a specified probability, Pcross, a

random crossover point is selected to divide the binary set into two parts. The portion of the chromosomes preceding the selected point is simply copied from the parent 1 to child 1 and parent 2 to child 2. The portion of the chromosome of parent 1 following the selected point is copied to child 2 in the corresponding position. Similarly, the remaining portion of the chromosome of parent 2 is placed in the corresponding position of child 1, as shown in figure 2.1. Otherwise, if the random variable is greater than Pcross, the entire chromosome of parent 1 is copied into child 1 and similarly for parent 2 and child 2. It can be seen that the operation of one-point crossover precludes the possibility of the first and last bit ever remaining on the same chromosome. The effect of crossover is to rearrange the genes with the objective of producing better combinations of genes to get more fit individuals. Typically, crossover probability between 0.6 and 0.8 has been found to work best in most situations. In this thesis, the probability of 0.75 has been chosen.

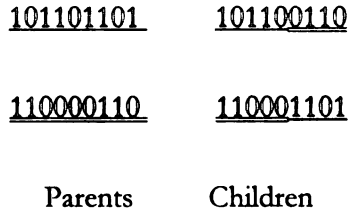

Figure 2.1. Example of the crossover procedure

2.1.1.3 Mutation Scheme

The mutation operator allows the possibility of a slight change in portions of the chromosome of the child. It tends to prevent the optimization process from being trapped in a local minimum. Thus, Mutation rate can affect the ability of the GA to locate a solution and gain more diversity. In mutation, if a random variable is less than the probability of the mutation, a binary element in the chromosome strings is randomly selected and changed. In most cases,

the mutation operator is not very effective to improve the GA's performance. A high mutation value often leads to the destruction of valuable information stored in the highly fit sequences. It usually disrupts the process toward to the optimal solution and interferes with the beneficial action of the selection and crossover. Basically, the mutation process should occur at low probability, usually in the range from 0.001-0.01(although in some cases values as high as 0.1 are used [24]). In this thesis a value of 0.001 is used. The mutation operator is illustrated in figure 2.2 in binary case. In this figure a randomly selected element in the chromosome is changed to a new value (0 to 1 or 1 to 0).

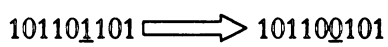

Figure 2.2. The mutation operator randomly changes the elements within the chromosome in case of P < P (mutation).

2.1.2 Fitness Functions

The fitness function, also known as the objective function or the cost function, is used to assign a fitness value to each individual in the GA population. This value represents the goodness of the individual. A desired objective value is specified and stored prior to the optimization process. The fitness value of every individual is calculated and assigned to the individual. By comparing the assigned value with the stored one, the goodness of the individual is obtained. In some complex problems, there may be more than one objective function. For instance, for an antenna problem, the radiation gain of the antenna is not the only objective value of interest; also important are the efficiency and voltage standing wave ratio (VSWR). The final objective function should be a combination of the three sub-objectives. The weighted value should be applied to each of them according to the importance

associated. The desired value assigned to each objective function may vary. It could be assigned as a minimum, a maximum or in a constrained range. Constraints are implemented by imposing a large penalty whenever the constraint is violated. A simple method is to define a function of the multiple objective optimizations:

$$F = \sum_{m=1}^{M} W_m |C_m - S_m| \tag{2.1}$$

Here F is the total raw fitness metric, M is the total number of the objective functions, W_m is the weight applied to the m^{th} basic fitness metric, C_m is output value of the m^{th} basic fitness metric and S_m is specified value of the m^{th} basic fitness metric.

2.2 GA-NEC

The GA-NEC program was developed by Dr. John Ross as part of the antenna modeling and design effort at Delphi Research Labs. It is a general purpose GA based optimizer for NEC2 with multiple functions for antenna design. In GA-NEC, parameters may be specified to control the selection, the crossover, the mutation operations, the generation gap, the convergence type and multiple fitness functions.

2.2.1 Selection, Crossover and Mutation

Based on the selection method used, parents are selected in pairs, and thus the number of the initial individuals in the population must be even. The population size used depends on the complexity of the problem and the length of the chromosome. Typically, longer chromosomes require larger population size. The population size can not be too large or too small. For a large population, the GA moves very slowly towards to the good points, and there are many

children in each generation, requiring many simulations. The large population along with its gene pool diversity overpowers these individuals by sheer numbers, and generally it is a large hill that will be exploited [25]. If the hill does not contain the best answer, the algorithm will often be trapped in local optimum. It is thus suboptimal. If the hill contains the best answer, it will take many simulations to arrive at good answers with such a large population. For a small population, there is not enough diversity to attain the optimal solution. It may make sense to solve a problem with several runs of a small generation GA rather than just one run of a large population GA under the same time cost. For binary chromosome, it is efficient to use a population of about four or five times of the number of bits in the chromosome. The size of the population is usually on the order of 20-500. Values around 100 are commonly used. In this study, there are most likely around ten parameters for the symmetric spline antenna and 13 for the asymmetric ones. The length of chromosome is at the range from 40 to 60. As the result of the rule, the population for the symmetric ones and asymmetric ones is set to 150 and 200 respectively in this study.

The selection strategy determines how the selection operator chooses the parents to generate the children. The *elitist strategy* is chosen along with roulette wheel selection. This strategy ensures that the best solution in each generation is most probably preserved. This will improve convergence. In the convergence criteria, the maximum number of generations that will be computed is specified. The number is set to 150 in this study.

The one-point crossover operation is adopted is this algorithm. The effect of the crossover is to rearrange the genes to produce better combinations of genes, and, as a result to get better

fit individuals. It has been found that the probability of crossover on the order of 0.6-0.8 works best in most problems [19]. This value is set to 0.7 in the GA-NEC program.

Mutation rate can affect the GA's ability of locating a solution to avoid the optimization process being trapped in local minima. Higher probability of mutation will destroy the valuable information that is already stored in the highly fit sequences. The value is set to 0.05 in this study.

2.2.2 Generation Gap

In the GA operation, the fraction of the population, the generation gap, to be selected as parents highly affects the GA convergence. It specifies the number of individuals involved in selection, crossover and mutation operations. A generation gap between 0.95 and 1 is adequate for most problems. It is set to 0.95 in this study.

2.2.3 Convergence

The convergence type is set to *none-use max generations* to specify that the run will stop only when the maximum number of generations has been reached. The convergence variable is set to *raw fitness minimum* to control the convergence. This is the common option because one is generally only interested in finding a single solution.

2.2.4 Fitness

Fitness is a single numerical quantity evaluated by a fitness function. It is assigned to each individual to describe how well an individual meets predefined design objectives and constraints. For multiple objectives, fitness can be computed based on the outputs of multiple analyses using a weighted sum. The definition of good fitness functions depends on the

problems themselves. For broadband antenna design problems, the three main objectives, the VSWR, efficiency, and gain, should be taken into consideration. The total fitness of an individual is the sum of the three weighted ones as shown in equation 1.

In order to design broadband traveling wave antennas with optimal characteristics, three fitness functions are specified. Each of them should be the summation of fitness values evaluated at certain frequencies from 200 MHz to 2 GHz. Since the VSWR plays a more important role, the corresponding weighting value should be considerably higher than that of efficiency and gain. We set the weighting value of VSWR, w_{VSWR} to 10000, and set $w_{efficiency}$ and w_{gain} to 100 and 1, respectively.

2.3 The applications of GA-NEC

GA has been shown to be a very powerful tool for antenna design. It is very efficient to design an antenna with special desired characteristics. The wire antenna design with special characteristics has received considerable attention in the literature. For instance, a circularly polarized antenna formed by several segments connected in series has been studied by Altshuler and Linden [26]. Ultra-wideband wire antennas have been designed by loading the wires with resonant RLC circuit [27-28]. In this application, the load location and the circuit elements have been optimized by a GA. The first GA designed Ultra-broadband antenna for communication was a loaded monopole with height of 1.75 m and frequency range of 30-450 MHz [29].

This study focuses on the topic of Ultra-broadband wire antenna design using a GA. The goal of this study was to design a wire antenna with loading at one end which had the desire

characteristics in terms of VSWR, efficiency, and the directivity over the frequency range 200 MHz to 2 GHz.

2.3.1 Coding the spline antennas

As discussed earlier, GA-NEC can not work on the antenna's parameters themselves. It must work on the binary strings or chromosomes that are formed by coding the parameters. Thus, the parameters that specify the physical information of the antennas must be determined before the optimization process can begin. The transient field produced by a traveling-wave wire antenna was studied by Rothwell [30]. It was shown that the traveling-wave time-domain antenna has the ability to directly radiate wideband waveforms for a certain impulse width. The optimal wideband properties can be attained by optimizing the shape of the antenna. Two types of spline antennas are taken into consideration: one with symmetric geometry as shown in figure 2.3, and the other with asymmetric geometry in figure 2.4. In order to use GA-NEC to optimize the shape of the antenna, the antenna parameters must be represented by binary strings.

2.3.1.1 Coding the symmetric spline antenna

There are several parameters that can affect the EM properties of the symmetric spline antenna. They are the length of the antenna, the radius of the wires, the shape of the curves and the load at the end of the antenna. In order to have GA-NEC optimize the antenna, the fitness function should be specified which defines the goal of the optimization process. All antenna parameters should be represented by binary strings since GA-NEC can't operate on the parameters themselves.

To obtain the spline shape antenna, an external program is called by GA-NEC. The external program is written in Visual Basic. Its purpose is to generate smooth "spline" curves by passing lines through several discrete points. Therefore, the shape of the curve is decided by the points which the curve should pass through. The optimal shape of antenna can be achieved by optimizing the positions of the points. The more points that are chosen, the more geometrical diversity the antenna has. But, more points means more binary strings are required. As a result, there will be a long chromosome which will slow down the process to find the best solution. In this particular study, eight points are selected to form one side of the curve. The other side is generated automatically by the symmetry of the geometry.

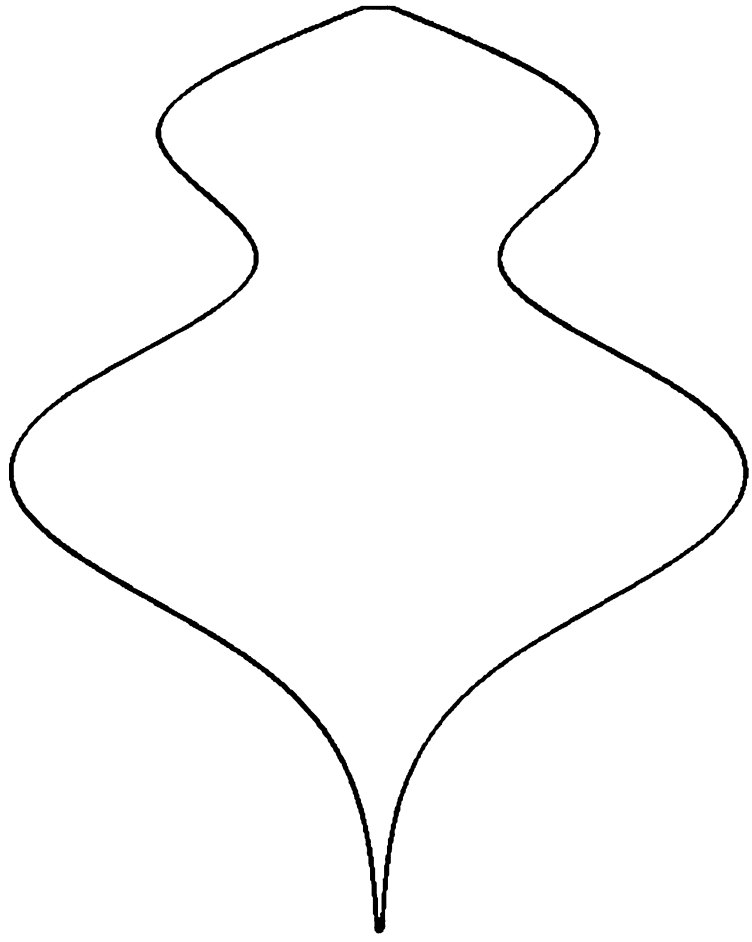

Figure 2.3. An example of antenna with symmetric geometry

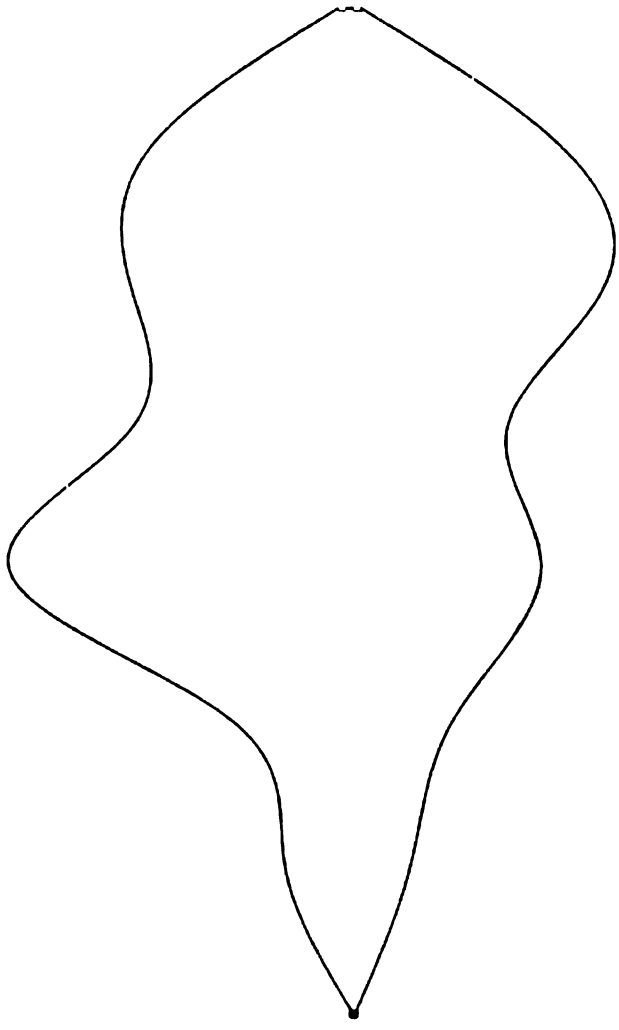

Figure 2.4. An example of antenna with asymmetric geometry

Fixing the beginning points, the shape of the antenna can be optimized based on the other seven points. There are also two other parameters, the radius of the wire and the load at the ends that should be optimized in order to reach the goal guided by the fitness functions. The nine parameters, also called the genes, represented in binary strings form one chromosome. One chromosome stands for an individual. In the real-valued chromosome, there are nine genes. Its representation is:

[P1 P2 P3 P4 P5 P6 P7 R1 L1]

Where the Ps are the position genes, R is the radius gene, and L is the load gene.

In binary representation, GA-NEC will use 5 bits for each position gene, 3 bits for the radius and 2 for the lumped load. The 40-bit chromosome will be constructed in the following typical way:

[P11...P15, P21...P25, P31...P35, P41...P45, P51...P55, P61...P65, P71...P75, R11 R12 R13, L11 L12]

Where the P's indicate the locations of each bit in the binary representation of the point positions variables, while the R's indicate the location of the 3 bits that make up the radius variable, and the L's indicate the 2 bits compose the third variable, the load. The first binary bit of each variable is the most significant one for that variable. It has higher weight than any others in the strings that compose that variable. One possible chromosome can be

[0010001011001001010000100100111010101111]

It represents one possible solution, an individual. For this individual, GA-NEC will translate it into a set of those parameters and pass them to the external program to generate the spline shaped antenna. In conjunction with NEC2, the antenna will be simulated and the

electromagnetic response of the antenna will be calculated. The results from the NEC2 analysis will be evaluated using the specified fitness functions. The yield value, the fitness value, is associated with the individual. The individuals in each generation are ranked according to their fitness values.

Several types of symmetric spline antennas are simulated in this study. They are varying, constraint and constant wire radius with closed and open end. GA-NEC only optimizes the point location and the load for a closed end. Hence, the number of binary strings can be reduced to 37 for open end and 39 for closed end. For the first case, the radius of the wire varies as a function of separation to keep the constant impedance (600 Ohms in this study). The second case allows the radius to vary over a specified range and GA-NEC optimizes the point location and the radius as well. The number of binary strings in this case will be 41 for the one with open end and 43 for the one with closed end. In the third case, the radius is set to constant along the whole antenna. GA-NEC optimizes the point locations and picks the optimal radius for the wire. In this case the number of binary strings is 39 for open end one and 41 for closed end.

2.3.1.2 Coding the asymmetric spline antenna

Similar to the symmetric antenna, the optimal asymmetric spline antenna can be achieved by optimizing the shape of the curves. But unlike the symmetric one, there are two wires that must be worked on. As a result, the number of points that need to be optimized will be twice that of the symmetric antenna. The population in each generation should be larger to have an efficient GA-NEC optimization. This will increase the simulation time for each run. The GA-NEC will move very slowly to the optimal solution. On the other hand, a large population can

bring more diversity, which may yield better-fitted value points. To speed up the simulation time and give GA-NEC more diversity, the number of points on each side is reduced to six instead of seven. Thus there are fourteen parameters that decide the characteristics of the asymmetric spline antenna. In the real-valued chromosome, there are fourteen genes. Its representation is:

[P1 P2 P3 P4 P5 P6 P7 P8 P9 P10 P11 P12 R1 L1]

As with the symmetric antenna, Ps represent the position gene, R the radius gene, and L the load gene.

The size of the gene or the number of bits used to represent a parameter is important to the accuracy of the solution and the time needed for GA-NEC to converge. In this case, GA-NEC uses 5 bits for each position gene, 4 bits for the radius and 2 bits to present the lumped load. This will bring enough accuracy to the solution and requires less time to converge. Each chromosome is encoded by 66 binary bits. The 66-bit chromosome can be constructed as:

[P11...P15, P21...P25, P31...P35, P41...P45, P51...P55, P61...P65, P71...P75, P81...P85, P91...P95, P101...P105, P111...P115, P121...P125, R1...R4,L1 L2]

One possible chromosome can be represented in binary strings as

[000110100111011100110101111101000000101100001100011000110001010111]

The number of bits in the chromosome is 66, which is bigger than that of the symmetric antenna, 40. This will enlarge the searching space. It seems that the asymmetric coding will obtain better solutions than the symmetric one if the population and number of runs are chosen properly. On the other hand, this will increase the simulation time.

2.3.2 The searching space

In order to run GA-NEC, the possible values of the parameters that will be optimized must be constrained. This will make the search space manageable. It is important that the ranges of the parameters should be large enough such that the optimal solution is likely to be included. Also, in GA-NEC, the number of bits that represent the parameters should be carefully chosen. This number together with the search space gives the possible value from which GA-NEC can choose. In the binary GA-NEC, the number of bits used to represent a parameter provides an integral number of different possible values of the parameter. If it is chosen to be small, it is possible that the optimal solution is not included in the search domain. But on the other hand, if it is big, as discussed previously, a large population is necessary to have GA-NEC search for the optimal solution efficiently. In this study, the point position search space is set from 0 to 1 meter. The radius varies from 0.0005-0.008 meters. The lumped load impedance search space is from 0 to 600 ohms with a step of 200 ohms.

2.3.3 The external Visual Basic program

The purpose of external program is to create the shape of the antenna using spline functions by working on the information in the input file that is generated by GA-NEC. In the input file, called spline.inp, the information that is needed to create the spline antenna is written in the proper order such that VB program can read it correctly. The first line of spline.inp specifies the total length of the antenna from the input end to the load end. The minimum separation is defined in the second line, which determines the minimum separation between the two halves of the antenna. Setting the proper minimum separation avoids segment separation violations when the NEC2 program is called. The third line specifies the input impedance at the input end of the antenna. The fourth line defines the number of segments that the antenna can be

divided into along the z-axis, the direction of the antenna. The fifth line specifies the number of points that the spline will pass through. The positions of the spline points are generated right after the fifth line. For an asymmetric spline antenna, the number of points is twice that of the symmetric one. The VB program will generate the antenna geometry data based on the information that is given in the input file, spline.inp.

In the VB program, there is a main function that defines the names of the input file and output file. Once these two files are specified in the main function block, a sub function is called to generate the antenna geometry. In the sub function block, the input file is opened and the parameters are read line by line as input information to create the antenna. The input file will close when the last line is fetched. After all the information is read from spline.inp, another function is called to create the curve that passes through the specified points.

In order to minimize reflections, it is desirable for the antenna to have constant transmission line impedance along its length. The separation and the radius of the wire determine the impedance of the antenna at a certain distance. Once the separation is known, the radius corresponding to impedance Z0 can be calculated by

$$\text{Radius} = \text{Separation} / (2 * \text{Cosh}(Z0/120)) \tag{2.2}$$

Here Cosh is the hyperbolic cosine function and Z0 is the input impedance of the feed twin lines.

After this process is complete, the information about segments that comprise the antenna is known. The information that is associated with the segments includes: the positions of the segments, the coordinates of each end, and the radius of the segments. The VB program then

writes this information to an output file, called spline.ni2, line by line. The information is formatted in the manner of a GW card that can be recognized by the NEC2 program. In the output file, each segment is written in its own GW card. All the GW cards for the segments that make up the spline antenna compose the spline.ni2 file. All the GW cards in this file are taken as part of the GA-NEC input file, which is the input of the NEC2 program. As mentioned earlier, the purpose of the VB program is to generate the geometry of the antenna and write it into a format which is readable by NEC2. Because the positions of the segments are unpredictable, it is almost impossible to write the GW cards for a spline antenna in a conventional manner, as might be done for a rhombic antenna. During the GA-NEC optimization process, each spline.inp and spline.ni2 file are associated with an individual. The program is called repeatedly by GA-NEC as the optimization process proceeds. For more details about this VB program, interested readers are referred to the appendix.

Chapter 3

THE OPTIMIZATION RESULTS AND ANALYSIS

The EM properties are mainly controlled by three system factors: the shapes of the antennas, the radius of the wires, and the load inserted at the end of these antennas. Therefore, optimization of the antenna properties is the goal of this study. The purpose of this chapter is to optimize the antenna properties. A set of spline antennas with the optimal wideband properties were studied in terms of gain along a certain direction, VSWR, and efficiency over a frequency range from 200 MHz to 2 GHz.

The GA-NEC program is used for optimization in conjunction with NEC2 (open version). The GA-NEC program performs optimization based on the NEC2 simulation results. In this study, both symmetric and asymmetric antenna geometry antennas are considered. The asymmetric geometry requires more binary strings to represent each individual than the symmetric one. As a result, it provides more diversity than the symmetric geometry, but needs a larger population and a longer run time. Both open ends and closed ends were studied for each geometric type. In the closed ends case, the lumped terminating load resistant was also optimized by GA-NEC.

The antennas were divided into 200 segments. Three criteria were used to optimize the radii of the segments: varying radius, constant radius and varying radius with constraint. The varying radii were calculated according to equation 2.2 to keep the characteristic impedance of the two-wire line constant. A constraint radius is to have the radius varying within a constrained range based on equation 2.2. The constant radius was optimized by GA-NEC with different

input impedances. The length of each of the antennas studied is 3 meters. An impedance of 600 ohms is chosen for varying radius case, 300 ohms for constraint radius antennas and 150 ohms for constant radius antennas. Table 3.1 shows all the cases that are discussed in this study.

Term definitions:

VSWR

An antenna's ability to receive power from a source is determined by the input impedance. For maximum power transfer, the input impedance should exactly match the output impedance of the source. For broadband antennas, the input impedance differs from the output impedance of the source. The complex reflection coefficient at the input of the antenna is

$$\Gamma = \frac{Z_{input} - Z_0}{Z_{input} + Z_0} \tag{3.1}$$

Here Z_{input} is the antenna's complex input impedance and Z_0 is the source impedance. The power reflected is equal to the incident power multiplied by the square of the magnitude of the complex input reflection coefficient. The net power accepted by the antenna is given by

$$P_{input} = P_{incident}(1 - \Gamma^2) \tag{3.2}$$

In terms of the reflection coefficient, the voltage standing wave ratio is given by

$$VSWR = \frac{1 + |\Gamma|}{1 - |\Gamma|} \tag{3.3}$$

The reflection coefficient, Γ, ranges from 0 to 1. The VSWR ranges from 1 to infinity. The VSWR is useful to describe the input match when the match is not good.

Antenna efficiency

The antenna efficiency, sometimes called the radiation efficiency, is defined as the ratio of the power radiated by the antenna to the net power accepted by the antenna from the connected transmitter. It can be described as:

$$P_{radiated} = P_{input} * \eta_{radiation} \tag{3.4}$$

Where $P_{radiated}$ is the power radiated by the antenna, P_{input} is the power accepted from the source, and $\eta_{radiation}$ is the antenna efficiency.

Radiated power

The radiated power is computed as the input power minus the structure and network loss. In this study, it is assumed that there is no network and the wire is lossless. The structure loss is ohmic loss in the load.

$$P_{radiated} = P_{input} - P_{load} \tag{3.5}$$

Power gain

The power gain of an antenna (in a given direction) is defined as the ratio of the intensity, in a given direction, to the radiation intensity that would be obtained if the power accepted by the antenna were radiated isotropically. The radiation intensity corresponding to the isotropically radiated power is equal to the power accepted (input) by the antenna divided by 4π [31]. The desired direction refers to along the length of the antenna (z-axis) in this study.

GA-NEC parameter setting

In the GA-NEC program, the initial population is set to 150. In some cases, GA-NEC does not converge after a long run time and therefore, the maximum number of generation is chosen to control the convergence. The value is set to 100 for all cases. The crossover probability is set to 0.75. The mutation probability is set to 0.008 and the generation gap is 0.95. The Elitist Strategy is chosen as the selection strategy.

The lengths of the antennas are 3 meters and the antennas are in yz-plane. The desired radiation direction is along the length of the antennas (z-axis). VB program generates the antennas by passing splines through 8 equally spaced points. 5 bits for symmetric geometry and 4 bits for asymmetric geometry are used to represent each point. The search domain for each point is from 0 to 1.2 meters. Two bits are used to represent the terminating load at the ends in the case of closed ends. For constraint or constant radii, the search space is from 0.001 to 0.01 m and is represented by 3 bits. As a result, in the cases of symmetric open ends, there are 35 bits for varying radii and 38 for constraint/constant radii. In the cases of symmetric closed ends, there are 32 and 35 bits in a chromosome for varying radii and constraint/constant radii, respectively. In the cases of asymmetric open ends, there are 56 bits for varying radii and 59 for constraint/constant radii. In the cases of symmetric closed ends, there are 50 and 53 bits in a chromosome for varying radii and constraint/constant radii, respectively. GA-NEC sweeps the frequency from 200 MHz to 2 GHz with a step of 100 MHz. GA-NEC only evaluates the value at integer of hundreds during the optimization process. A voltage source of 1 volt is chosen to excite the antennas. The goal of the fitness function is chosen as "constrain within range". As discuss in chapter 2, a penalty will be

applied if the value is out of the range. In this study, the constraint range of VSWR is set to range from 1 to 3, 5 to 20 for the power gain and 80 to 100 for efficiency.

Table 3.1 Different study cases

Geometry	**Ends type**	**Impedance (Ohms)**	**Radius type**	**Optimization points**	**Bits**
Symmetric	Open ends	600	varying	7	35
		300	constraint	7	38
		150	constant	7	38
	Closed ends	600	varying	6	32
		300	constraint	6	35
		150	constant	6	35
Asymmetric	Open ends	600	varying	14	56
		300	constraint	14	59
		150	constant	14	59
	Closed ends	600	varying	12	50
		300	constraint	12	53
		150	constant	12	53

3.1 Antennas with Symmetric Geometry

The shape of the antenna is generated by spline curves passing through certain points. GA-NEC2 optimizes the shape of the antenna by optimizing the positions of these points. For the symmetric antennas, the number of points optimized is just half of that for the asymmetric antenna. As shown in table 3.1, the number of optimization points is 6 for antennas with closed ends and 7 for that with open ends. There are 8 points along the antennas equally spaced along the length of the antennas. One point at one end is fixed in the case of open ends and two points at the ends are fixed in the case of closed ends.

3.1.1 Symmetric geometry with open ends

For symmetric antennas with open ends, the current is zero at the ends. The input power is radiated when the current travels along the antenna. In this case, the shape of the antenna and the radius of the wire dominate the EM properties. Several cases with different input impedance are studied (table 3.1). Optimizing the shape and the radius of the wire is the goal for this situation.

3.1.1.1 Feed impedance of 600 Ohms

Because of the symmetric geometry, there are only seven parameters that need to be optimized in GA-NEC. They are the positions of the seven points that the wire passes trough. The radius of the wire is obtained with equation 2.2. Figure 3.1 shows the geometry of a 3-meter antenna. The thickness of the line is proportional to the radius of the wire. It varies from 0.00013 to 0.013 meters. Some segments with small radii near the ends cannot be displayed in figure 3.1.

In Figure 3.2, the real part of input impedance is close to Z0 (600 Ohms) and the imaginary part tends to zero as the frequency increases. The VSWR (to Z0) varies from higher that three at low frequency to just over one at high frequency. Therefore, the radiated power changes in a large range at low frequency and become stable at high frequency (Figure 3.4). There is no ohmic loss when the wave travels along the antenna and therefore, the efficiency is 100 percent for the entire frequency range (Figure 3.5). In Figure 3.6, the power gain of the antenna is 4 dB at 200 MHz and increases to about 9 dB at 2000 MHz. It indicates that the antenna has higher directivity at higher frequency. As shown in Figure 3.7, the antenna has lower directivity in both xz-plane and yz-plane at low frequency. When frequency increases, the side lobes become smaller (Figure 3.8 - 3.10). Figure 3.1 -3.10 indicates that this antenna

has high radiation efficiency (100 percent), low VSWR (ranging from 1.01 - 3.3), and good directivity at higher frequency Furthermore, it will show in chapter 4 that it also has good GMC pulse response in transmission.

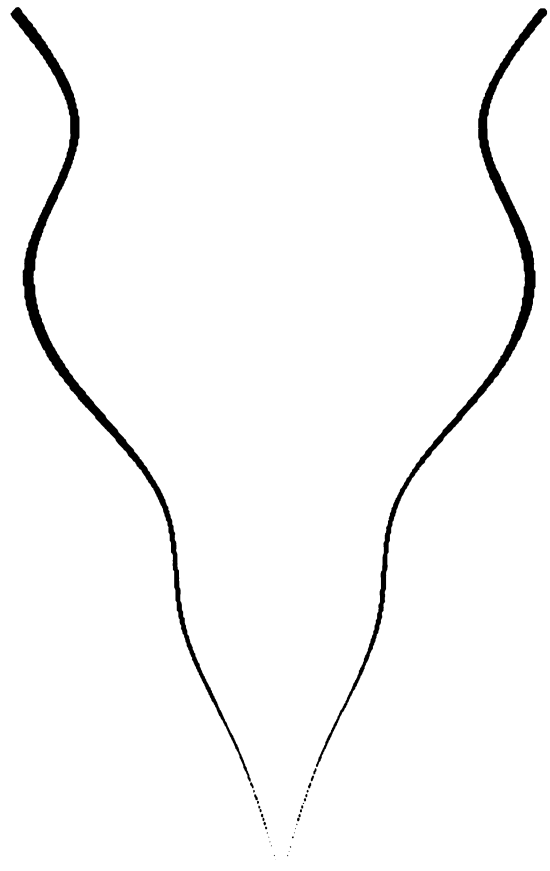

Figure 3.1 Antenna Geometry

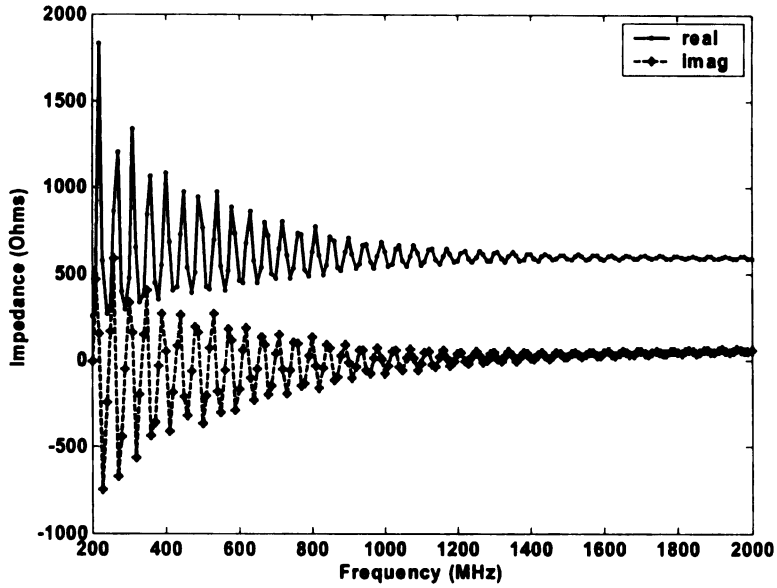

Figure 3.2 Input Impedance vs. Frequency

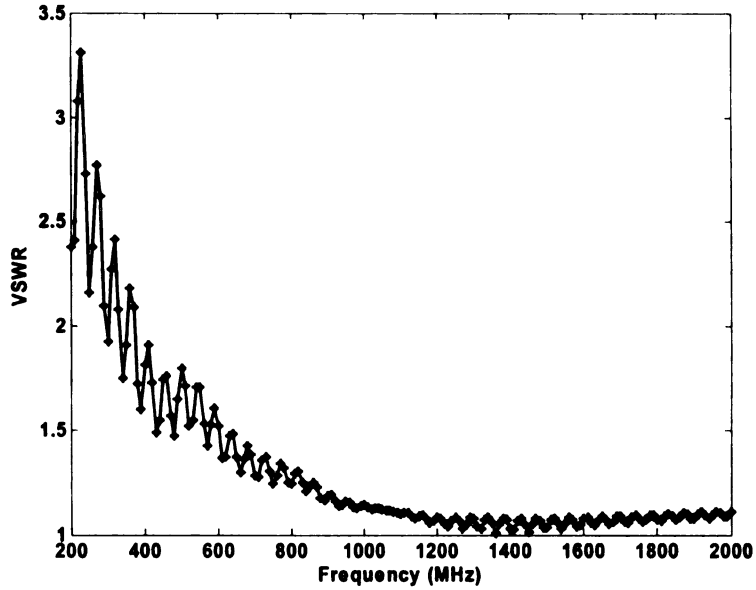

Figure 3.3 VSWR vs. Frequency

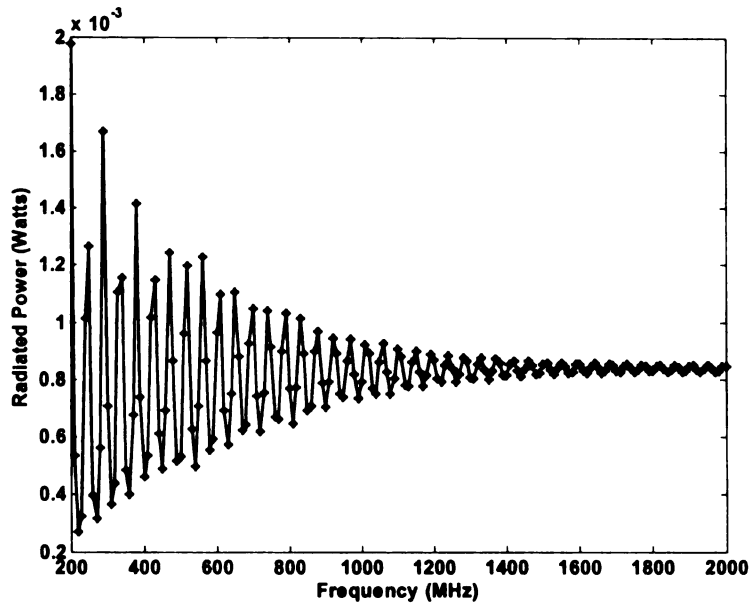

Figure 3.4 Radiated Power vs. Frequency

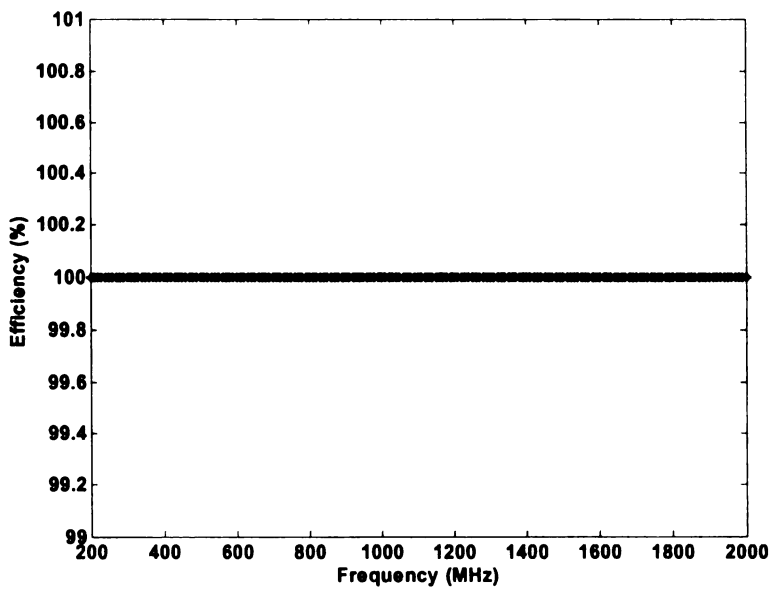

Figure 3.5 Efficiency vs. Frequency

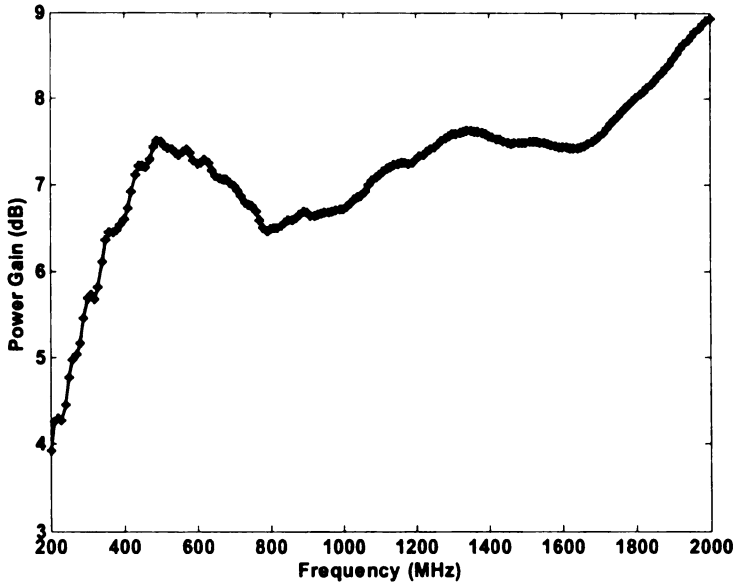

Figure 3.6 Power Gain vs. Frequency

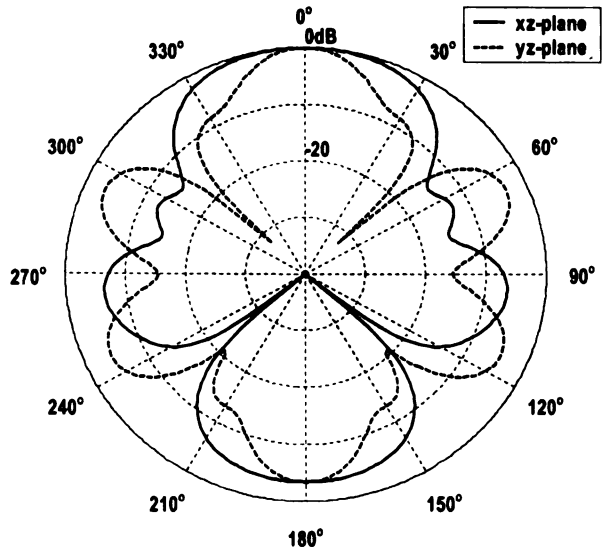

Figure 3.7 E_ϕ (xz-plane) and E_θ (yz-plane) patterns at 200 MHz

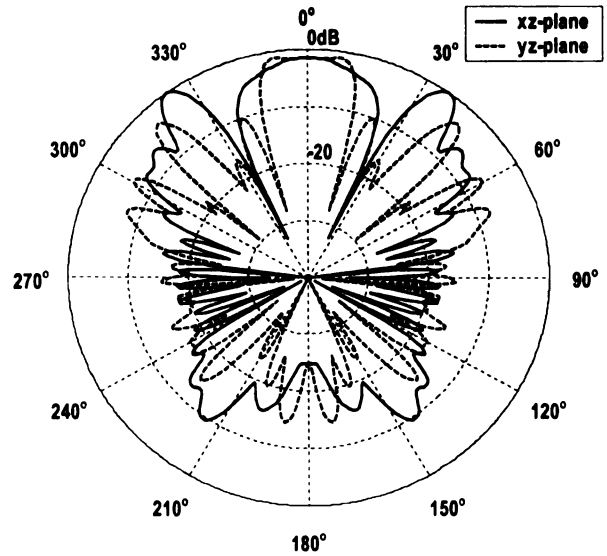

Figure 3.8 E_ϕ (xz-plane) and E_θ (yz-plane) patterns at 800 MHz

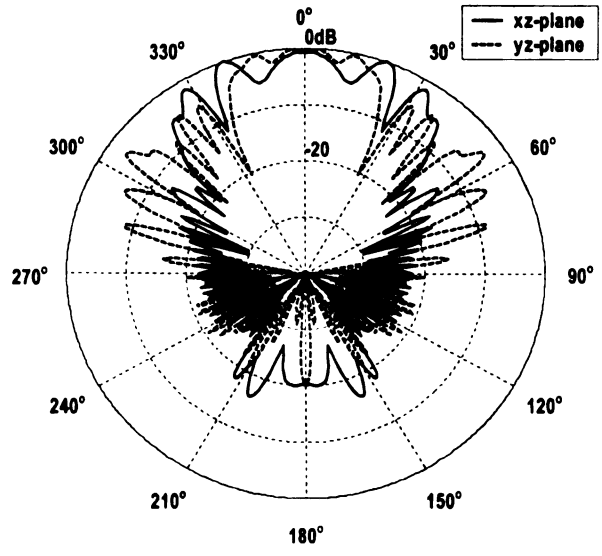

Figure 3.9 E_ϕ (xz-plane) and E_θ (yz-plane) patterns at 1400 MHz

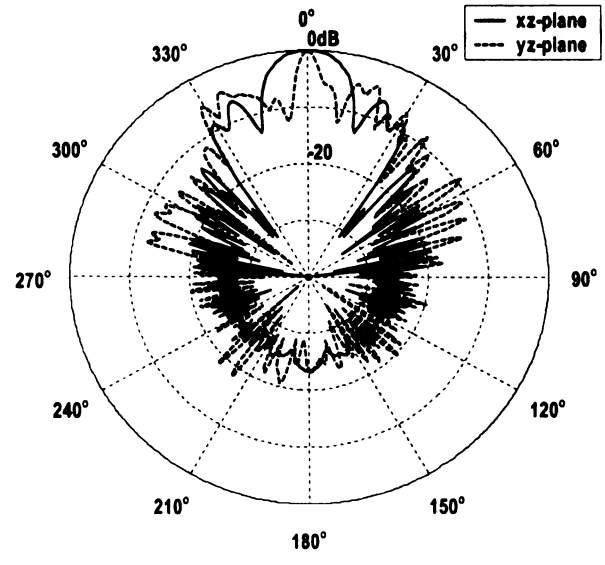

Figure 3.10 E_ϕ (xz-plane) and E_θ (yz-plane) patterns at 2000 MHz

3.1.1.2 Feed impedance of 300 Ohms

As in the 600 ohms case, there are seven points to be optimized. The VB program calculates the radii of the segments (equation 2.2) and constrains the value in the constraint range if the calculated results are out of it. Figure 3.11 shows the optimized result. Most of the radii have a value of 0.01 meter except for a few segments near the feeding point that have radii varying from 0.00163 to 0.01 meter.

In Figure 3.12, the real part of the input impedance is close to 300 ohms as frequency increases. The VSWR is in a range of 1.08 - 2.46 (Figure 3.13). More power is radiated at higher frequency (Figure 3.14). The efficiency is 100 percent since there is no loss (Figure 3.15). Figure 3.16 show that the power gains have several dips at frequency 550, 850 and 1600 MHz. The antenna is not very directive at low frequency (Figure 3.17). Moreover, there are more side lobes at higher frequency. The directivity is not as good as that of the previous case as seen in Figure 3.17 – 3.20.

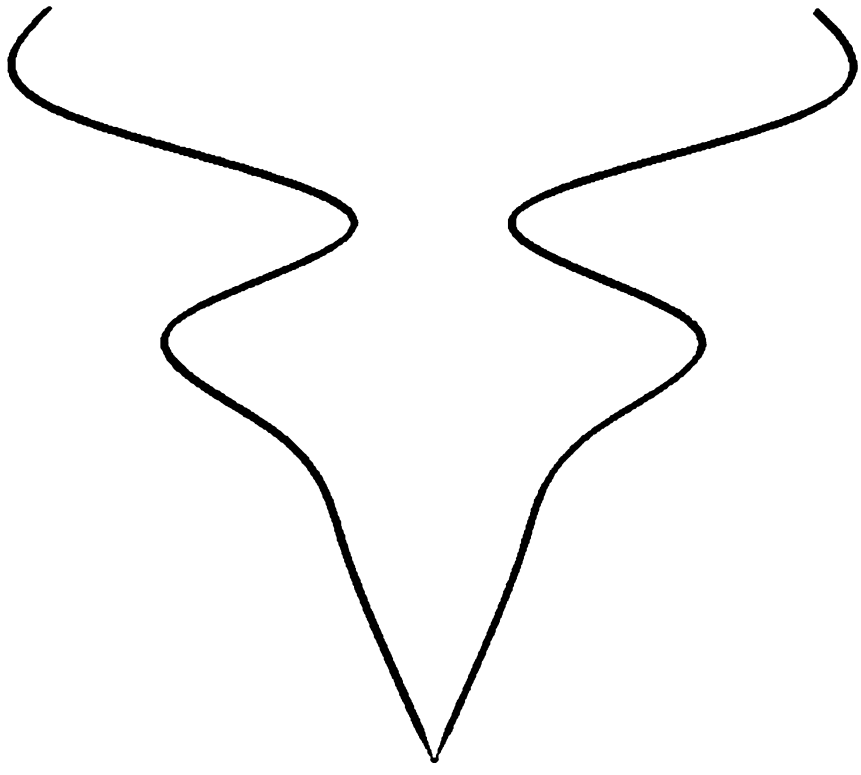

Figure 3.11 Antenna Geometry

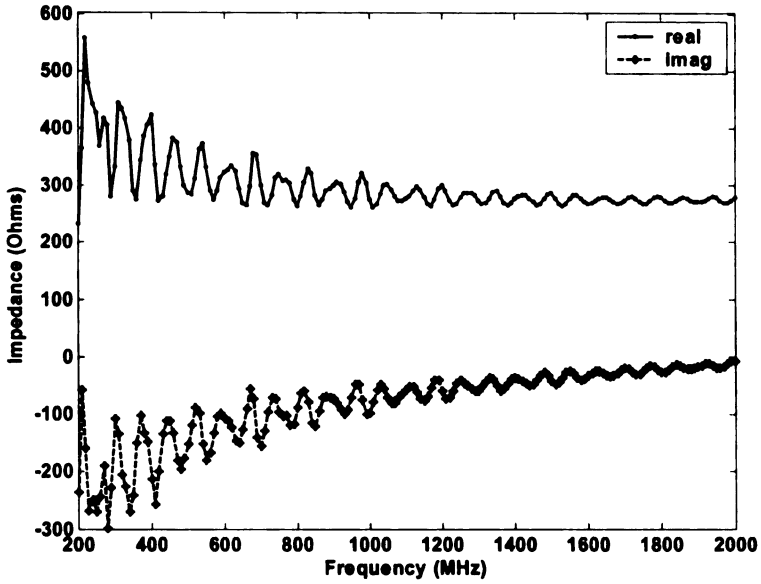

Figure 3.12 Input Impedance vs. Frequency

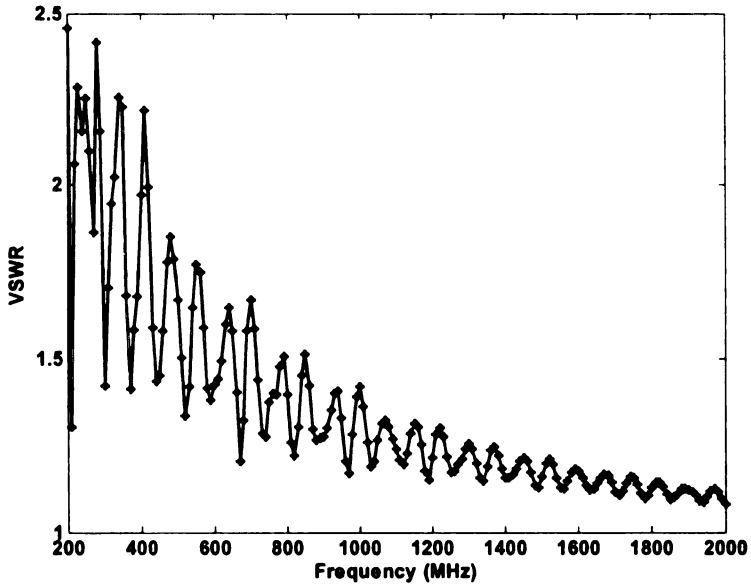

Figure 3.13 VSWR vs. Frequency

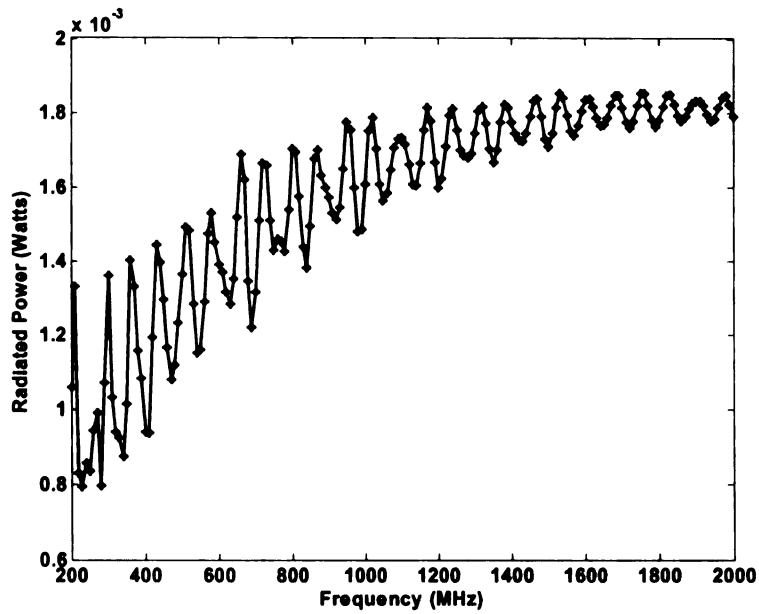

Figure 3.14 Radiated Power vs. Frequency

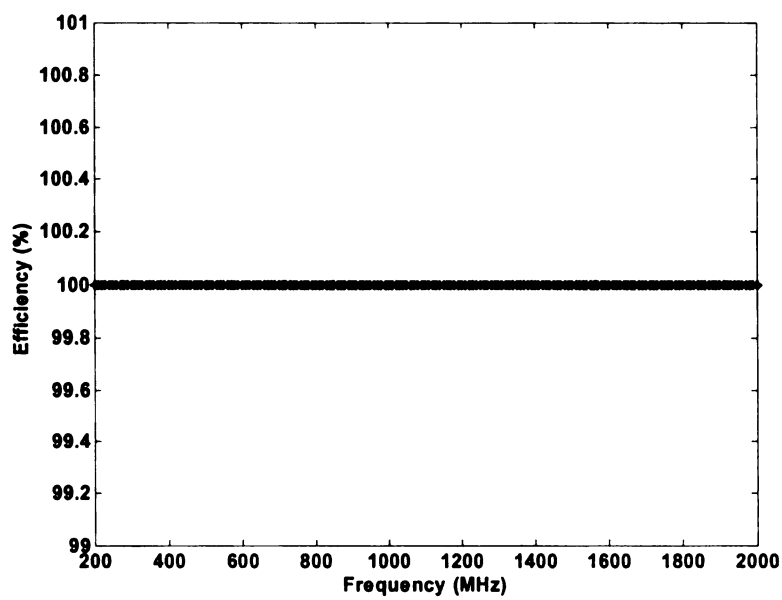

Figure 3.15 Efficiency vs. Frequency

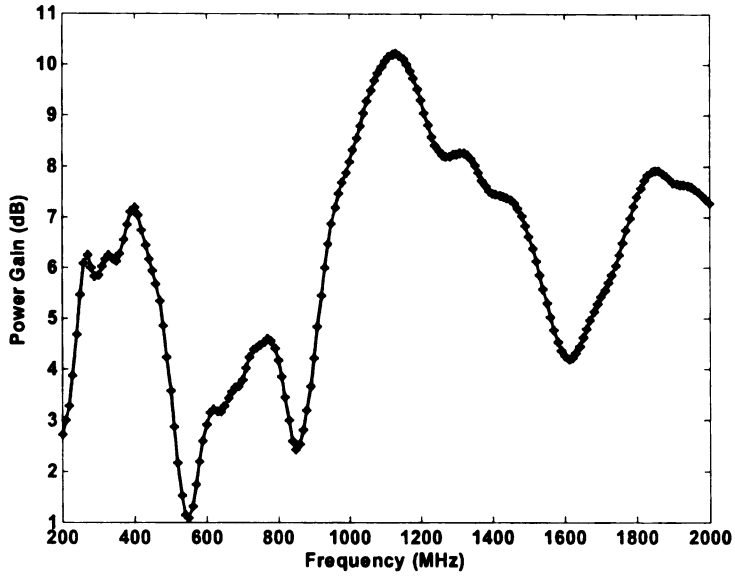

Figure 3.16 Power Gain vs. Frequency

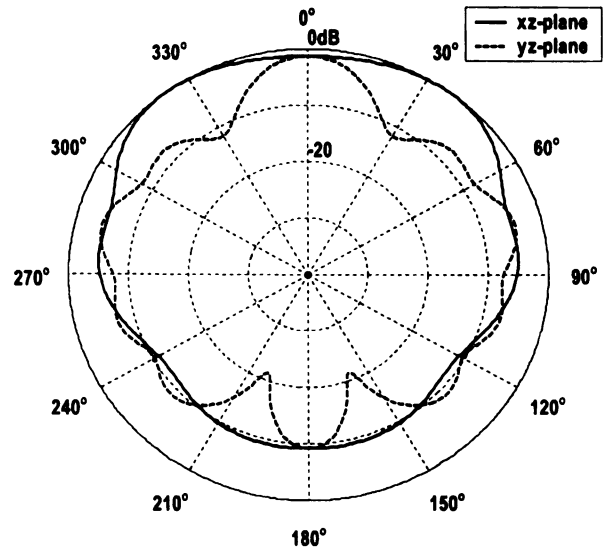

Figure 3.17 E_ϕ (xz-plane) and E_θ (yz-plane) patterns at 200 MHz

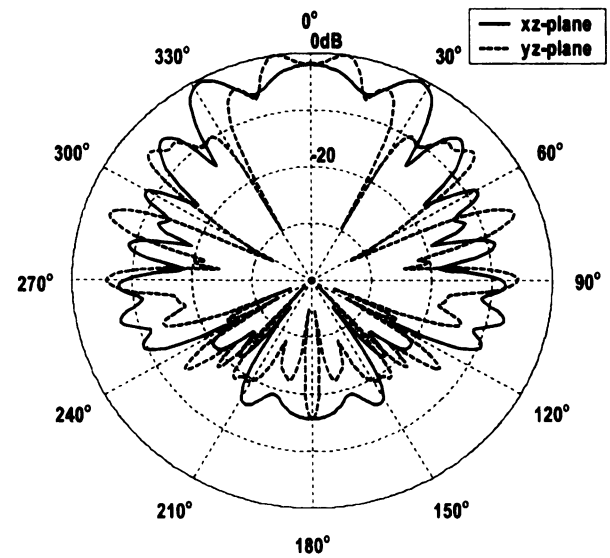

Figure 3.18 E_ϕ (xz-plane) and E_θ (yz-plane) patterns at 800 MHz

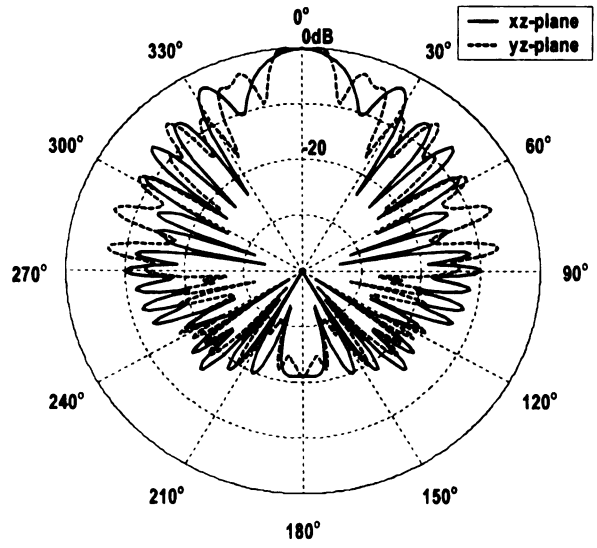

Figure 3.19 E_ϕ (xz-plane) and E_θ (yz-plane) patterns at 1400 MHz

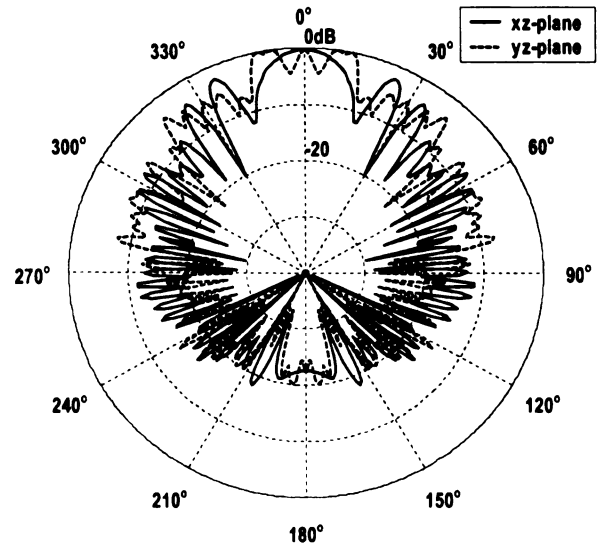

Figure 3.20 E_ϕ (xz-plane) and E_θ (yz-plane) patterns at 2000 MHz

3.1.1.3 Feed impedance of 150 Ohms

The radii of the segments are constant throughout the antenna. The program optimizes the value in a range of 0.001 – 0.01 m. Figure 3.21 shows the optimized antenna shape. The GA-NEC optimized radius value of segments is 0.0058 m.

The real part of the input impedance is close to 150 ohms as frequency increases while the imaginary part is close to -50 ohms (Figure 3.22). Figure 3.23 shows the VSWR is in a range of 1.3 - 3.44. The radiated power increases at higher frequency (Figure 3.24). In Figure 3.26, the power gain has several dips at frequency 300, 550 and 1250 MHz. There is no ohmic loss for this antenna (Figure 3.25). The directivity is not as good as that of the previous ones as shown in Figure 3.27 – 3.30. The direction of maximum radiation is around 60 degree instead of 0 degree at 200 MHz (Figure 3.27).

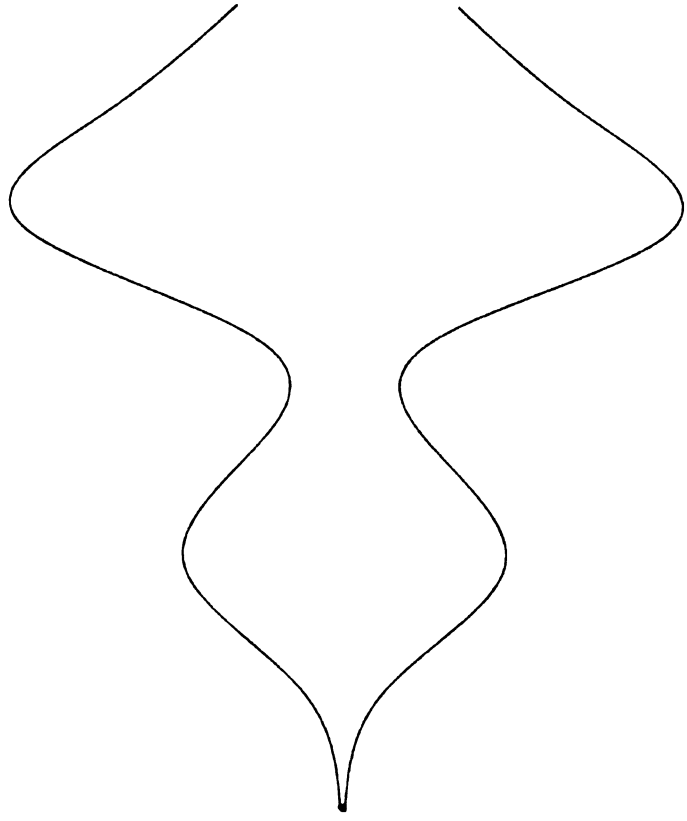

Figure 3.21 Antenna Geometry

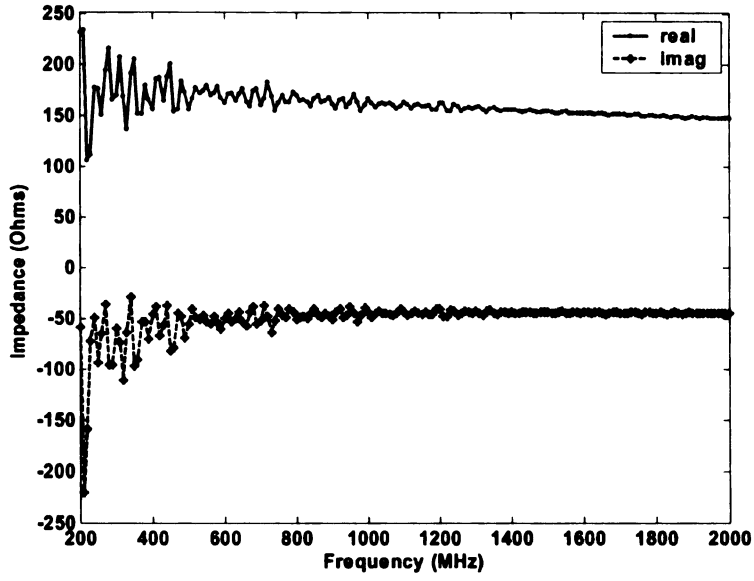

Figure 3.22 Input Impedance vs. Frequency

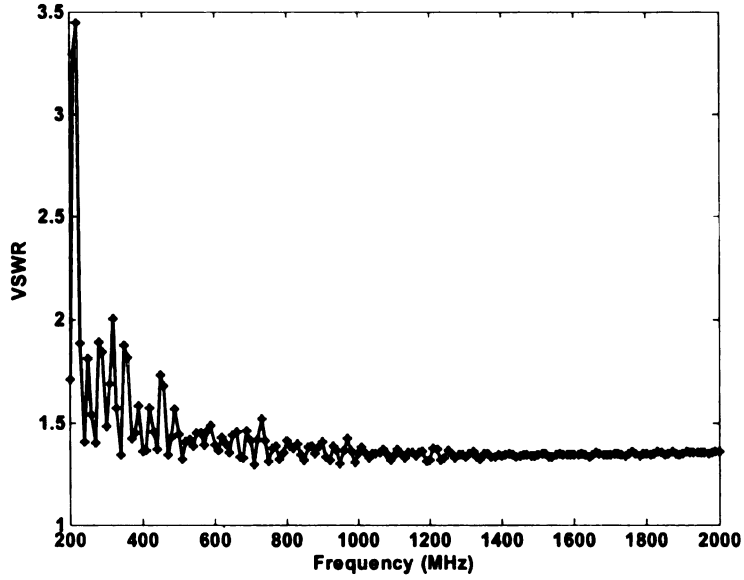

Figure 3.23 VSWR vs. Frequency

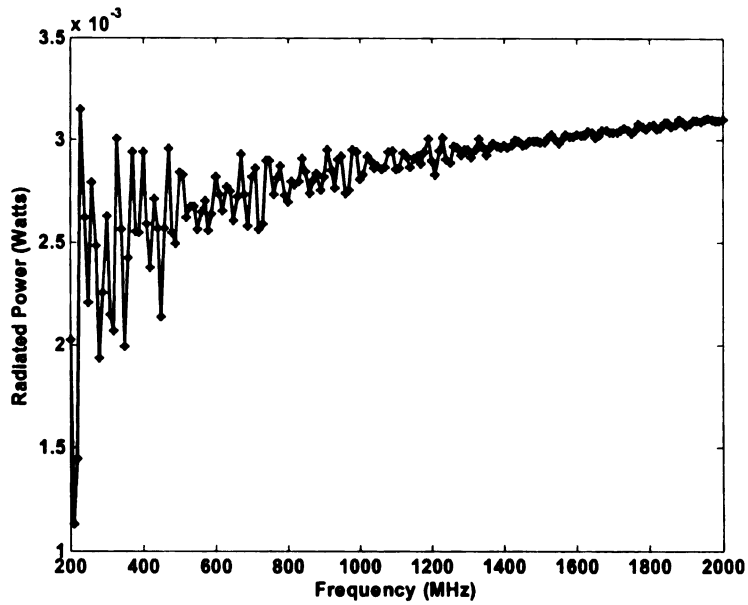

Figure 3.24 Radiated Power vs. Frequency

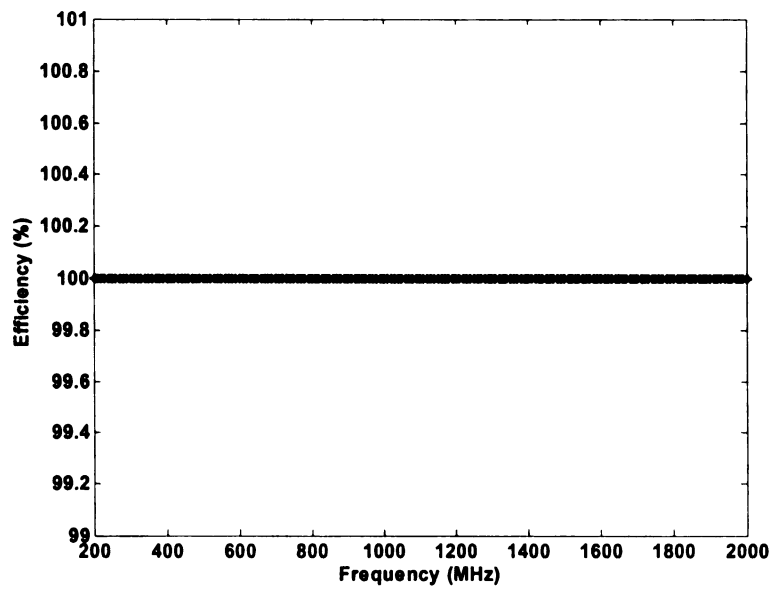

Figure 3.25 Efficiency vs. Frequency

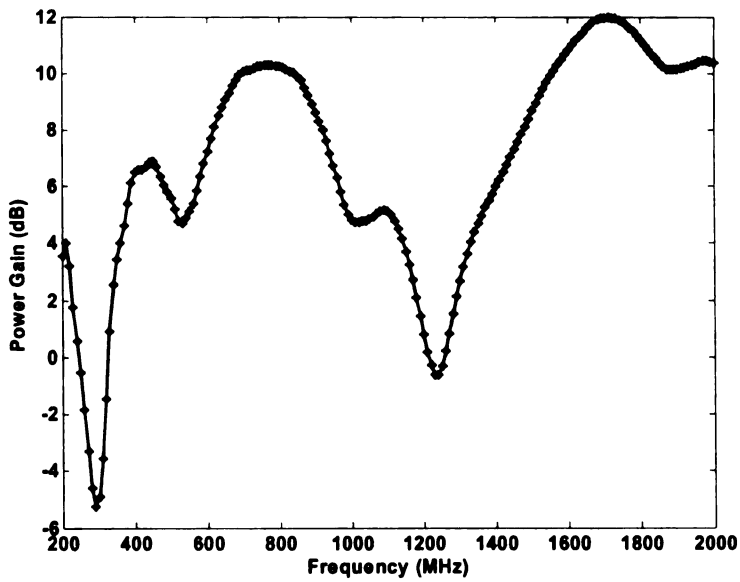

Figure 3.26 Power Gain vs. Frequency

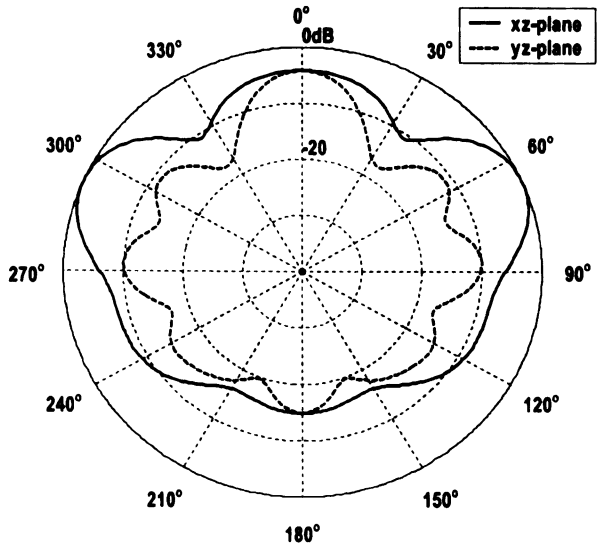

Figure 3.27 E_ϕ (xz-plane) and E_θ (yz-plane) patterns at 200 MHz

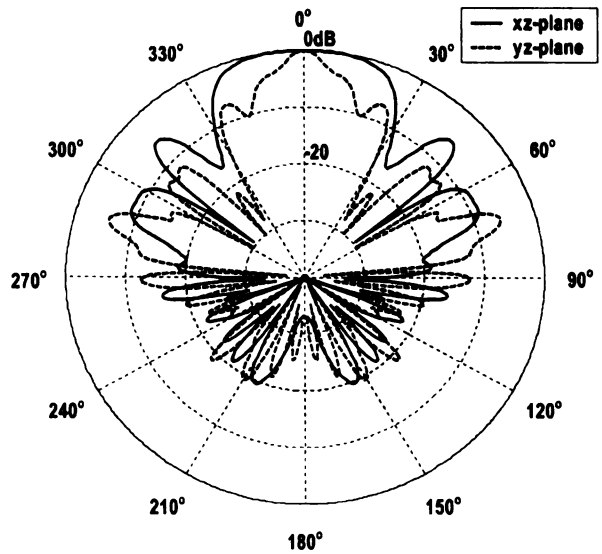

Figure 3.28 E_ϕ (xz-plane) and E_θ (yz-plane) patterns at 800 MHz

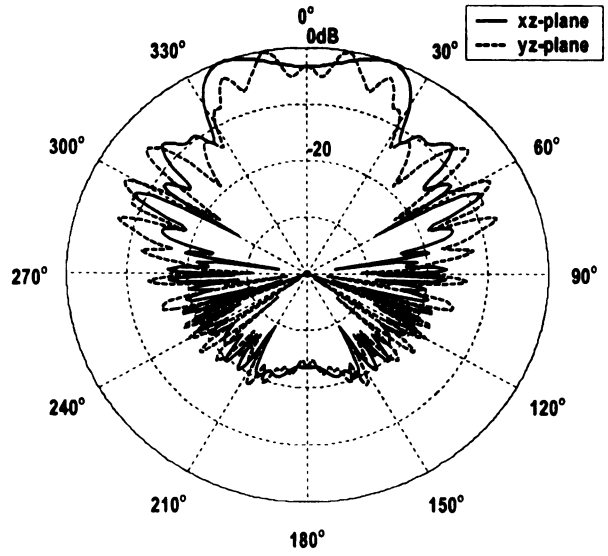

Figure 3.29 E_ϕ (xz-plane) and E_θ (yz-plane) patterns at 1400 MHz

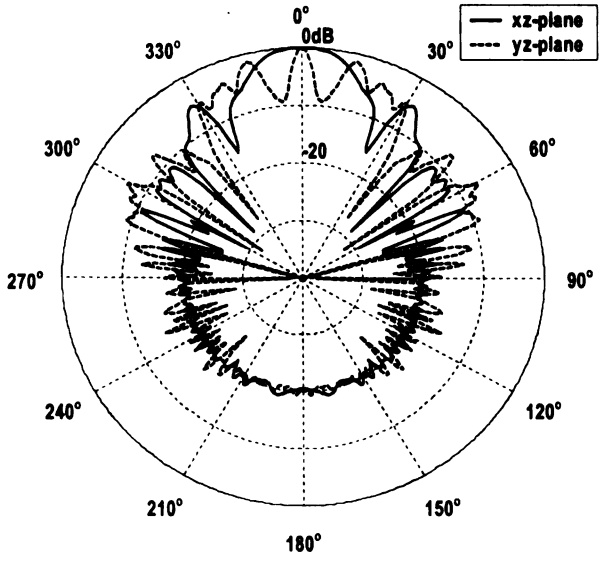

Figure 3.30 E_ϕ (xz-plane) and E_θ (yz-plane) patterns at 2000 MHz

3.1.2 Symmetric geometry with closed ends

For symmetric antenna with closed ends, the current may not be zero at the end. The input power is radiated as the current travels along the antenna. Some of the power may be lost in the load. In this case, the EM properties are affected by three factors: the shape of the antenna, the radius of the wire, and the load on the antenna. Several cases with different input impedance are studied (Table 3.1) to optimize the shape, the radii of the composed segments and the terminating load to the antenna. Since the ends are closed, only 6 points control the shape of the antenna.

3.1.2.1 Feed impedance of 600 Ohms

The optimized geometry is shown in Figure 3.31. Some segments with small radii near the ends cannot be displayed. The thickness of the line represents the radii of these segments, which vary from 0.00013 to 0.01123 m. The load to the end segment is 600 ohms which is equal to the characteristic impedance of the two-wire line.

Figure 3.32 shows that the real part of the input impedance is around 600 ohms and the imaginary part is around zero. The VSWR varies from 1 to 2.6 (Figure 3.33). In Figure 3.35, the efficiency is 100 percent over the frequency band because there is no current passes through the load. In figure 3.36, the power gain is higher than 2.2 dB over the frequency band and reaches to 12 dB at around 1600 MHz. The direction of maximum radiation is 90 degree at 200 MHz (Figure 3.37). It is in the desired direction at higher frequency as seen in figure 3.38 – 3.40.

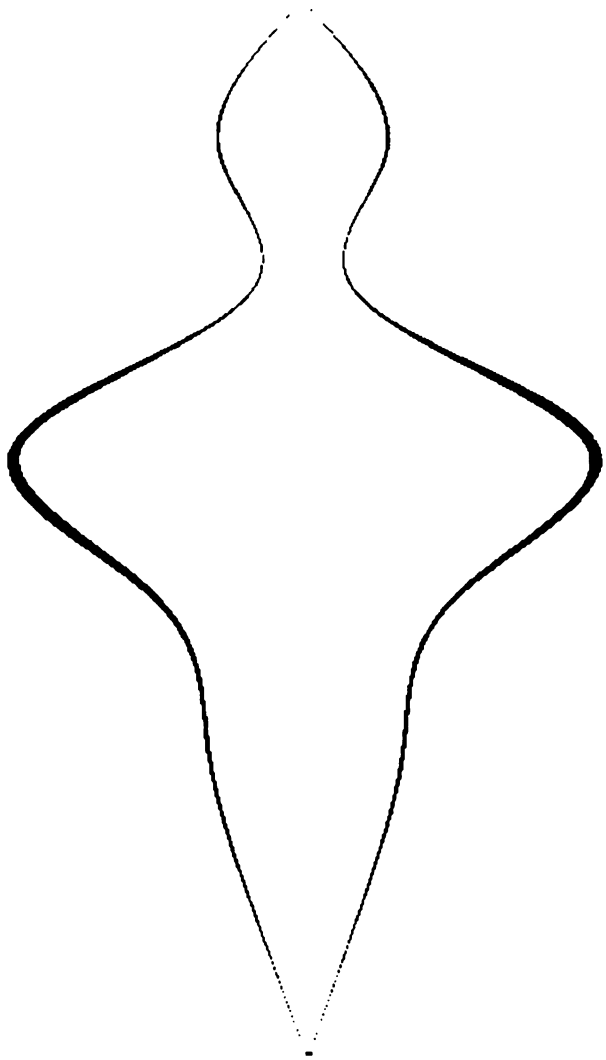

Figure 3.31 Antenna Geometry

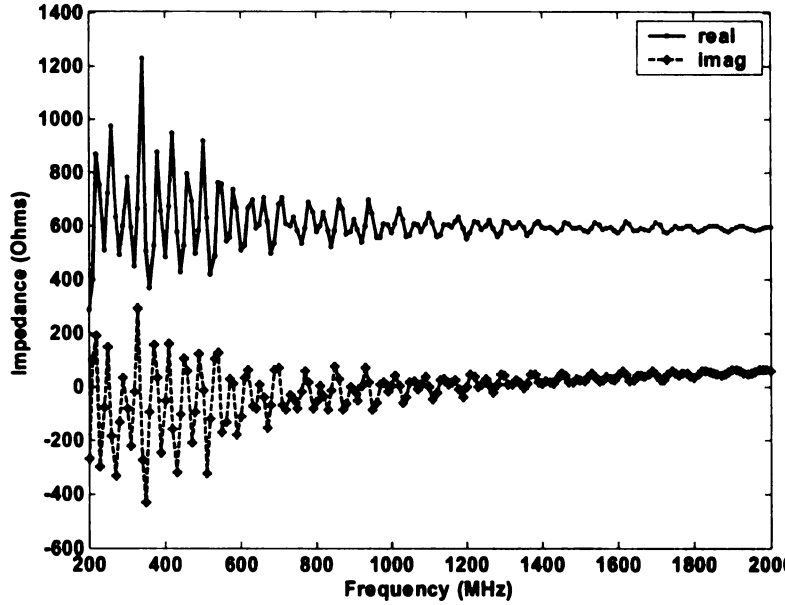

Figure 3.32 Input Impedance vs. Frequency

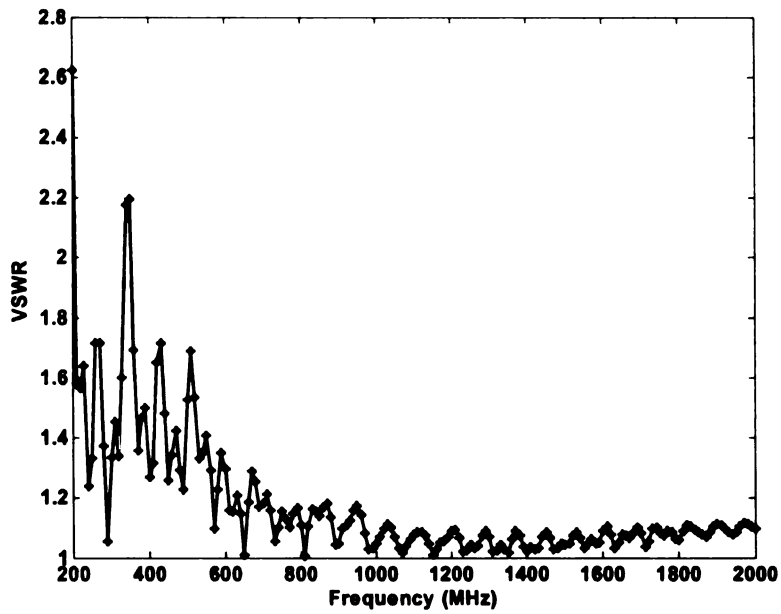

Figure 3.33 VSWR vs. Frequency

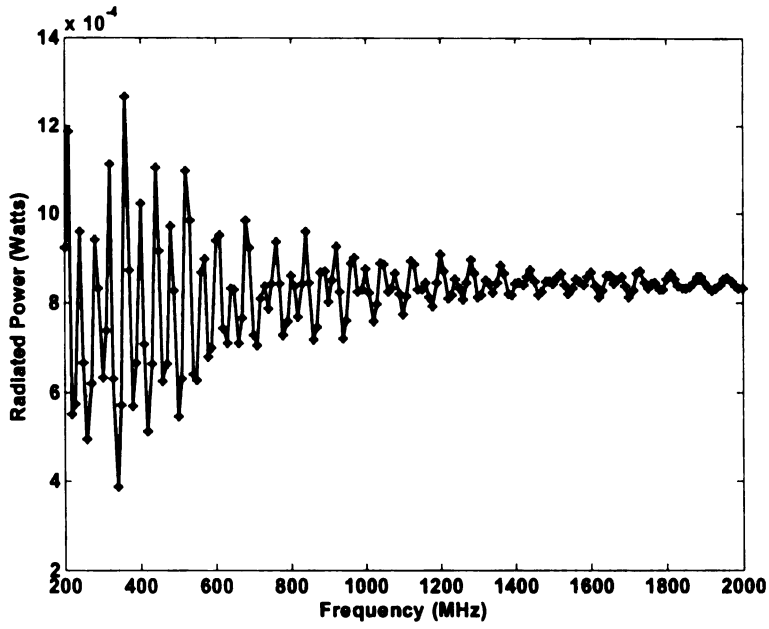

Figure 3.34 Radiated Power vs. Frequency

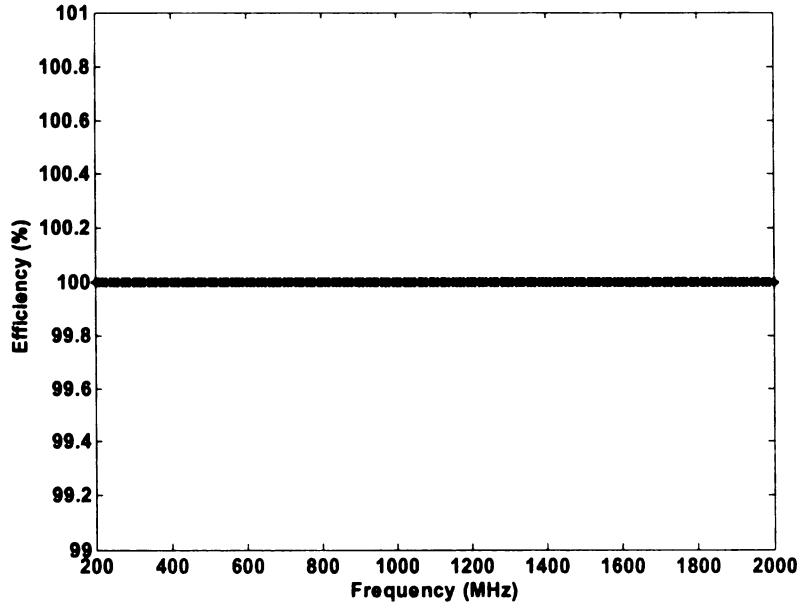

Figure 3.35 Efficiency vs. Frequency

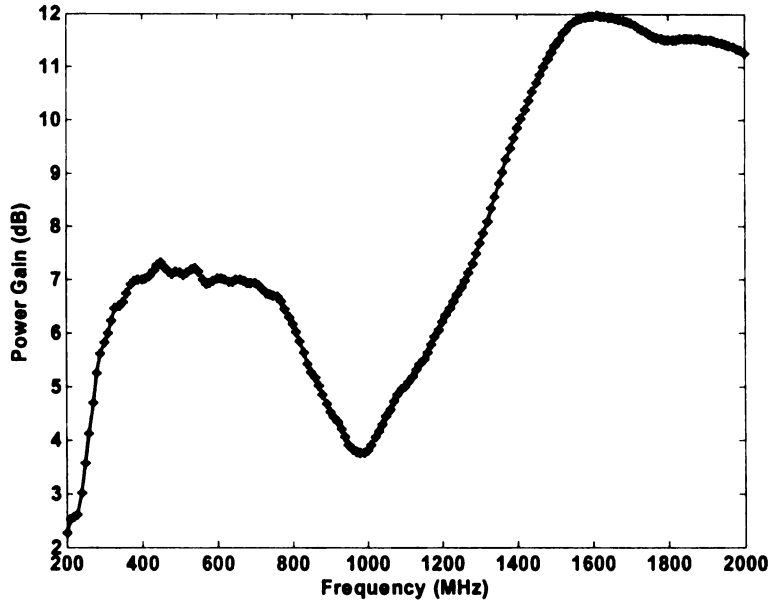

Figure 3.36 Power Gain vs. Frequency

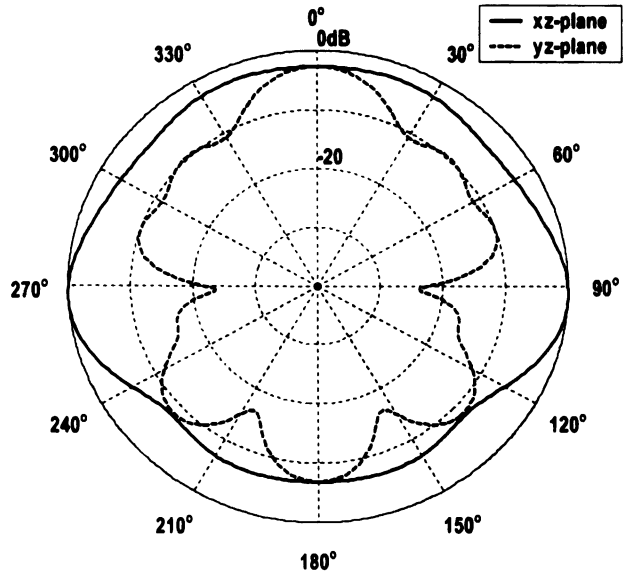

Figure 3.37 E_ϕ (xz-plane) and E_θ (yz-plane) patterns at 200 MHz

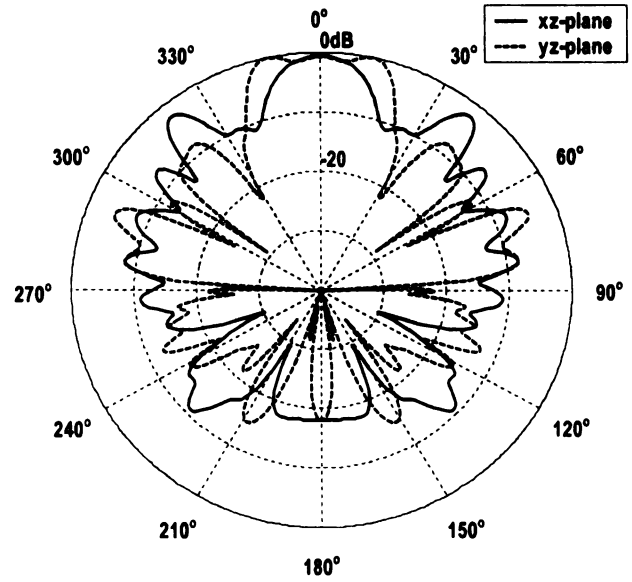

Figure 3.38 E_ϕ (xz-plane) and E_θ (yz-plane) patterns at 800 MHz

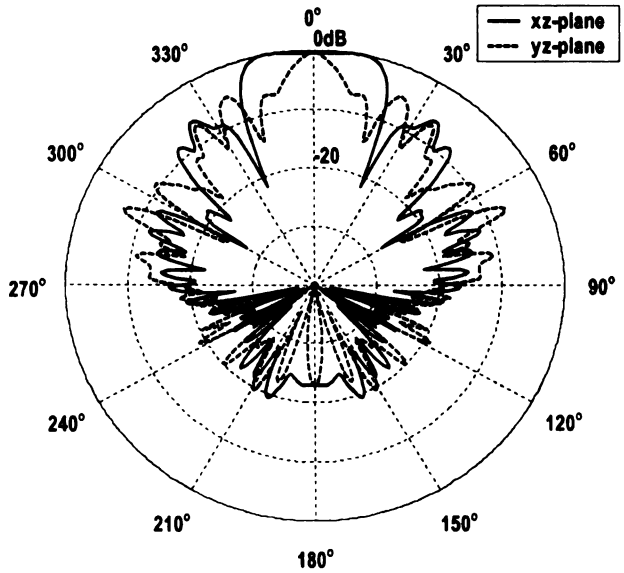

Figure 3.39 E_ϕ (xz-plane) and E_θ (yz-plane) patterns at 1400 MHz

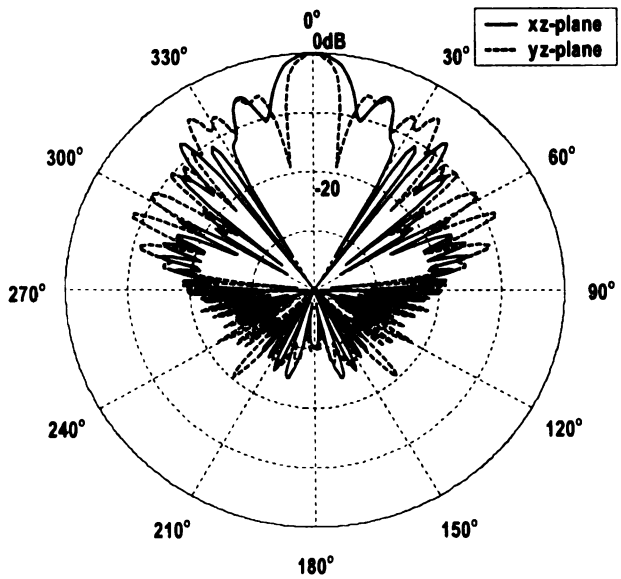

Figure 3.40 E_ϕ (xz-plane) and E_θ (yz-plane) patterns at 2000 MHz

3.1.2.2 Feed impedance of 300 Ohms

GA-NEC optimizes the shape of the antenna and constrains the radii of the composed segments in a specified range of 0.002 – 0.01 m. Figure 3.41 shows the optimized result in this case. The radii vary from 0.002 – 0.009 m. The optimal load to the end is 600 ohms.

The real part of input impedance becomes stable at 300 ohms and the imaginary part tends to zero as frequency increases (Figure 3.42). Figure 3.43 shows that the VSWR is from 1.03 to 3.85. There is a VSWR burst around frequency 250 MHz. This is because GA-NEC only evaluates the value at integer of hundreds during the optimization process. The radiated power varies at different frequencies (Figure 3.44). Figure 3.45 shows the power radiation efficiency is 100 percent through the study frequency band. The power gain along the length of the antenna is between 4.88 and 11.62 dB (Figure 3.46). From Figure 3.47 to 3.50, it can be seen that this antenna become more directive at higher frequency. In figure 3.47, there are three big side lobes in yz-plane the antenna there is not directive in xz-plane. The side lobes getting smaller at higher frequency indicate that the antenna is more directive.

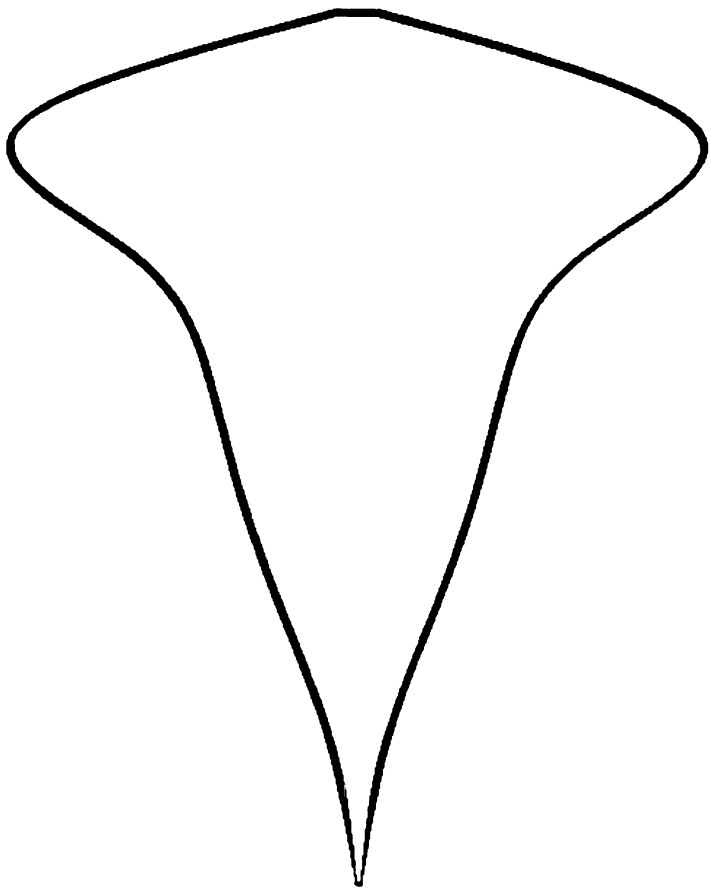

Figure 3.41 Antenna Geometry

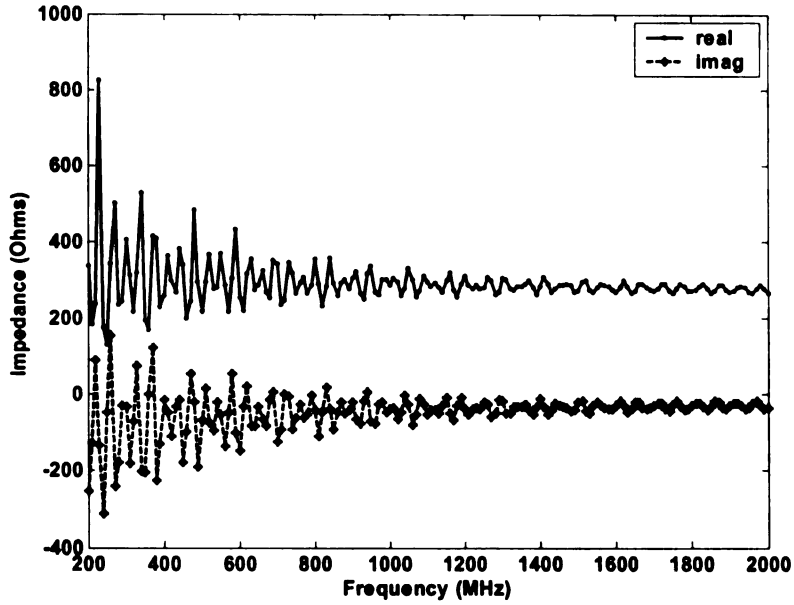

Figure 3.42 Input Impedance vs. Frequency

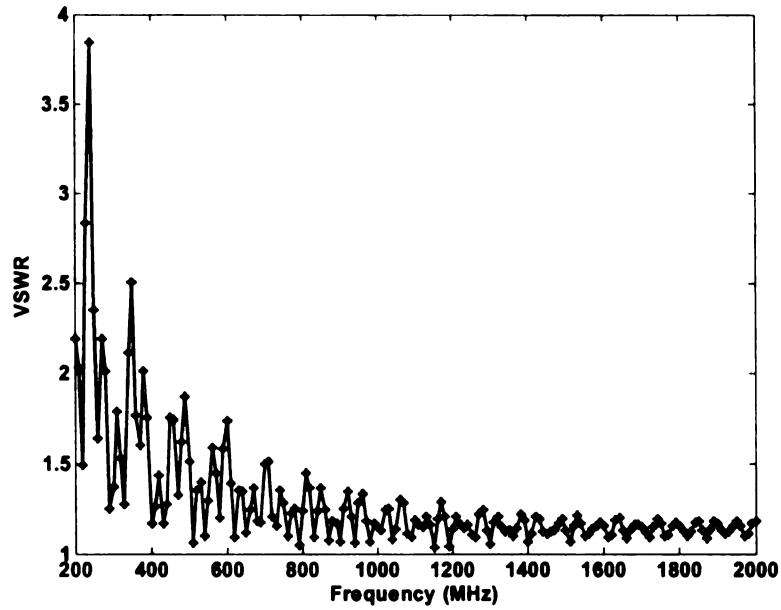

Figure 3.43 VSWR vs. Frequency

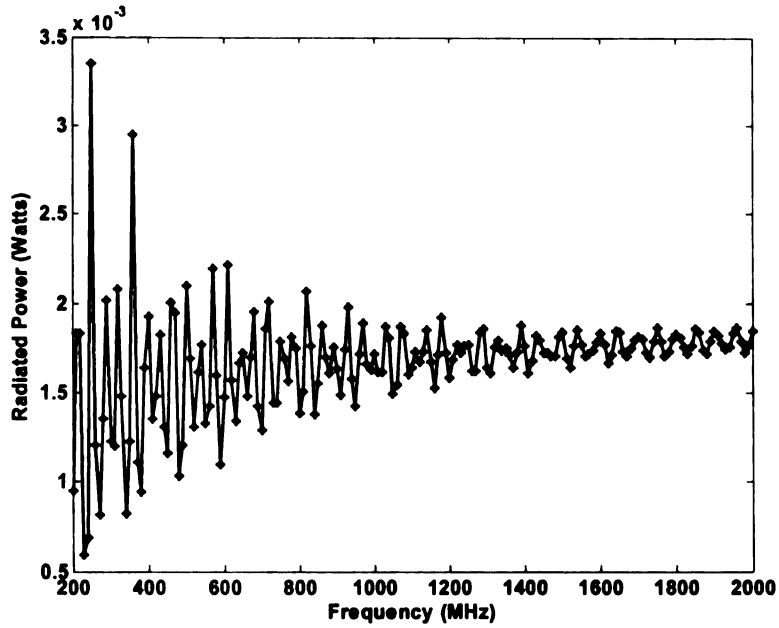

Figure 3.44 Radiated Power vs. Frequency

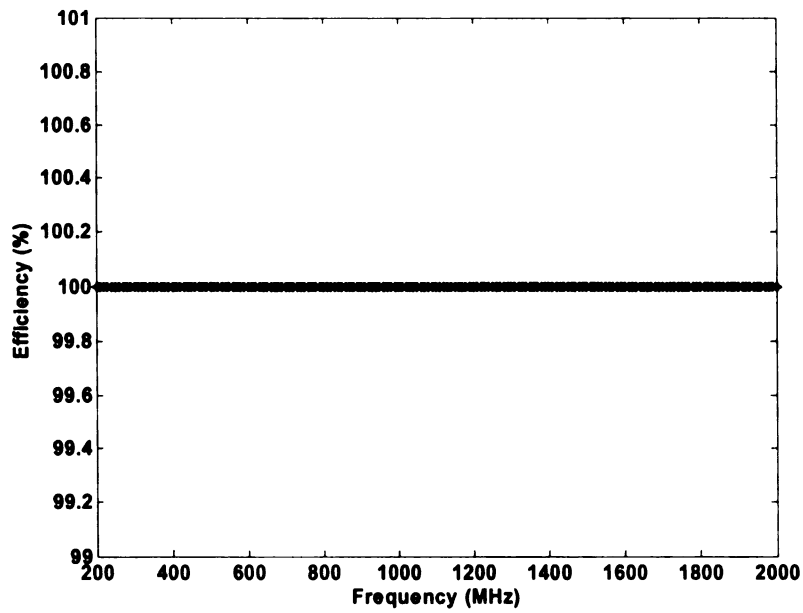

Figure 3.45 Efficiency vs. Frequency

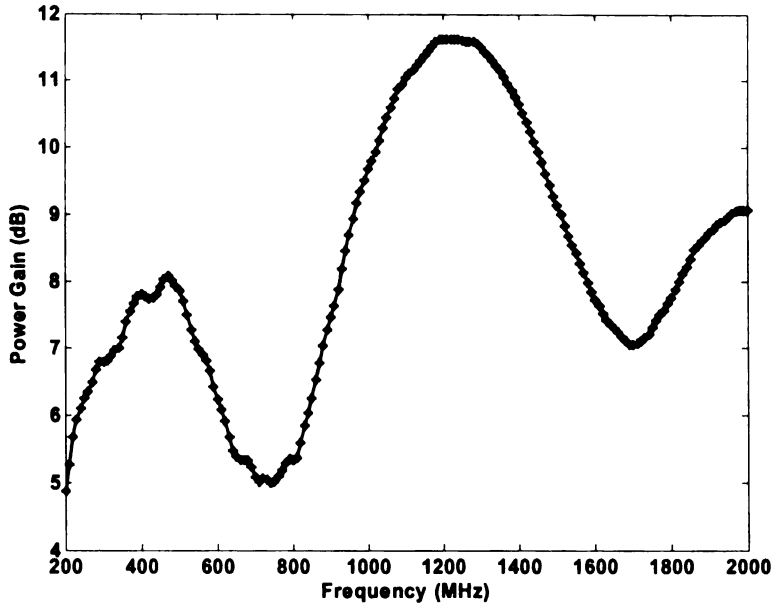

Figure 3.46 Power Gain vs. Frequency

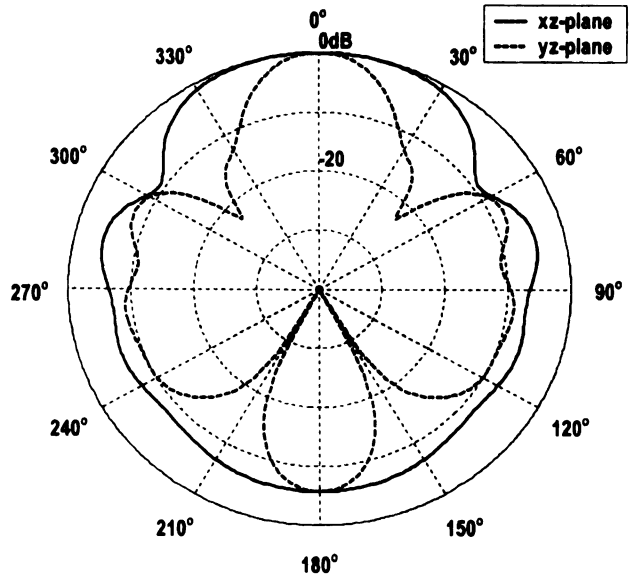

Figure 3.47 E_ϕ (xz-plane) and E_θ (yz-plane) patterns at 200 MHz

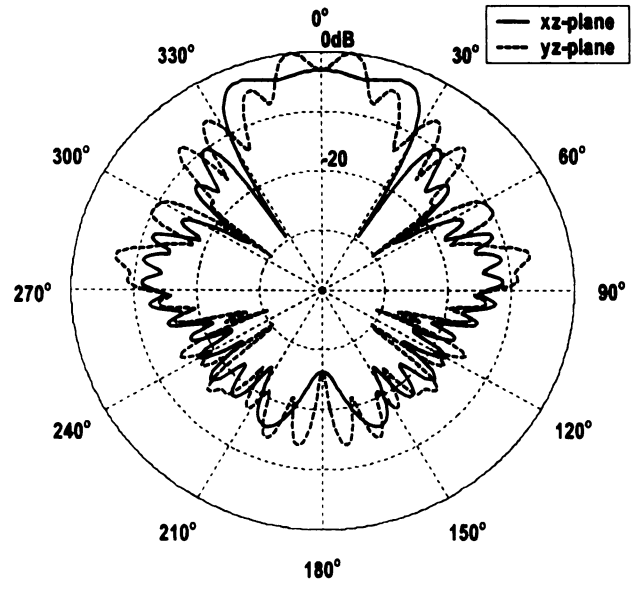

Figure 3.48 E_ϕ (xz-plane) and E_θ (yz-plane) patterns at 800 MHz

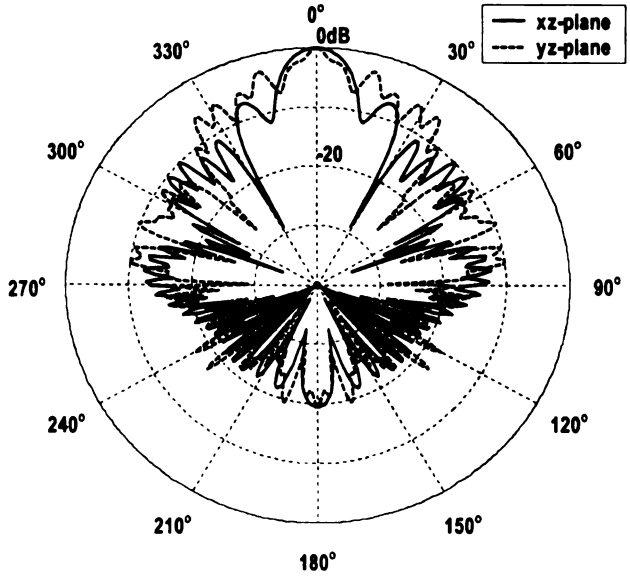

Figure 3.49 E_ϕ (xz-plane) and E_θ (yz-plane) patterns at 1400 MHz

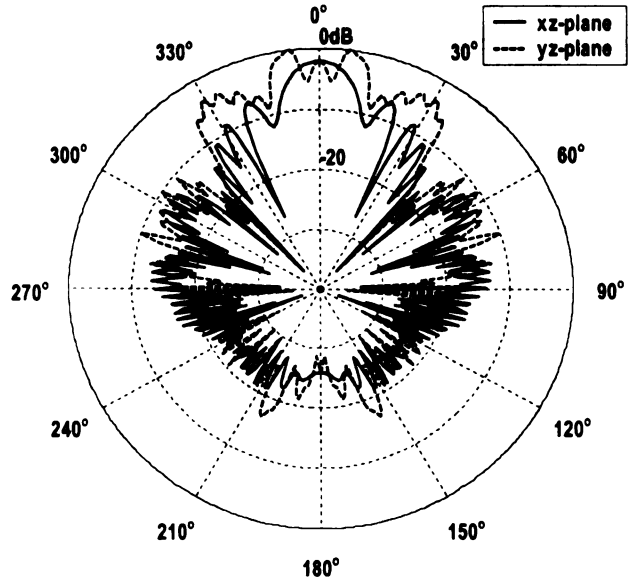

Figure 3.50 E_ϕ (xz-plane) and E_θ (yz-plane) patterns at 2000 MHz

3.1.2.3 Feed impedance of 150 Ohms

In this case, the radii of the segments of the antenna are set to be constant. The GA-NEC optimizes the value in a range of 0.001 – 0.016 m. The optimized geometry is shown in figure 3.51. The segments that made the wires have constant radii of 0.005 m. The load to the ends is 600 ohms.

Figure 3.52 shows that the real part of the input impedance is around 150 ohms and the imaginary part is around -50 ohms. The VSWR values are in a range of 1.15 – 2.8, but most of them are larger than 1.4 (Figure 3.53). The radiated power increases at higher frequency (Figure 3.54). The efficiency is 100 percent (Figure 3.55). It can be seen that there are three big dips in the power gain at around 450, 950 and 1450 MHz (Figure 3.56). The worst one is around 950 MHz at which there is almost no radiation along the antenna. Figure 3.57 shows that the antenna has low directivity at lower frequency. There is a subtle improvement at higher frequency.

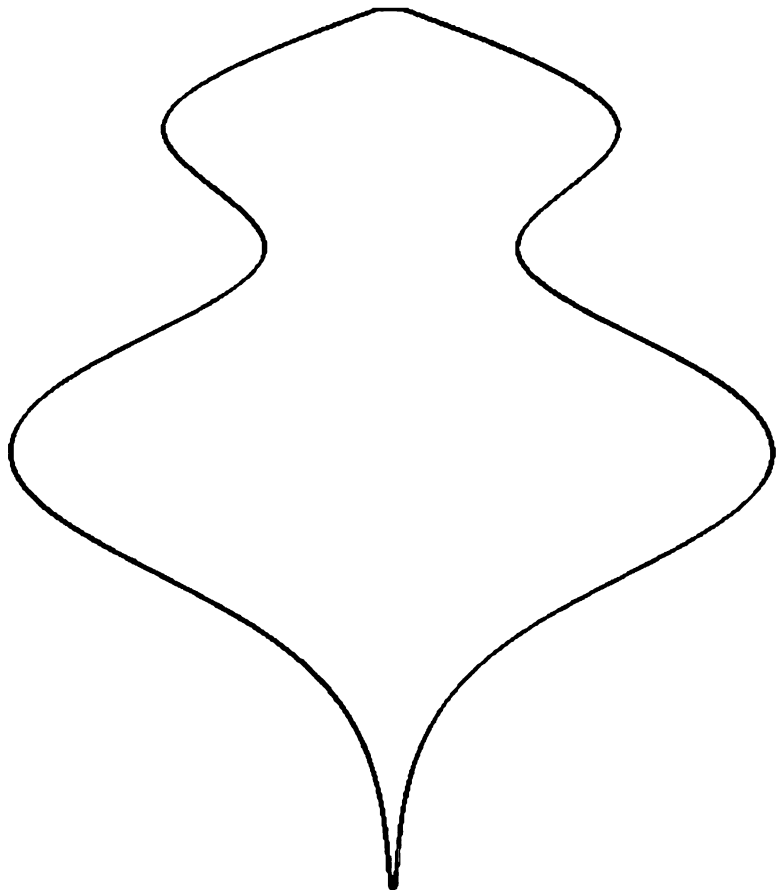

Figure 3.51 Antenna Geometry

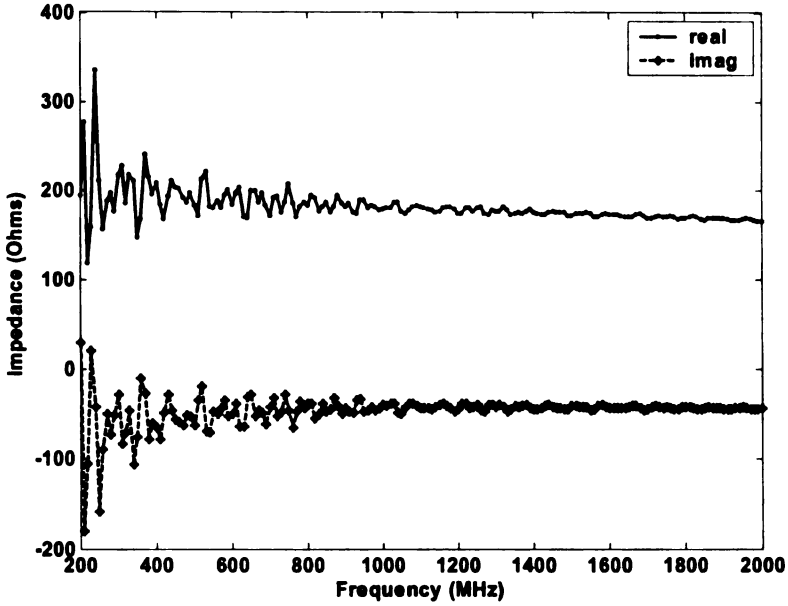

Figure 3.52 Input impedance vs. Frequency

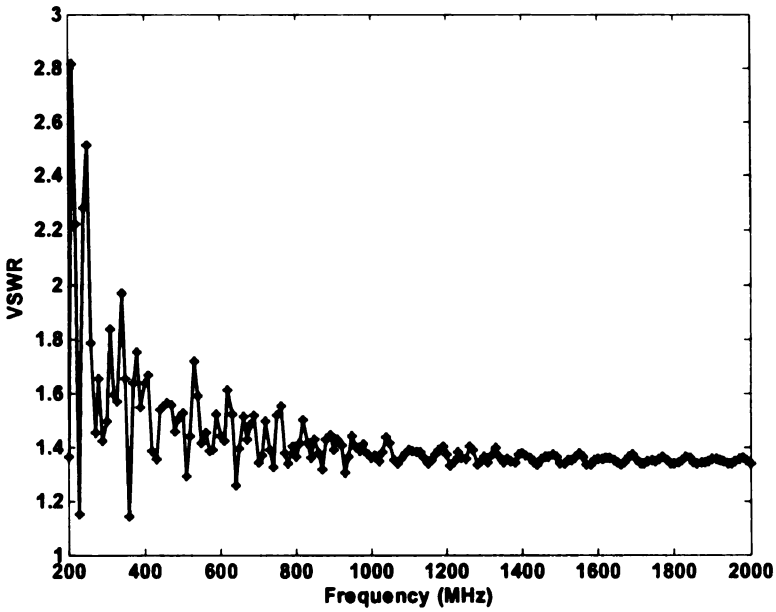

Figure 3.53 VSWR vs. Frequency

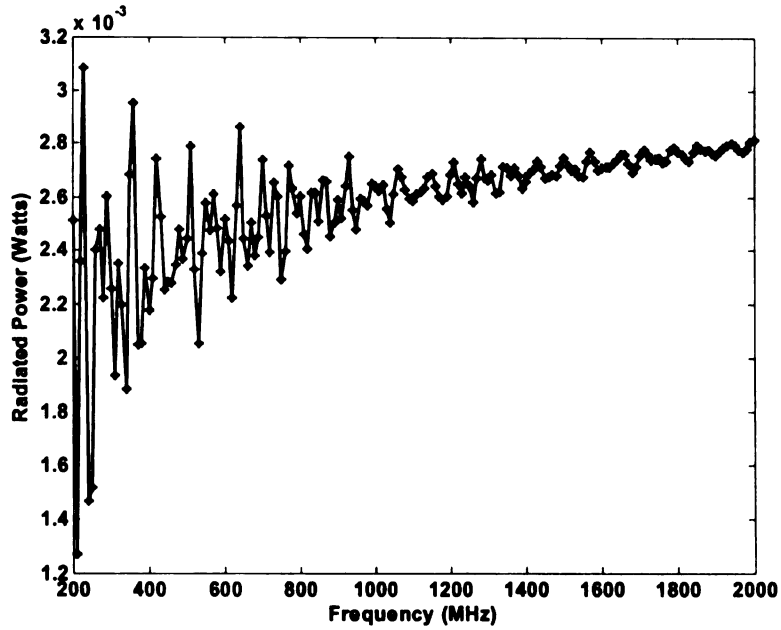

Figure 3.54 Radiated Power vs. Frequency

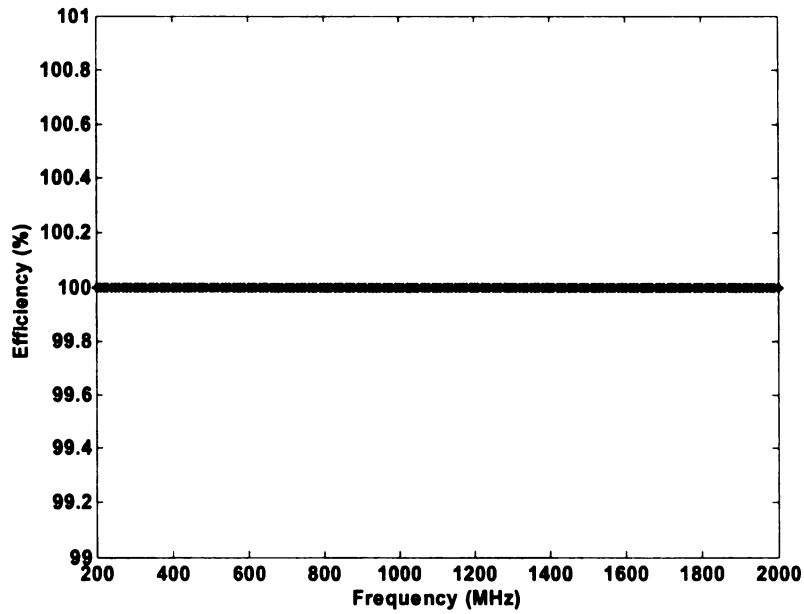

Figure 3.55 Efficiency vs. Frequency

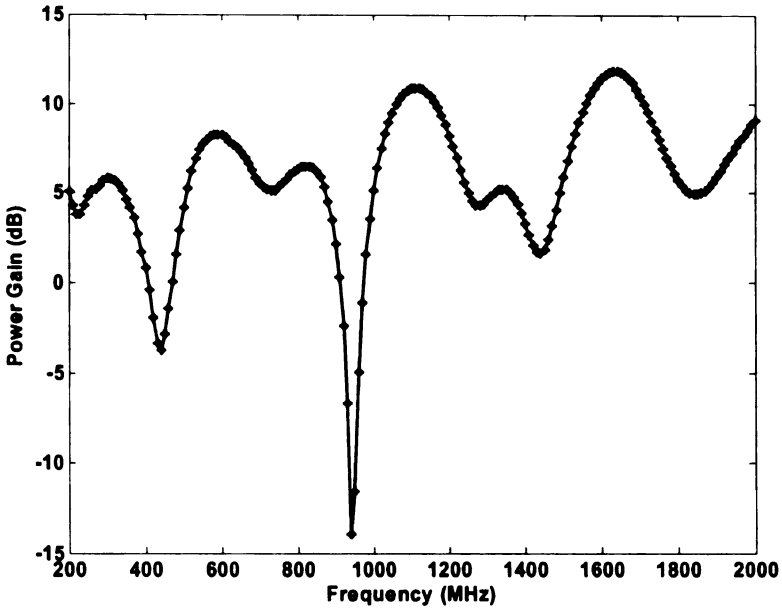

Figure 3.56 Power Gain vs. Frequency

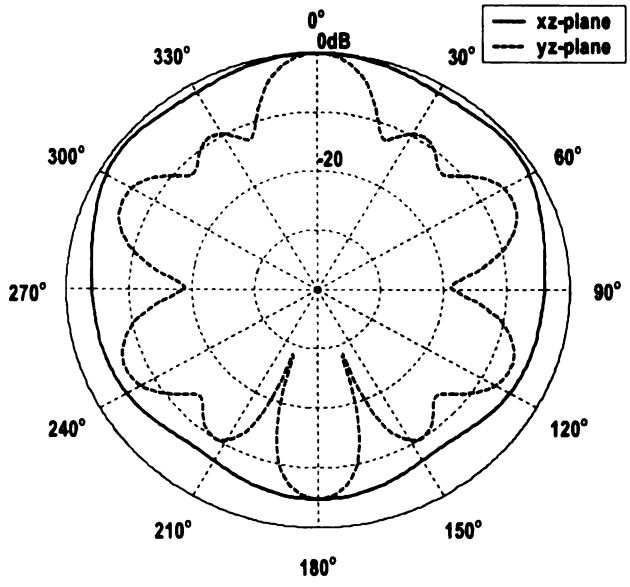

Figure 3.57 E_ϕ (xz-plane) and E_θ (yz-plane) patterns at 200 MHz

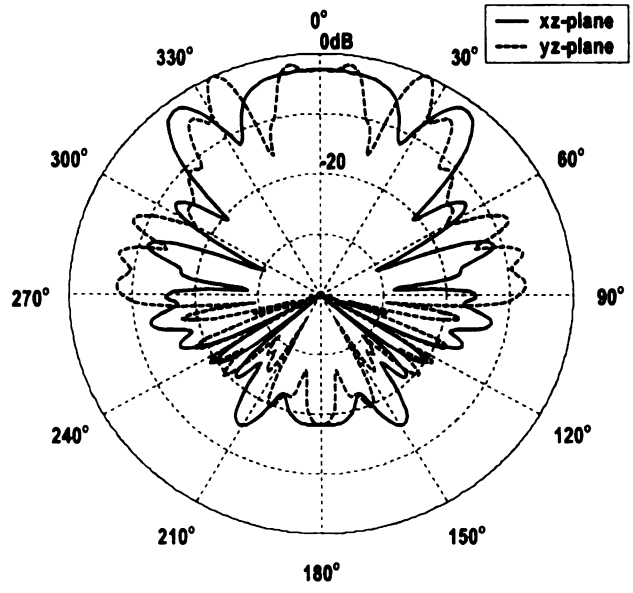

Figure 3.58 E_ϕ (xz-plane) and E_θ (yz-plane) patterns at 800 MHz

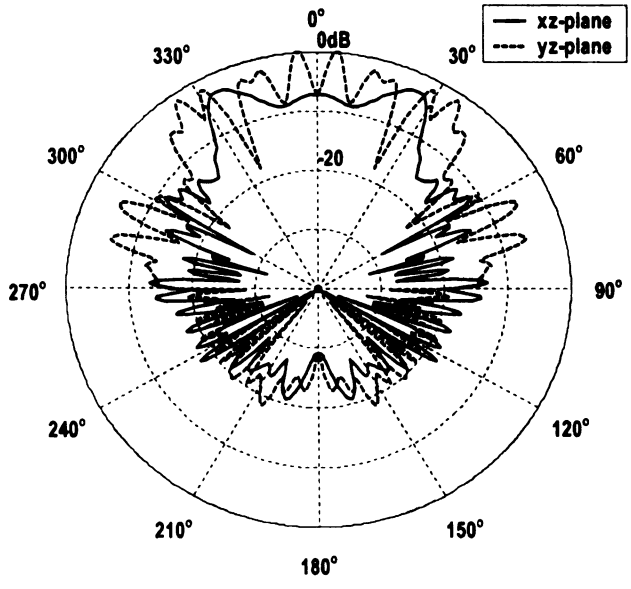

Figure 3.59 E_ϕ (xz-plane) and E_θ (yz-plane) patterns at 1400 MHz

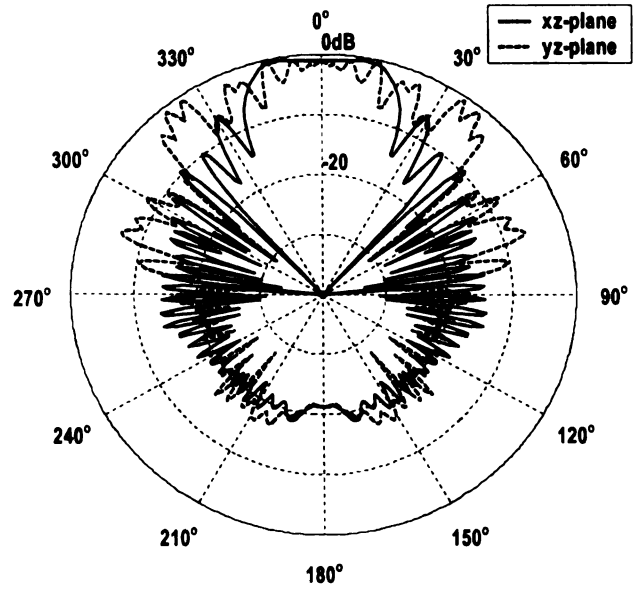

Figure 3.60 E_ϕ (xz-plane) and E_θ (yz-plane) patterns at 2000 MHz

3.2 Antennas with asymmetric Geometry

As shown in table 3.1, 14 points in open ends cases and 12 in closed ends cases define the shape of the asymmetric antenna. More binary strings are required than in the symmetric case to code these parameters in GA-NEC. The length of the chromosome to represent an individual is almost twice of that in symmetric cases. As discussed in chapter 2, this gives more diversity, and the program searches the optimal solution in a larger domain. Therefore, a bigger number of individuals in the initial population and more running time are needed. In this study, the initial population is set to 200 and the maximum number of generations is 100.

3.2.1 Antennas with open ends

3.2.1.1 Feed impedance of 600 Ohms

The radii of the segments are calculated with equation 2.2. The characteristic impedance of the two wires is a constant of 600 ohms. Figure 3.61 shows the geometry of the optimized antenna. The thickness of the line is proportional to the radius of the segments ranging from 0.00013 to 0.01189 m. Some segments with small radii near the ends cannot be displayed in Figure 3.61.The real part of the input impedance varies around 600 ohms and the imaginary part varies around 0 ohms (Figure 3.62). The input VSWR is below 2.8 (Figure 3.63) and the efficiency is 100 percent over the frequency band (Figure 3.65). The radiated power versus frequency is shown in figure 3.64. In Figure 3.66, the antenna has good power gains. The direction of the maximum radiation is around 10 degrees away from the desired direction at 800 MHz (Figure 3.68) and 15 degrees away at 2000 MHz (Figure 3.70). The antenna pattern is

not symmetric. In Figure 3.68 - 3.69, the direction of the maximum radiation is close to the desired direction (along the length of the antenna).

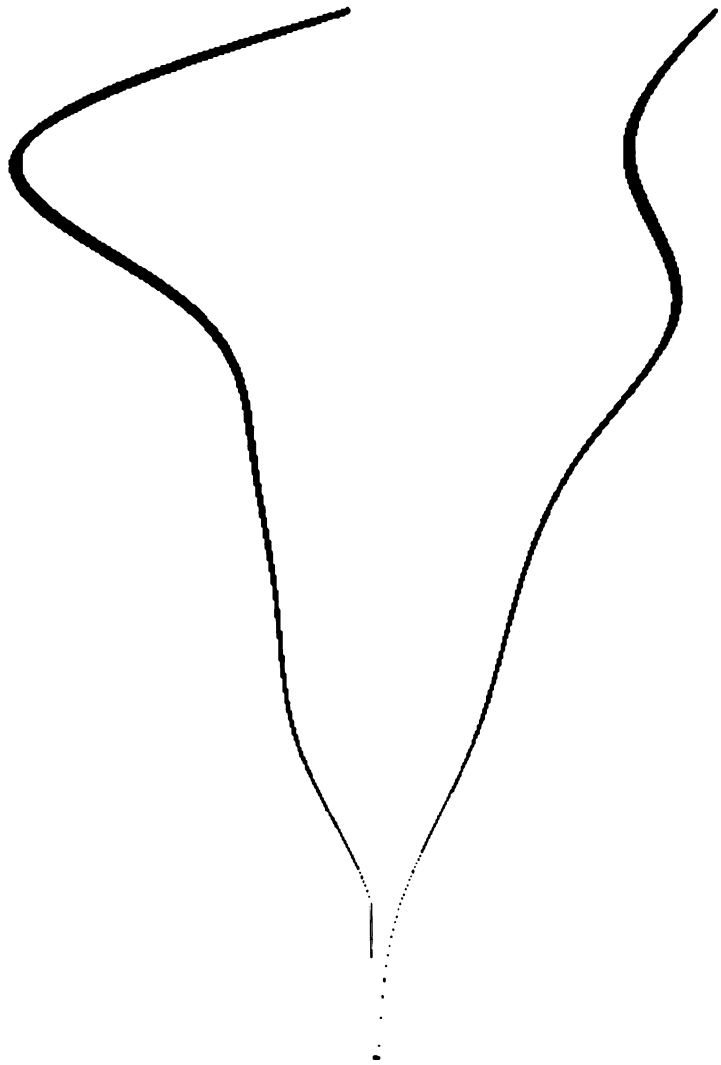

Figure 3.61 Antenna Geometry

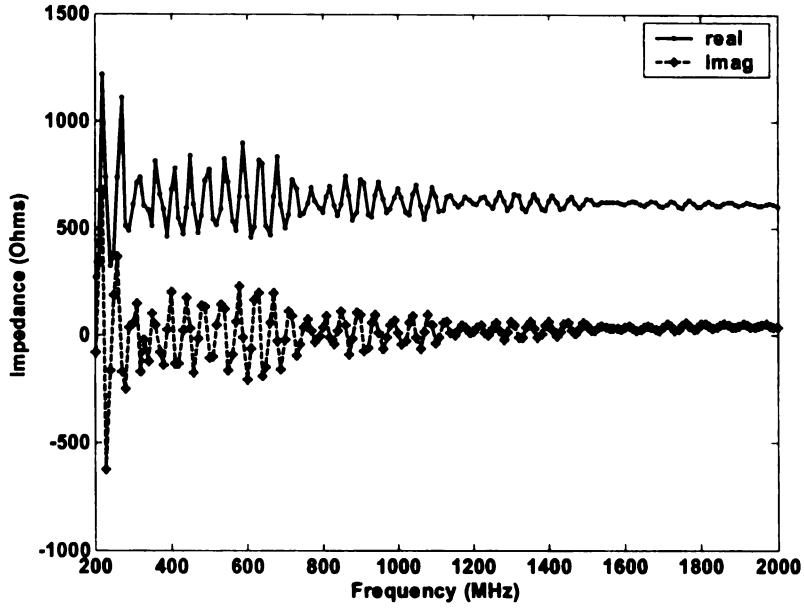

Figure 3.62 Input Impedance vs. Frequency

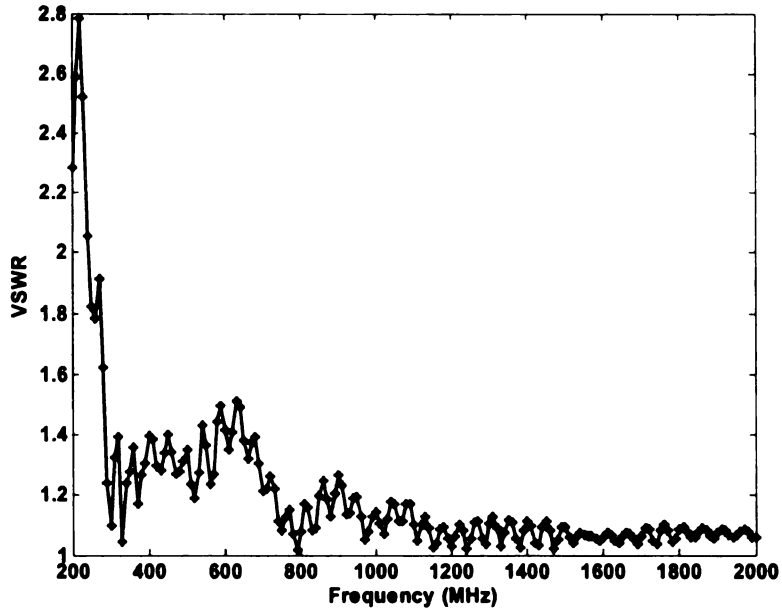

Figure 3.63 VSWR vs. Frequency

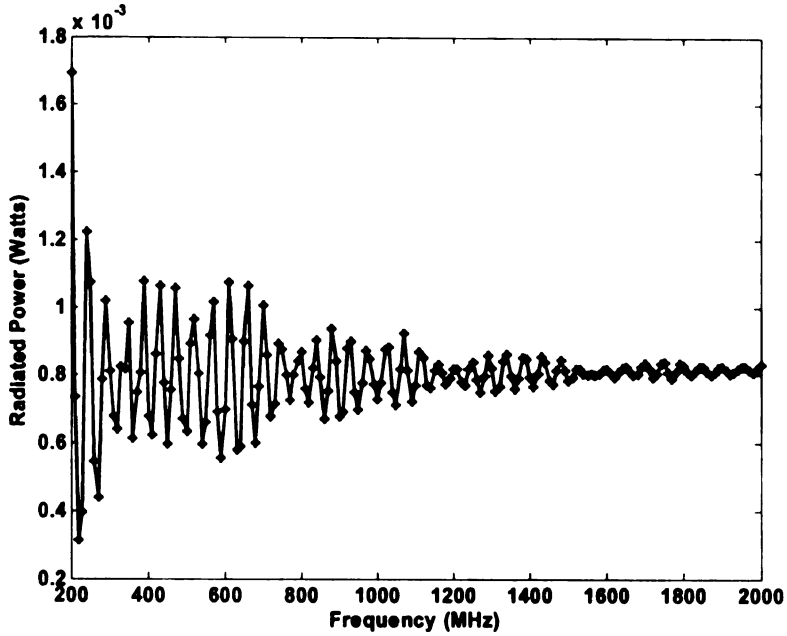

Figure 3.64 Radiated Power vs. Frequency

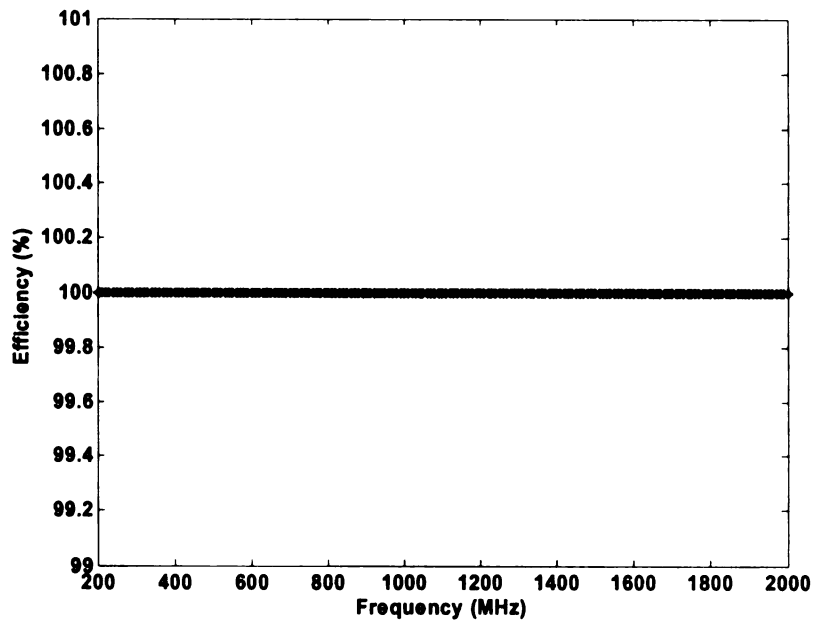

Figure 3.65 Efficiency vs. Frequency

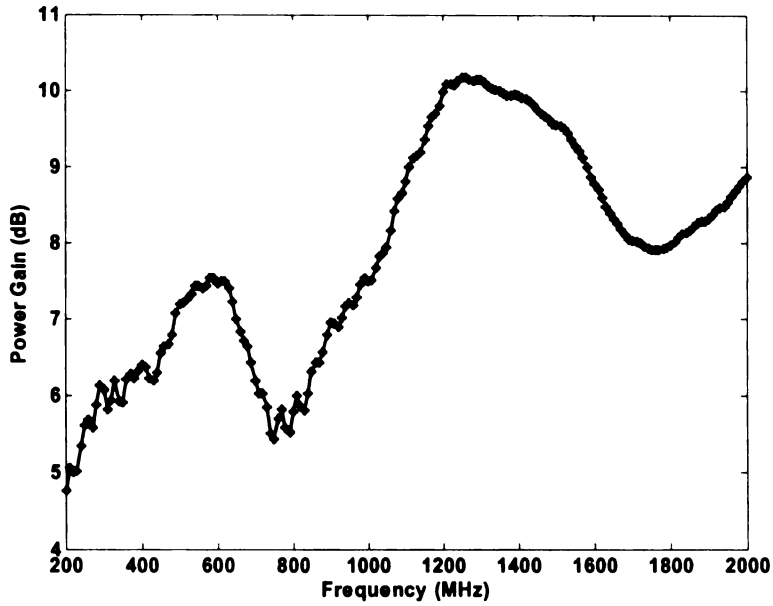

Figure 3.66 Power Gain vs. Frequency

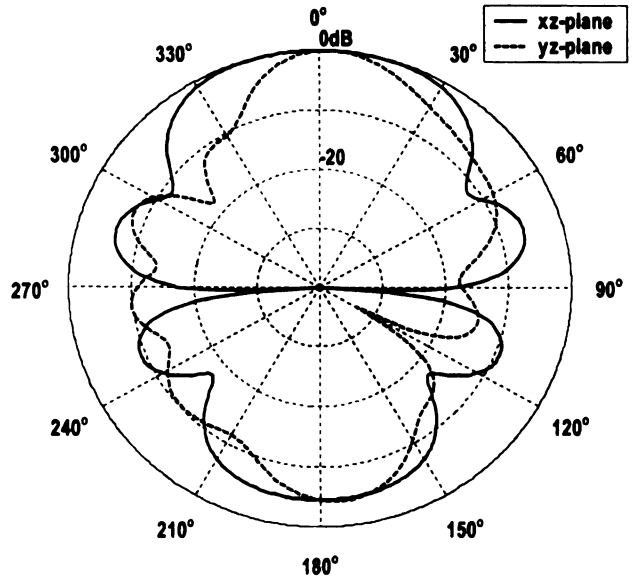

Figure 3.67 E_ϕ (xz-plane) and E_θ (yz-plane) patterns at 200 MHz

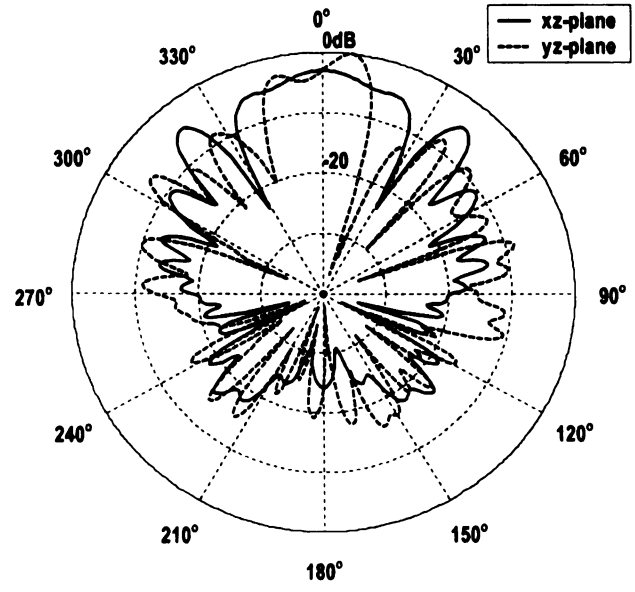

Figure 3.68 E_ϕ (xz-plane) and E_θ (yz-plane) patterns at 800 MHz

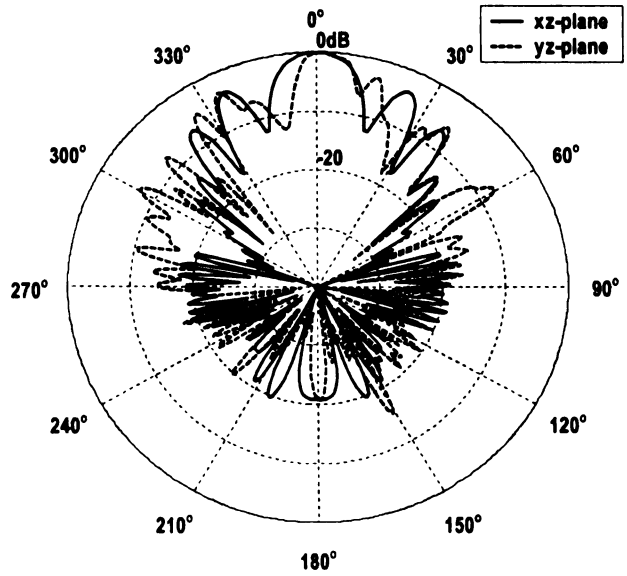

Figure 3.69 E_ϕ (xz-plane) and E_θ (yz-plane) patterns at 1400 MHz

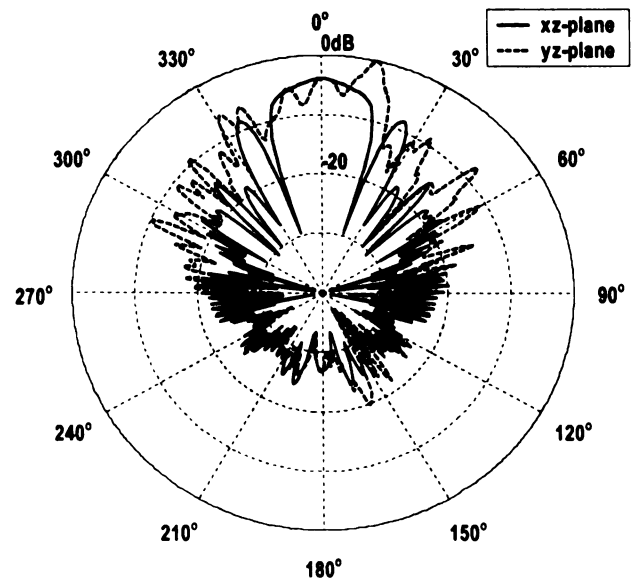

Figure 3.70 E_ϕ (xz-plane) and E_θ (yz-plane) patterns at 2000 MHz

3.2.1.2 Feed impedance of 300 Ohms

Figure 3.71 shows the optimized antenna shape. The thickness of the wire is proportional to the radius. Most of the radii of segments of the antenna are 0.005 m except for a few segments near the feeding point that have radii values varying from 0.00165 to 0.005 m. Figure 3.72 shows the input impedance to the antenna. The real part of the impedance varies around 300 ohms (the desired impedance), and the imaginary part has the mean value about zero. The input VSWR ranges from around 1 to less than 2.6 (Figure 3.73). Figure 3.74 shows the radiated power as a function of frequency. The radiation efficiency is 100 percent over the frequency band (Figure 3.75). In figure 3.76, all power gains along the length of the antenna are above 4 dB. There are two small dips at around 650 MHz and 1500 MHz. Figure 3.77 indicates that this antenna is more directive that the previous one at low frequency in the desired direction. But, it is not as good at higher frequency (Figure 3.78 – 80). The direction of the maximum value is around 10 degree away from the desired one.

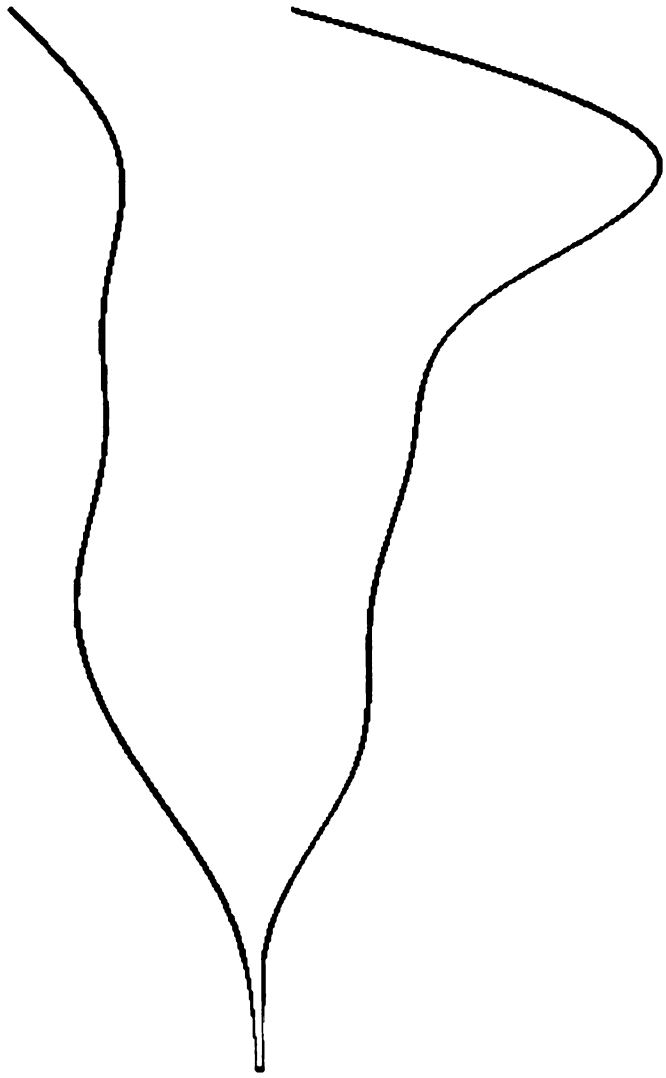

Figure 3.71 Antenna Geometry

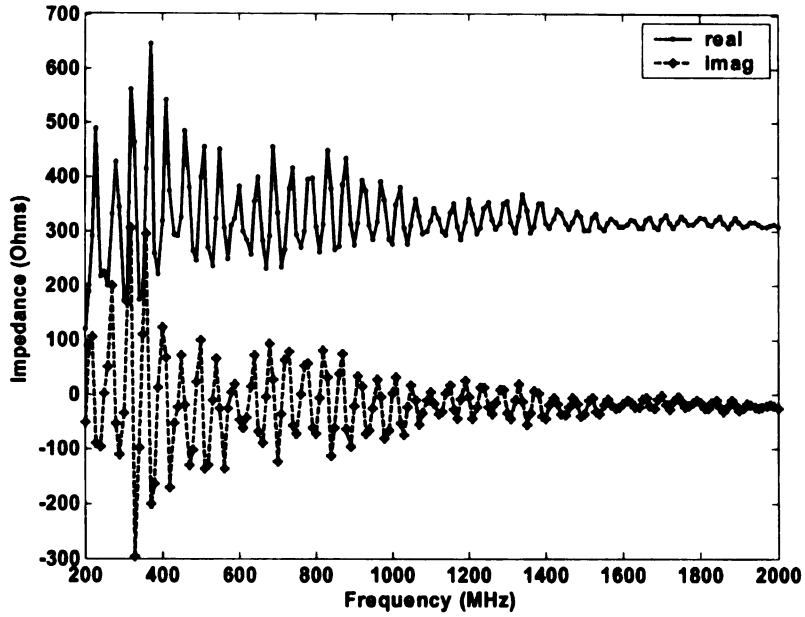

Figure 3.72 Input Impedance vs. Frequency

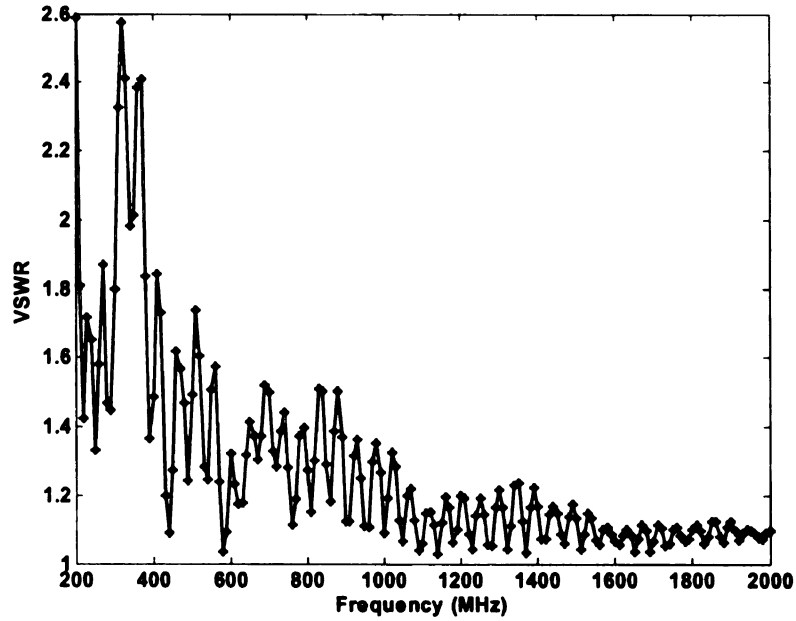

Figure 3.73 VSWR vs. Frequency

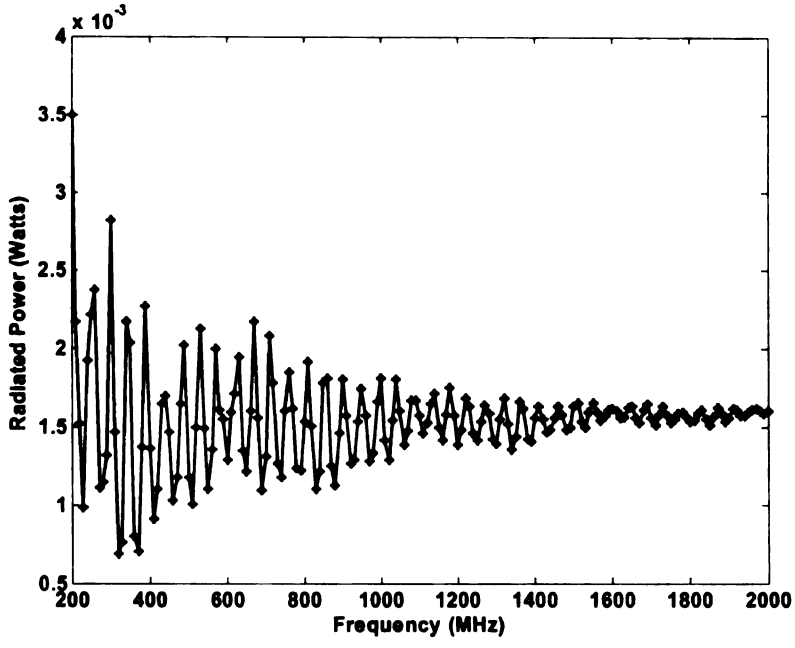

Figure 3.74 Radiated Power vs. Frequency

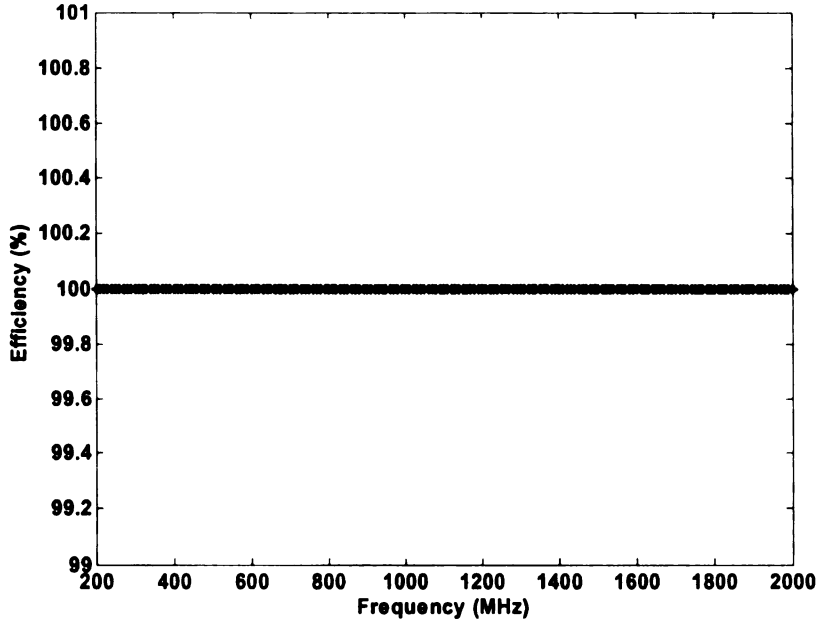

Figure 3.75 Efficiency vs. Frequency

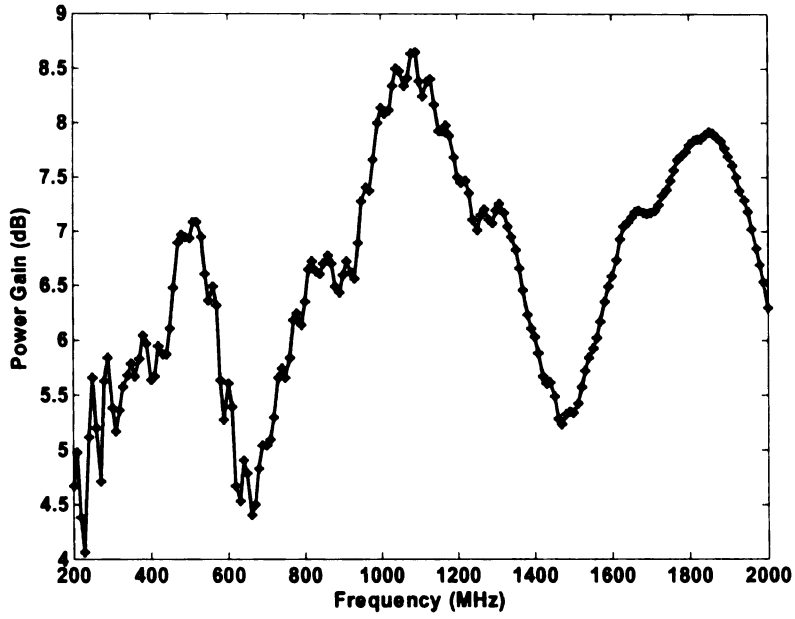

Figure 3.76 Power Gain vs. Frequency

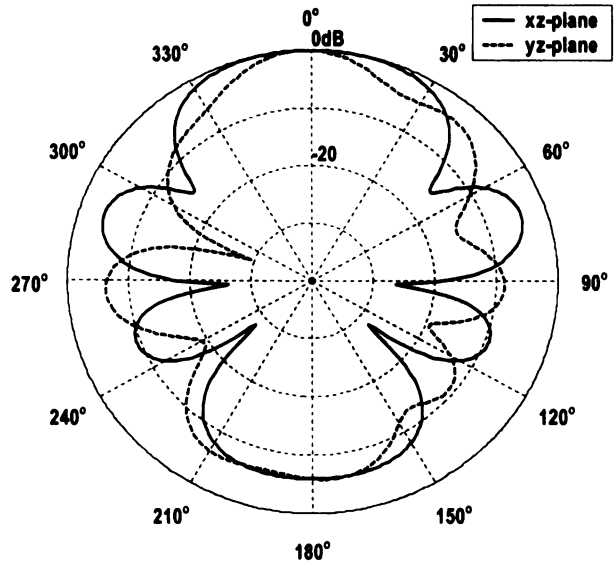

Figure 3.77 E_ϕ (xz-plane) and E_θ (yz-plane) patterns at 200 MHz

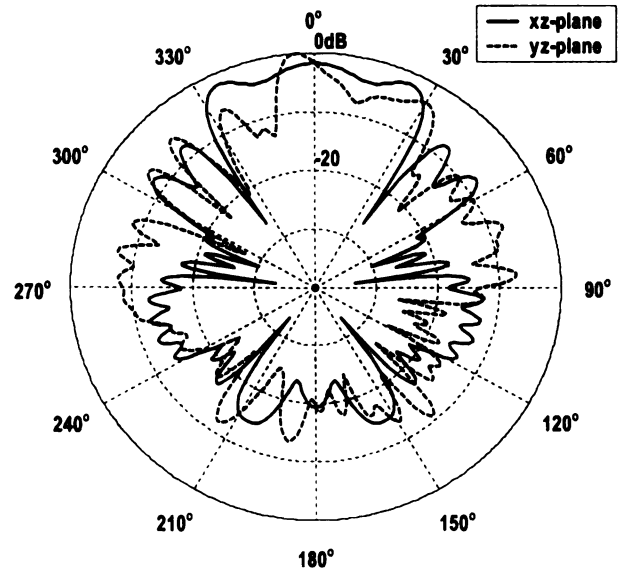

Figure 3.78 E_ϕ (xz-plane) and E_θ (yz-plane) patterns at 800 MHz

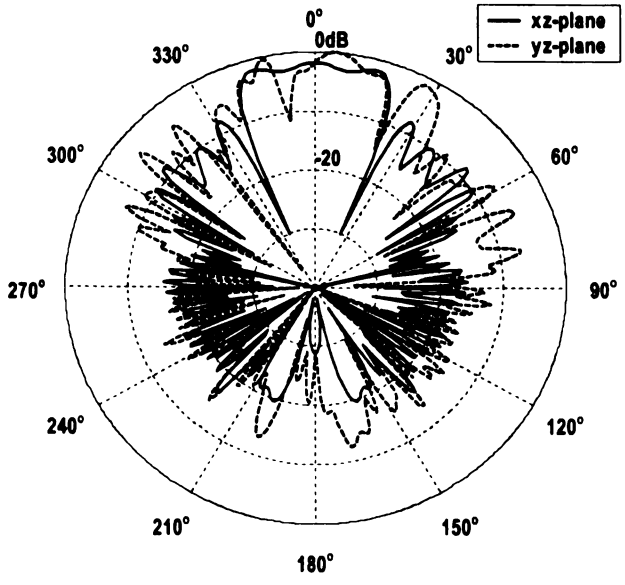

Figure 3.79 E_ϕ (xz-plane) and E_θ (yz-plane) patterns at 1400 MHz

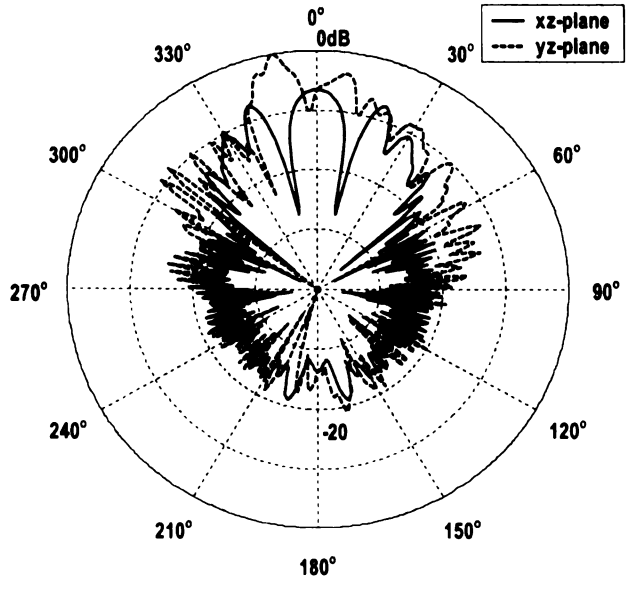

Figure 3.80 E_ϕ (xz-plane) and E_θ (yz-plane) patterns at 2000 MHz

3.2.1.3 Feed impedance of 150 Ohms

The range of the radii of all the segments is from 0.0005 to 0.01 m. The optimized value is 0.00864 m. Figure 3.81 shows the shape of the antenna. In Figure 3.82, the input impedance changes as a function of frequency. The VSWR is in a range of 1.7 – 2.65 (Figure 3.83). In figure 3.84, more power is radiated as the frequency increases. The radiation efficiency is 100 percent over the frequency range (figure 3.85). All of the power gains of the antenna are above 4.8 dB over the whole frequency band (Figure 3.86). There is a dip at around 750 MHz and a peak at 1300 MHz. The maximum radiation in the length of the antenna direction is shown in Figure 3.87. It is 20 degrees away in the xz-plane at 800 MHz (Figure 3.88) and 10 degrees away in yz-plane (Figure 3.89). At 2 GHz, the maximum radiation is 15 degrees away in the yz-plane.

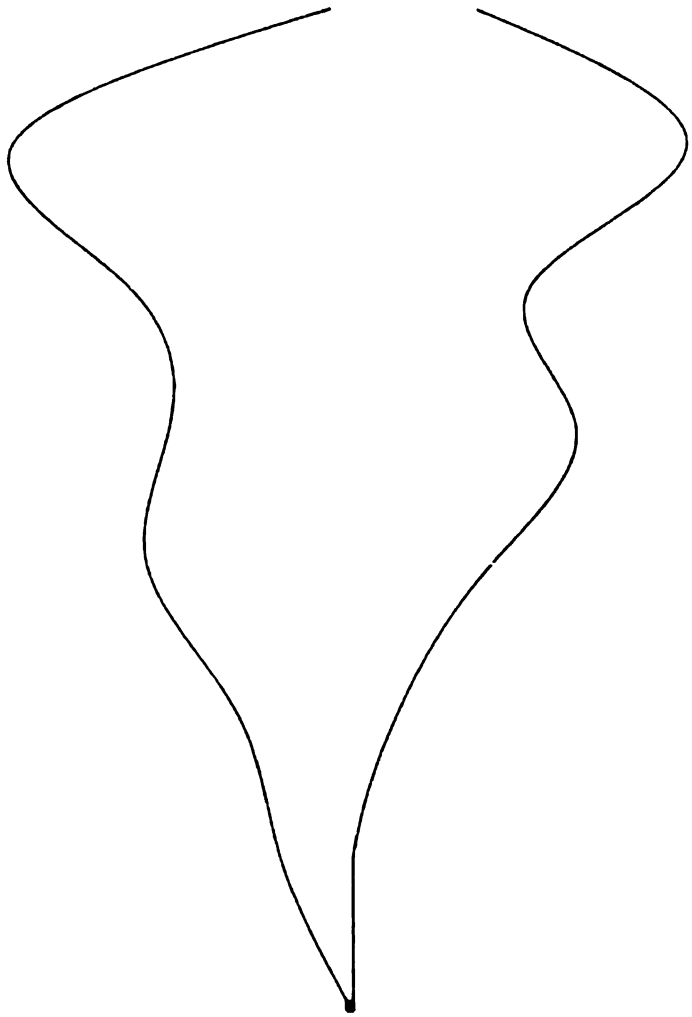

Figure 3.81 Antenna Geometry

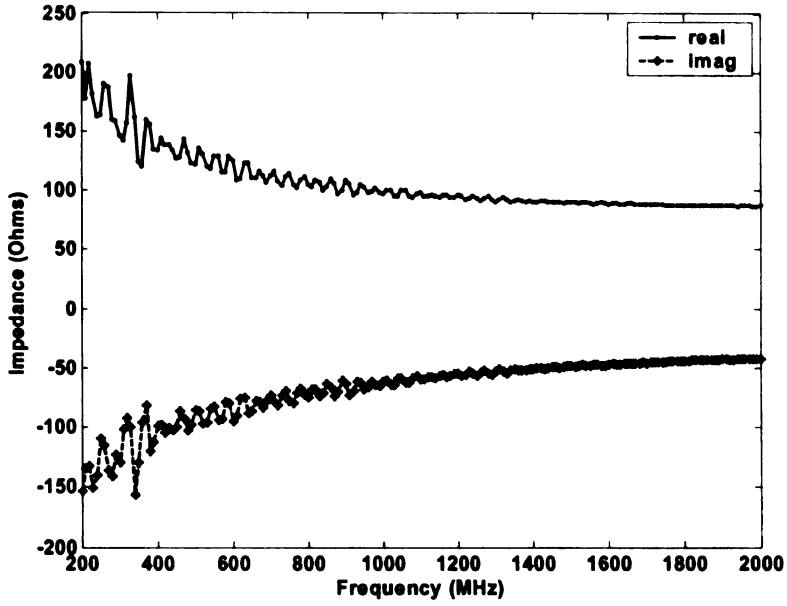

Figure 3.82 Input Impedance vs. Frequency

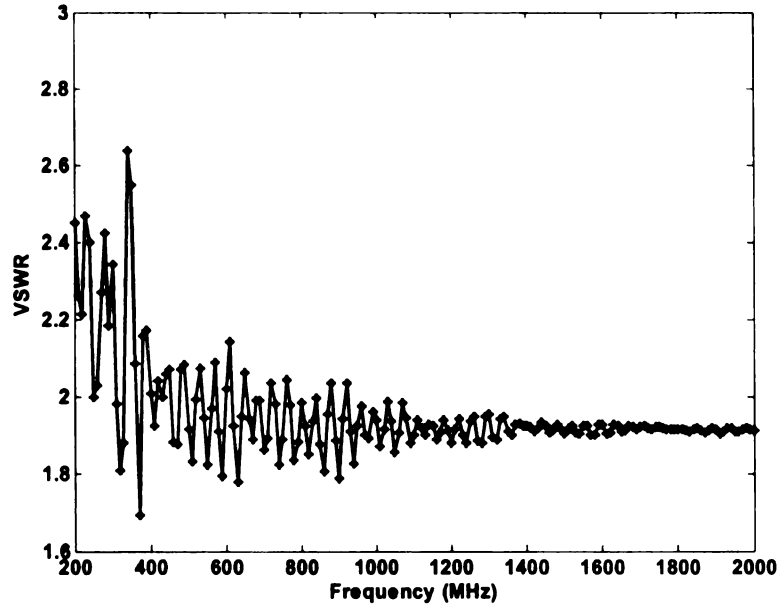

Figure 3.83 VSWR vs. Frequency

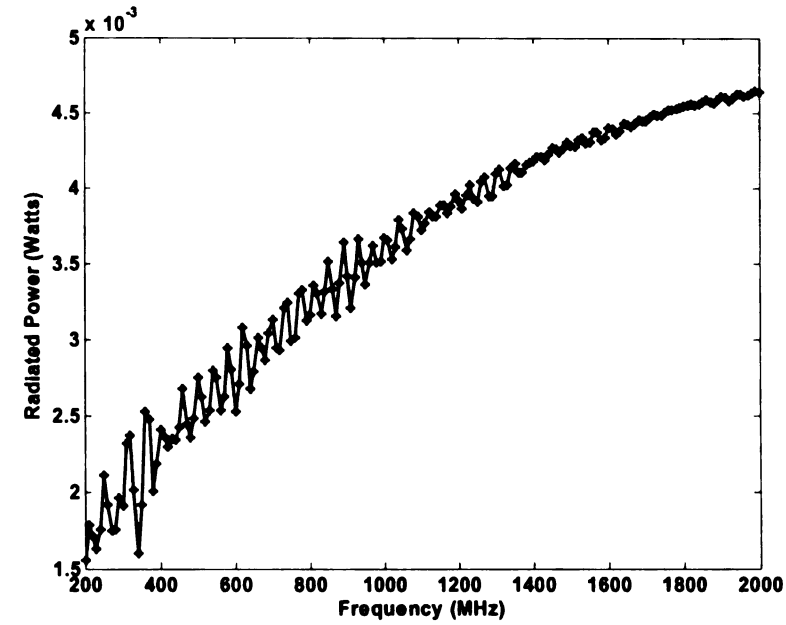

Figure 3.84 Radiated Power vs. Frequency

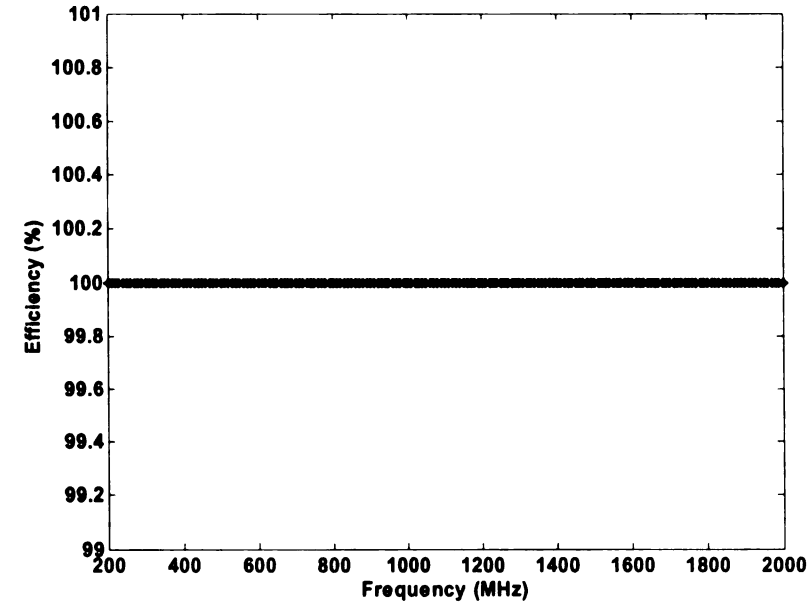

Figure 3.85 Efficiency vs. Frequency

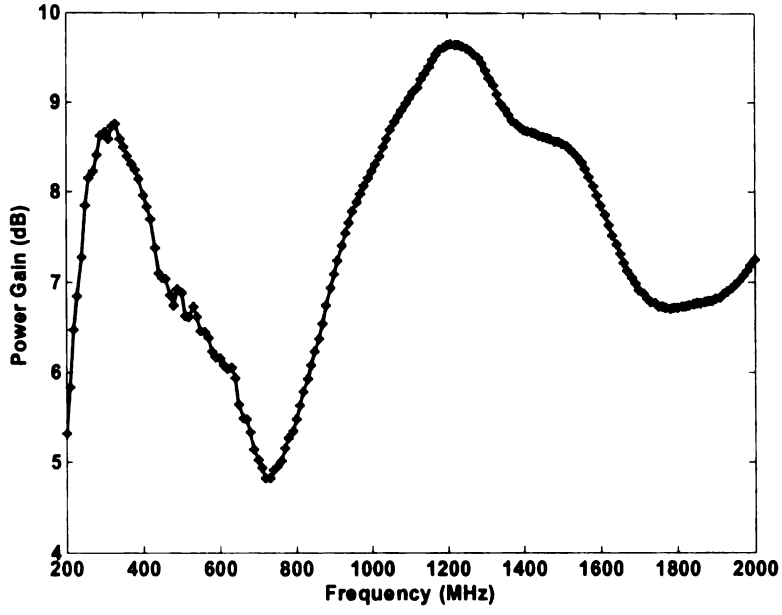

Figure 3.86 Power Gain vs. Frequency

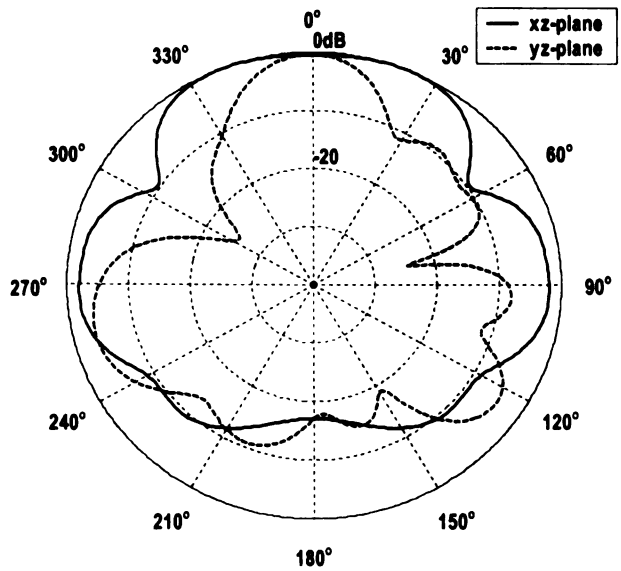

Figure 3.87 E_ϕ (xz-plane) and E_θ (yz-plane) patterns at 200 MHz

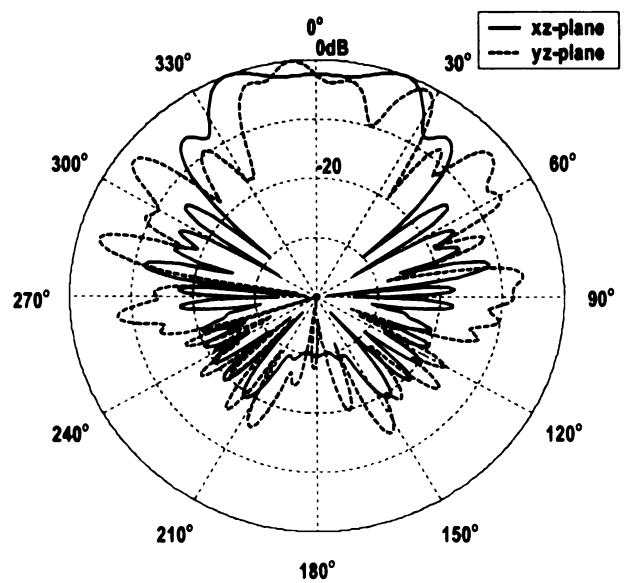

Figure 3.88 E_ϕ (xz-plane) and E_θ (yz-plane) patterns at 800 MHz

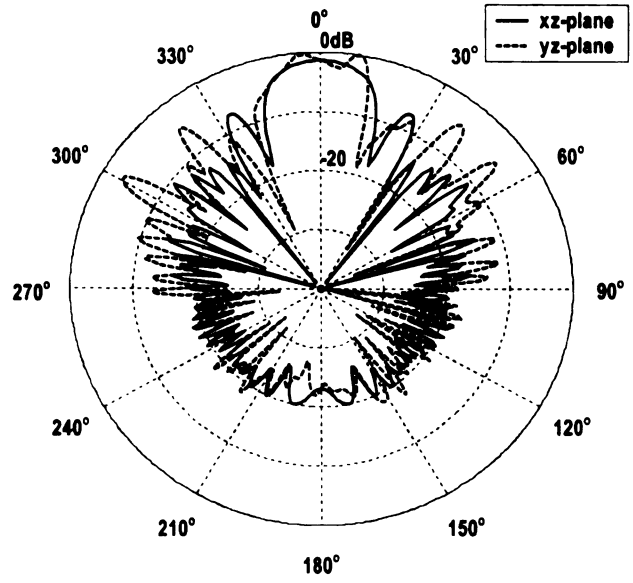

Figure 3.89 E_ϕ (xz-plane) and E_θ (yz-plane) patterns at 1400 MHz

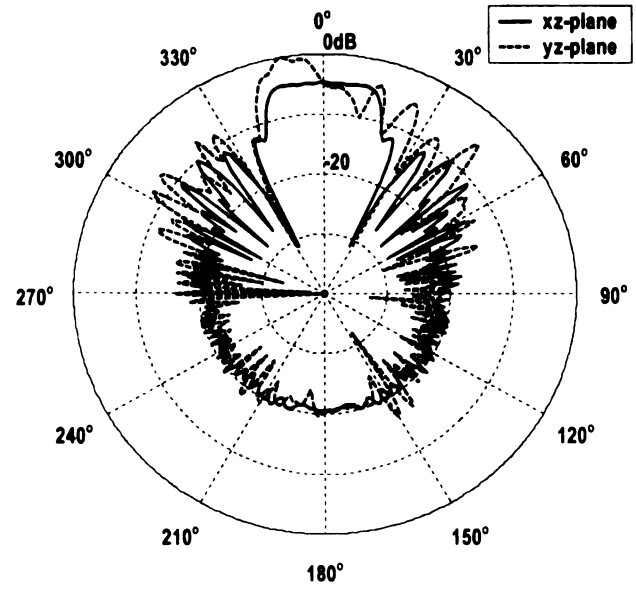

Figure 3.90 E_ϕ (xz-plane) and E_θ (yz-plane) patterns at 2000 MHz

3.2.2 Antennas with closed ends

3.2.2.1 Feed impedance of 600 Ohms

Figure 3.91 shows the optimized shape of the antenna. The radii of these segments vary from 0.0005 m to 0.01125. Some of the radii are too small to be displayed, especially at the two ends. The input impedance as a function of frequency is shown in Figure 3.92. It shows that the input impedance is not as a smooth function as that of the symmetric antenna. The VSWRs vary from 1.01 to 2.5 and the mean value is around 1.5 (Figure 3.93). It is not a smooth function of frequency. Figure 3.94 shows the radiated power as a function of frequency. The power gain is above 3.3 dB over the frequency band (Figure 3.95). It reaches 9.5 dB at 600 MHz and drops to 5 db at around 1150 MHz. As shown in figure 3.97, the maximum radiation direction is 30 degrees away in the xz-plane at 200 MHz, and about 3 degrees away in the yz-plane at 800 MHz (Figure 3.98). The maximum radiation is in the yz-plane which is 5 and 10 degrees away from the desired direction as show in figure 3.89 and figure 3.90, respectively.

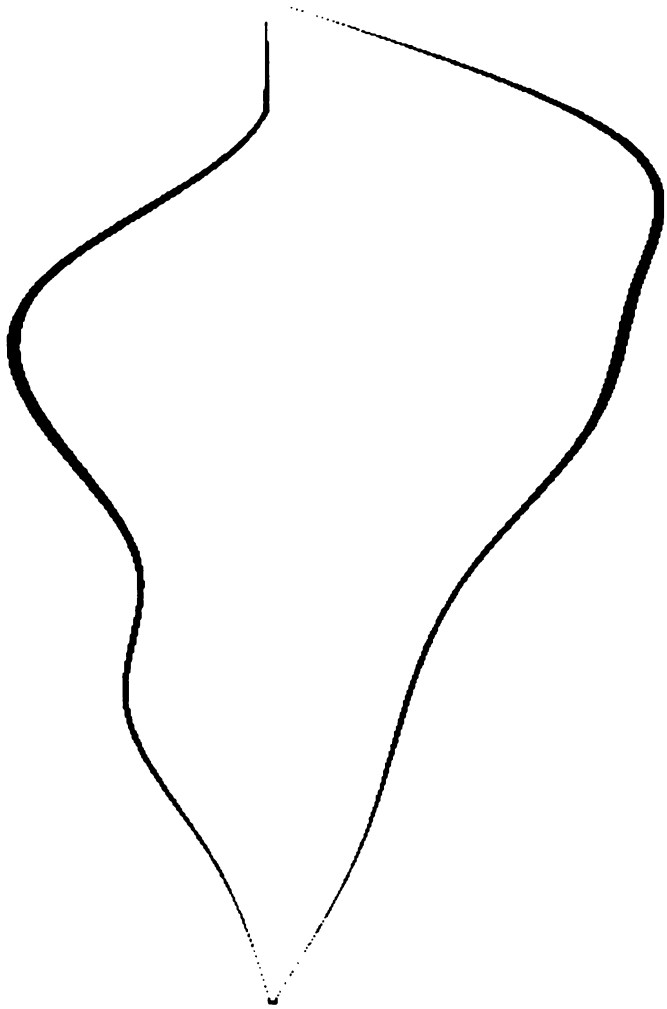

Figure 3.91 Antenna Geometry

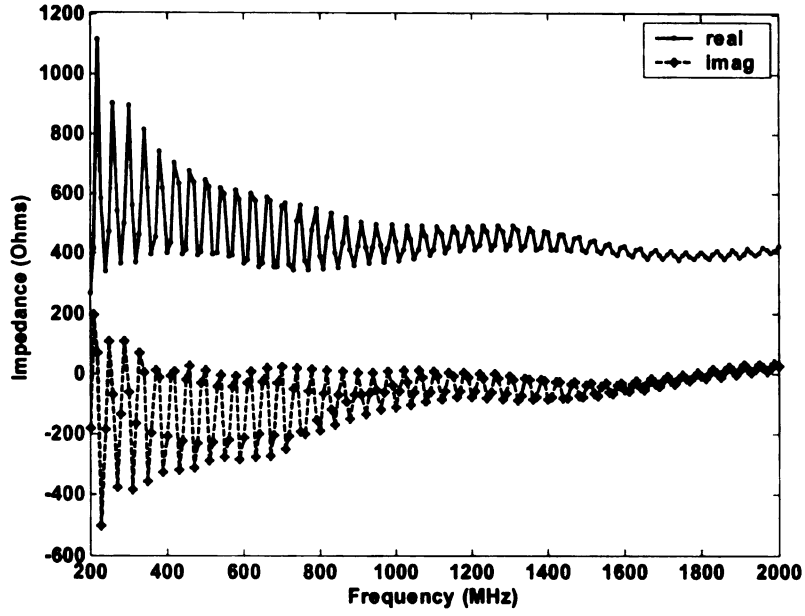

Figure 3.92 Input Impedance vs. Frequency

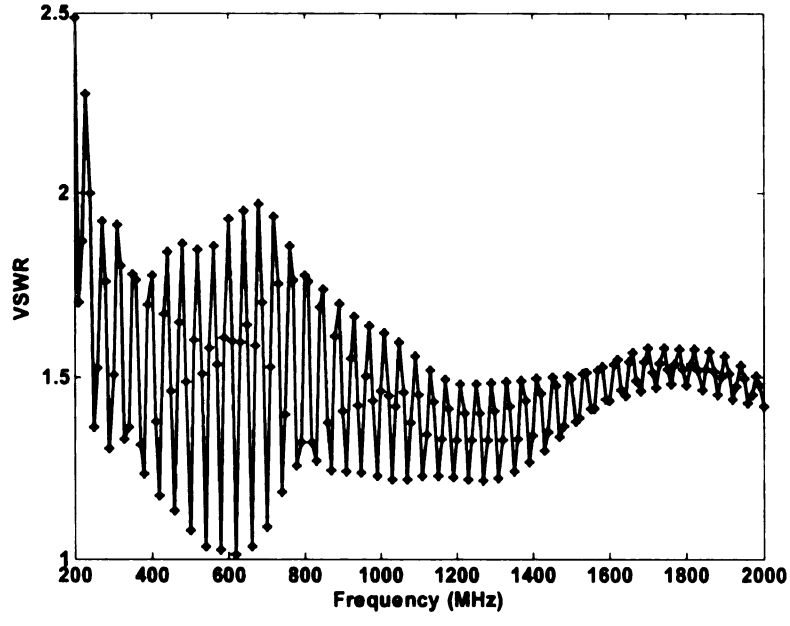

Figure 3.93 VSWR vs. Frequency

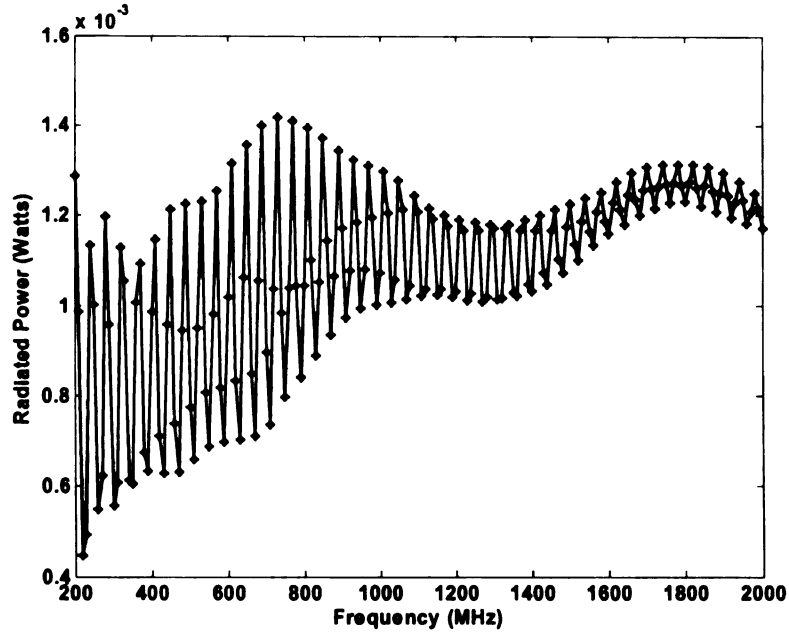

Figure 3.94 Radiated Power vs. Frequency

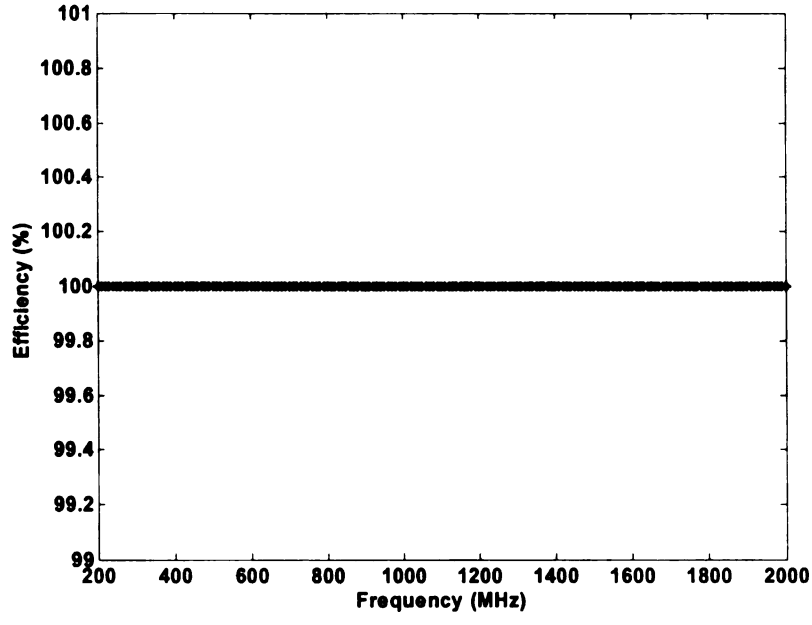

Figure 3.95 Efficiency vs. Frequency

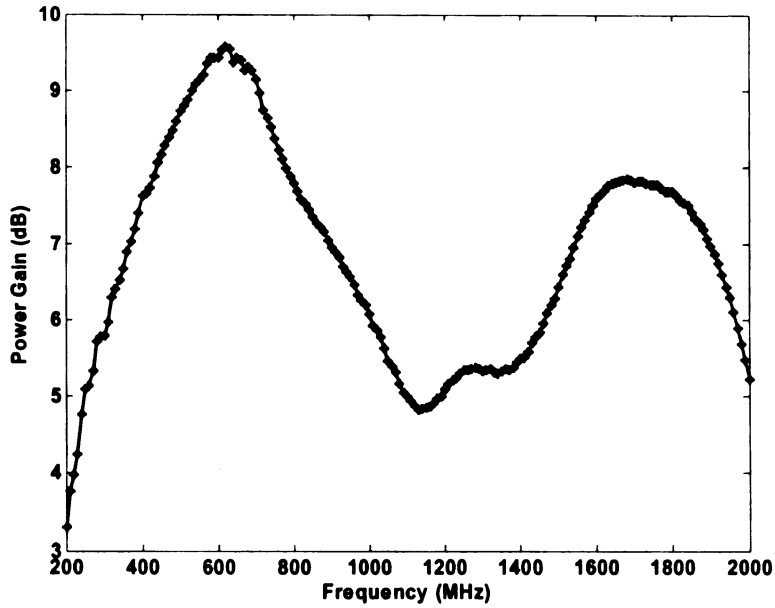

Figure 3.96 Power Gain vs. Frequency

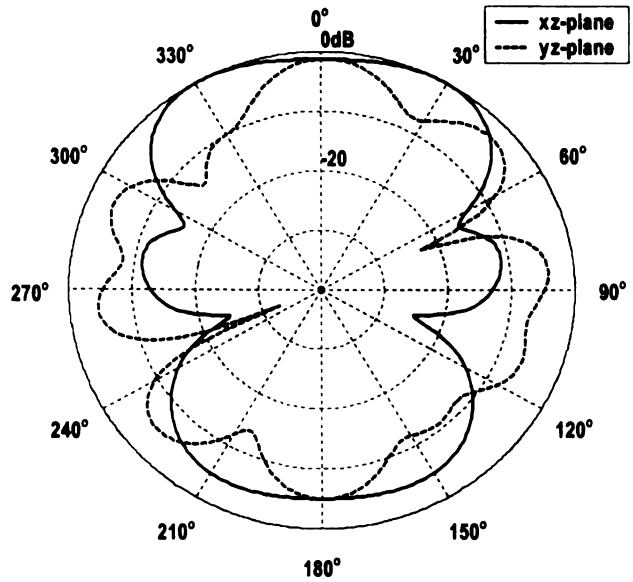

Figure 3.97 E_ϕ (xz-plane) and E_θ (yz-plane) patterns at 200 MHz

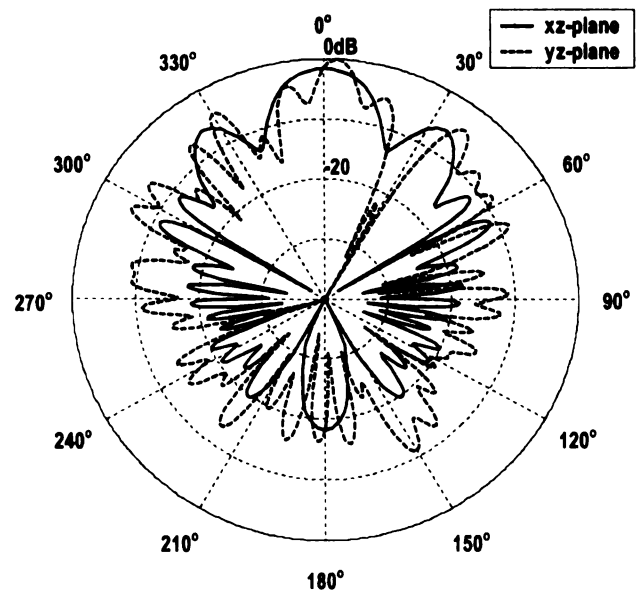

Figure 3.98 E_ϕ (xz-plane) and E_θ (yz-plane) patterns at 800 MHz

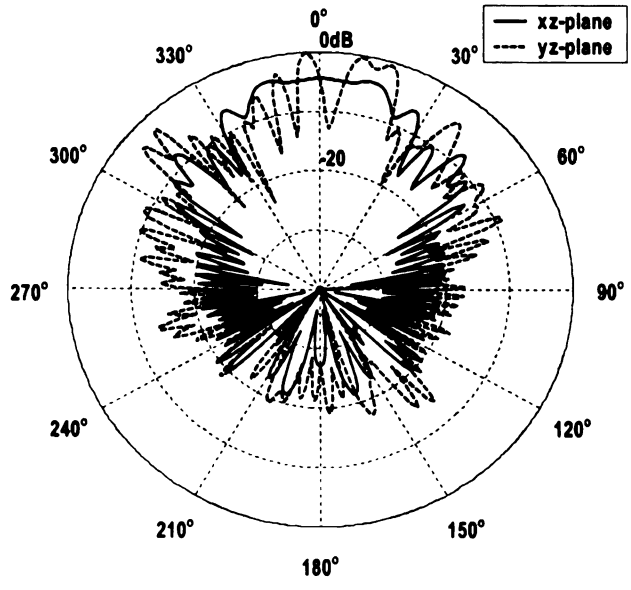

Figure 3.99 E_ϕ (xz-plane) and E_θ (yz-plane) patterns at 1400 MHz

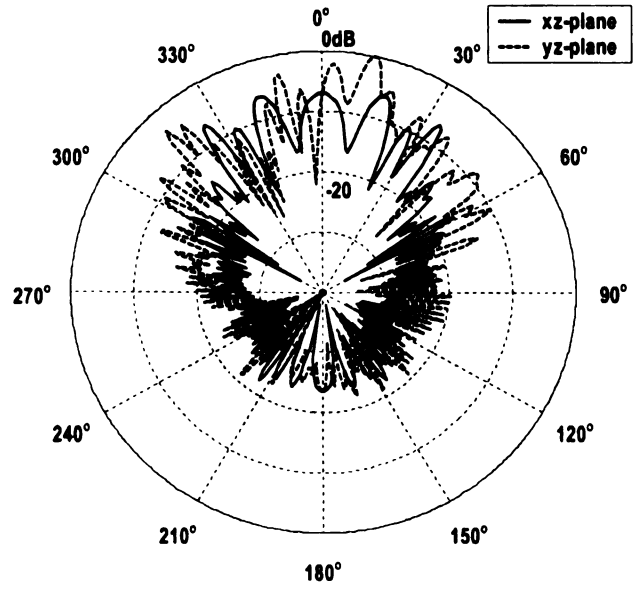

Figure 3.100 E_ϕ (xz-plane) and E_θ (yz-plane) patterns at 2000 MHz

3.2.2.2 Feed impedance of 300 Ohms

The optimized shape is shown in figure 3.101. The radii of these segments vary from 0.00163-0.006 m. The terminating load to the ends is zero (short circuit). The input impedance versus frequency is shown in figure 3.102. The VSWR varies from 1.05 to 2.5 (Figure 3.103). The radiated power and efficiency are shown in Figure 3.104 and Figure 3.105, respectively. The power gain starts from 3.5 dB at 200 MHz and reaches 12.8 dB at 2000 MHz (Figure 3.106). It indicates that this antenna has good directivity along the length of the antenna. Figure 3.107 – 120 show the radiation pattern in xz-plane and yz-plane. The maximum radiation direction is not always along the length of the antenna in yz-plane over the frequency band.

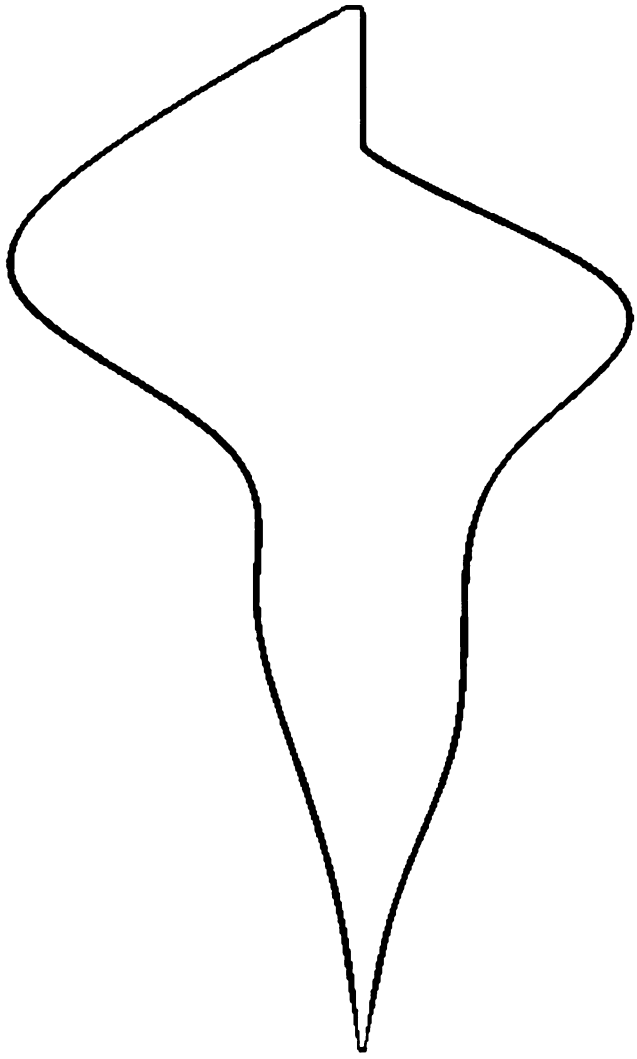

Figure 3.101 Antenna Geometry

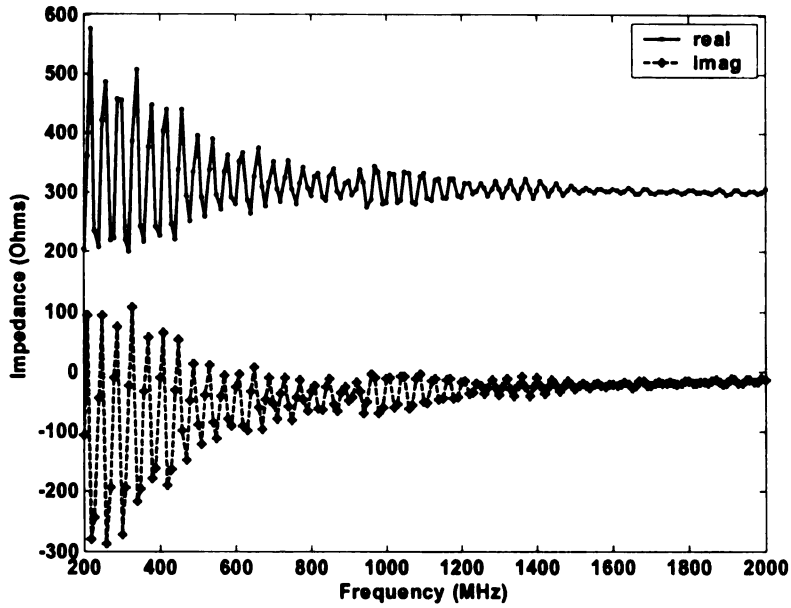

Figure 3.102 Input Impedance vs. Frequency

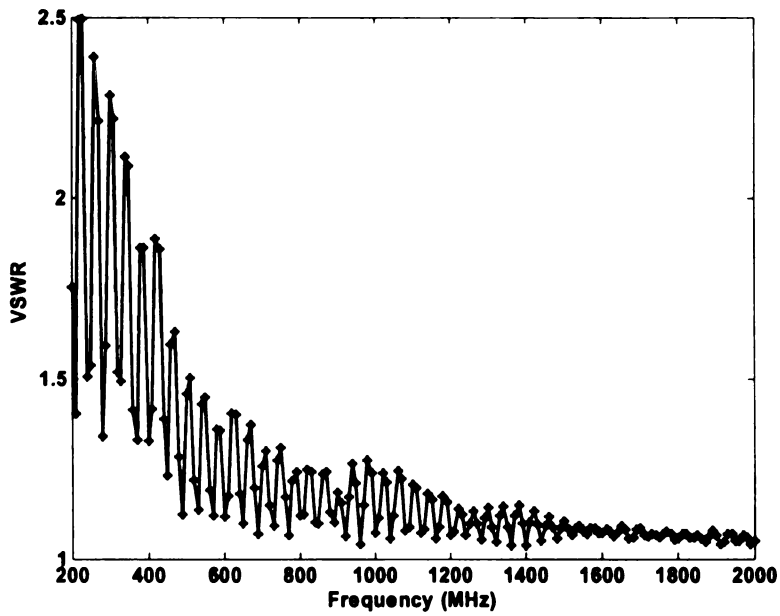

Figure 3.103 VSWR vs. Frequency

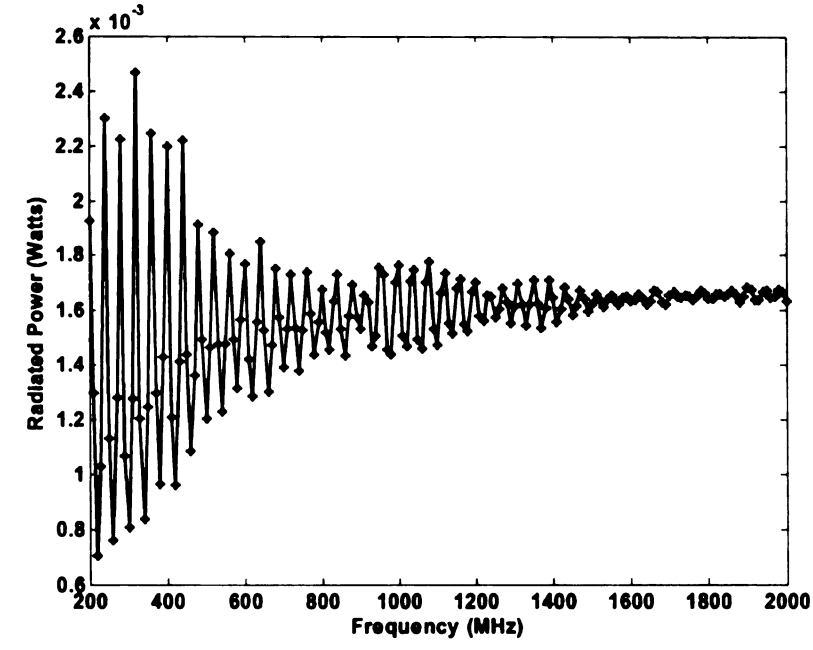

Figure 3.104 Radiated Power vs. Frequency

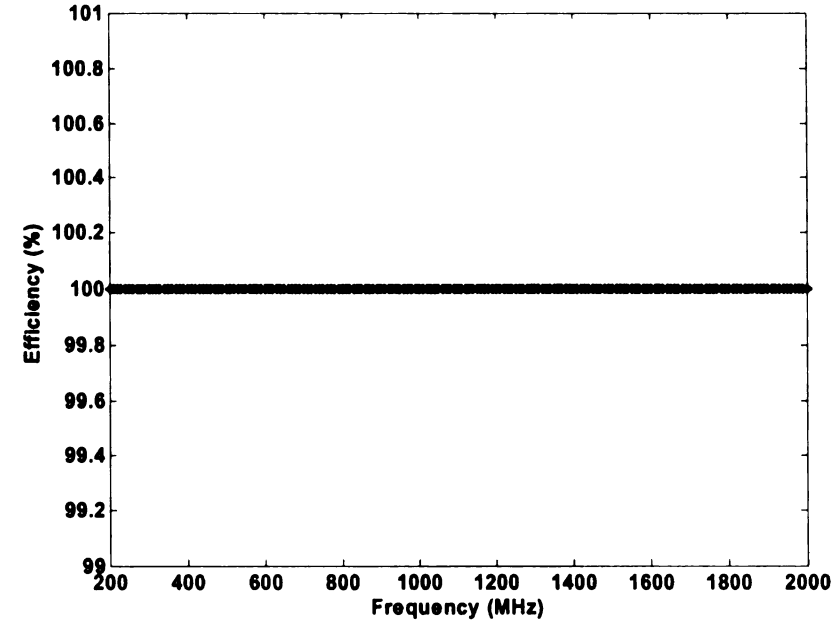

Figure 3.105 Efficiency vs. Frequency

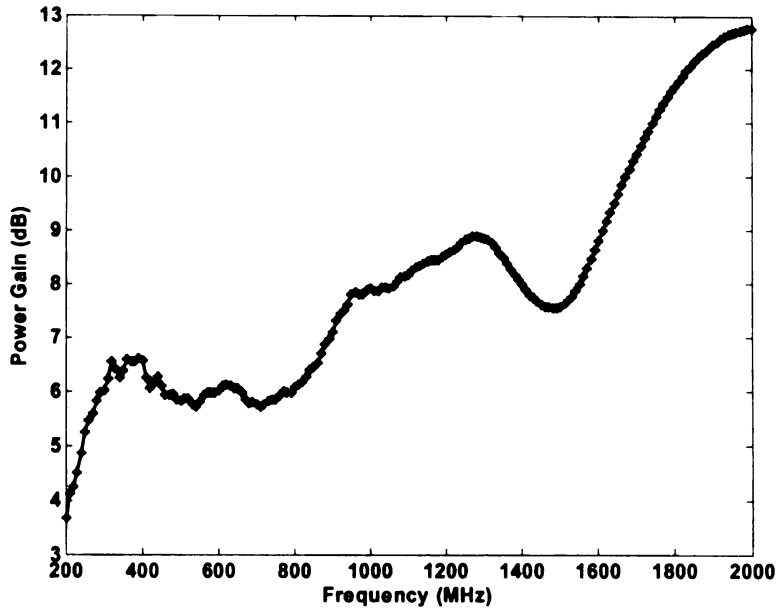

Figure 3.106 Power Gain vs. Frequency

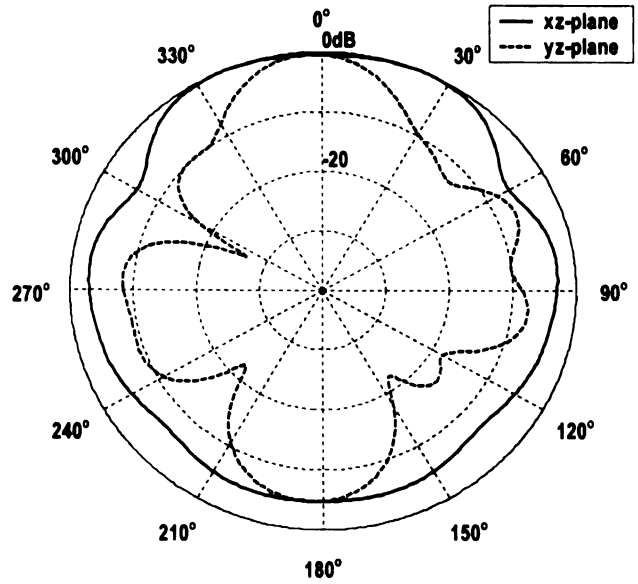

Figure 3.107 E_ϕ (xz-plane) and E_θ (yz-plane) patterns at 200 MHz

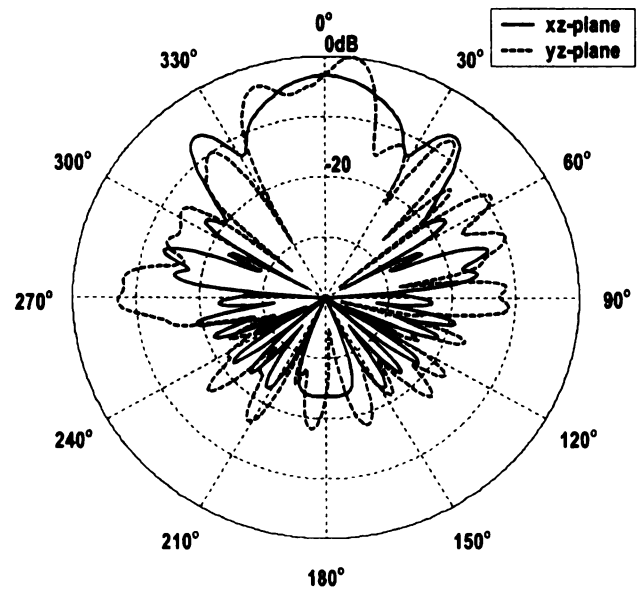

Figure 3.108 E_ϕ (xz-plane) and E_θ (yz-plane) patterns at 800 MHz

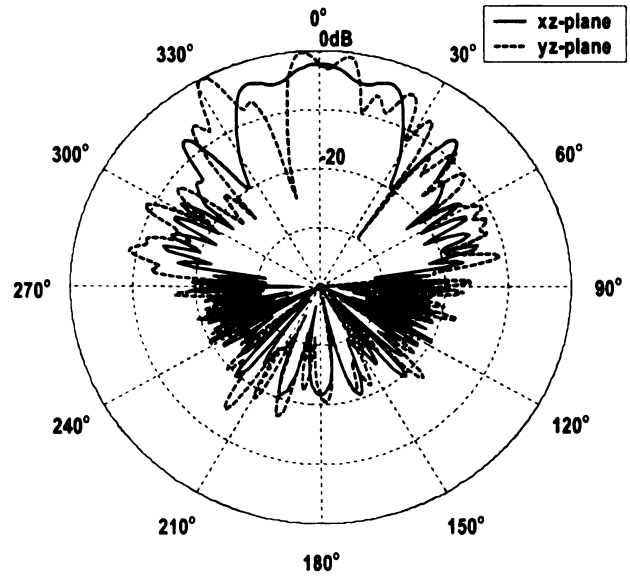

Figure 3.109 E_ϕ (xz-plane) and E_θ (yz-plane) patterns at 1400 MHz

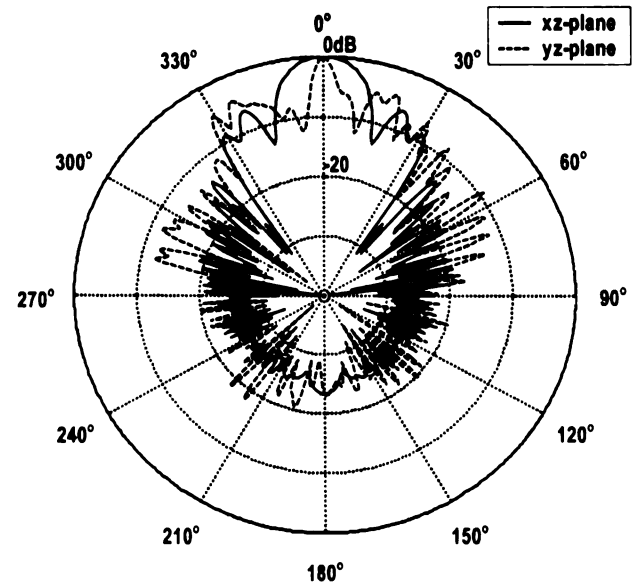

Figure 3.110 E_ϕ (xz-plane) and E_θ (yz-plane) patterns at 2000 MHz

3.2.2.3 Feed impedance of 150 Ohms

This antenna has the optimized constant radius of 0.007 m and the shape is shown in Figure 3.111. The terminating load to the ends is 300 ohms. The real part of the input impedance varies around 150 ohms and the imaginary part is close to -50 ohms as frequency increases (Figure 3.112). The VSWR varies from 1.28 to 2.0 and the mean value is around 1.45 (Figure 2.113). The radiated power increases with frequency (Figure 3.14). The antenna efficiency is from 81.5 percent at 200 MHz to 99.7 percent at 2000 MHz (Figure 3.115). The input power is loss due to the ohmic loss at the load. The antenna has good power gain along the length except there are two dips at around 1000 MHz and 1500 MHz. In Figure 3.117, the direction of maximum radiation is around 30 degrees away from the desired direction in the xz-plane at 200 MHz. It is at around 10 and 15 degrees away in the yz-plane at 800 MHz (Figure 3.118). The maximum radiation is in yz-planes but not in the desired directions (Figure 3.119-120).

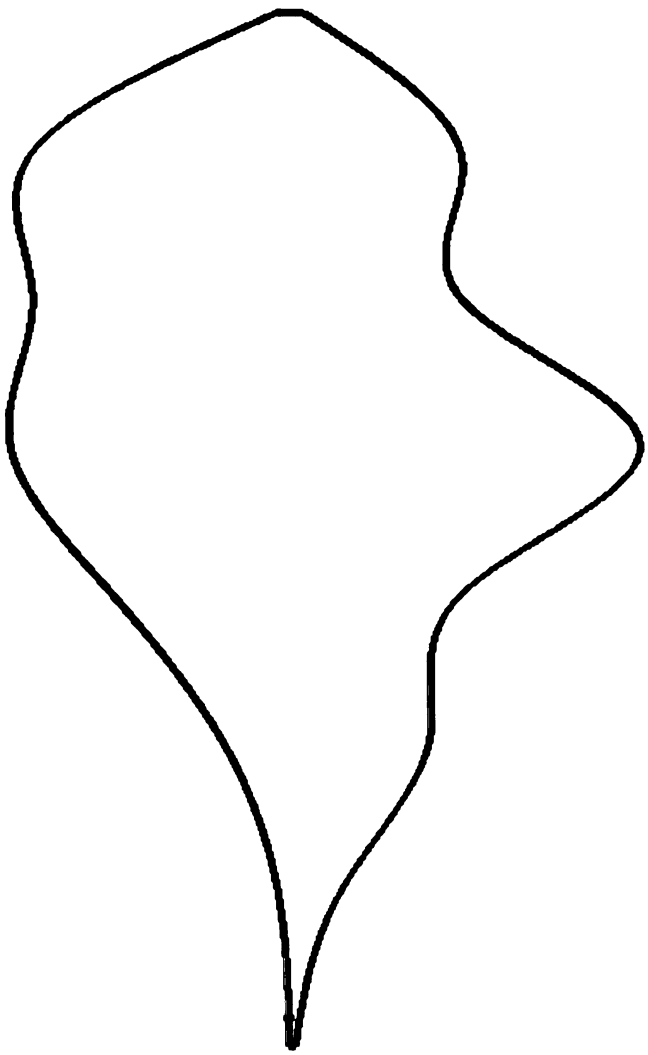

Figure 3.111 Antenna Geometry

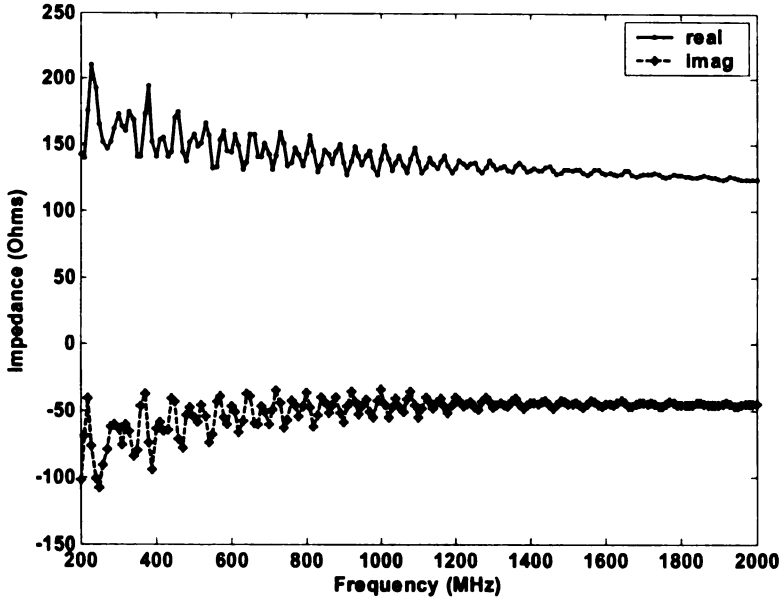

Figure 3.112 Input Impedance vs. Frequency

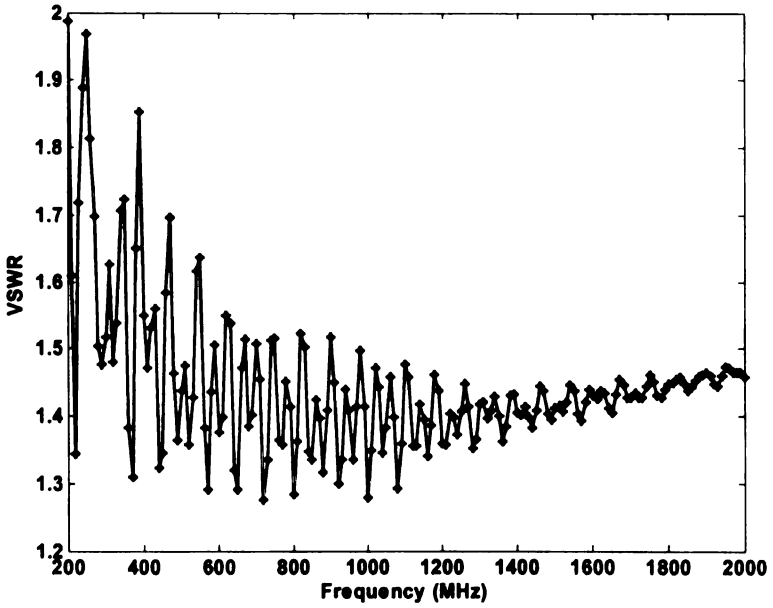

Figure 3.113 VSWR vs. Frequency

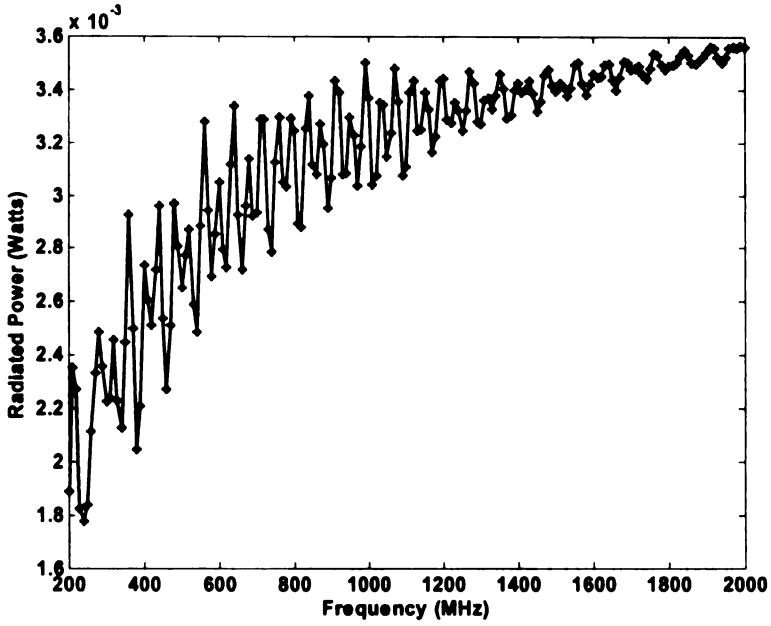

Figure 3.114 Radiated Power vs. Frequency

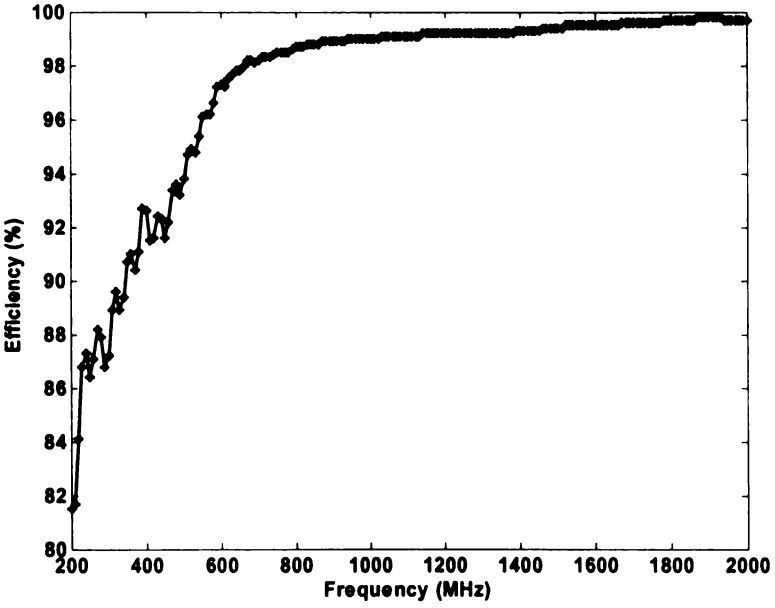

Figure 3.115 Efficiency vs. Frequency

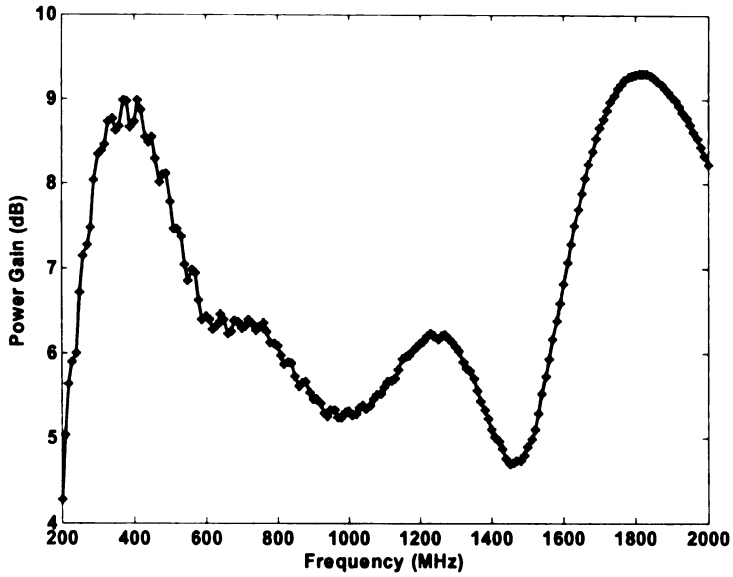

Figure 3.116 Power Gain vs. Frequency

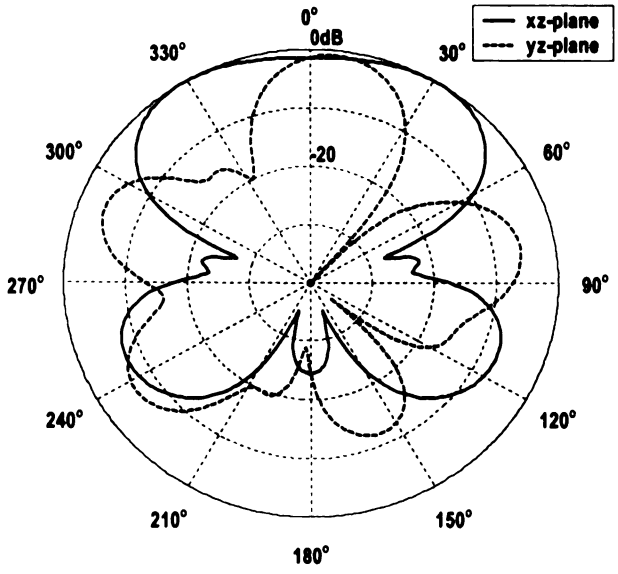

Figure 3.117 E_ϕ (xz-plane) and E_θ (yz-plane) patterns at 200 MHz

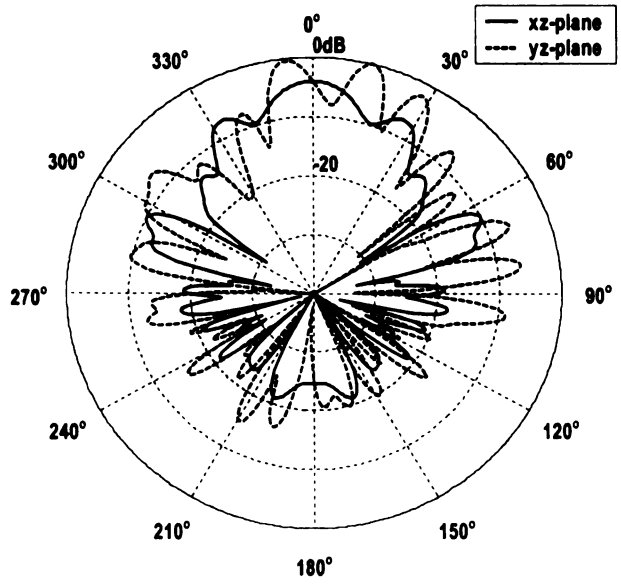

Figure 3.118 E_ϕ (xz-plane) and E_θ (yz-plane) patterns at 800 MHz

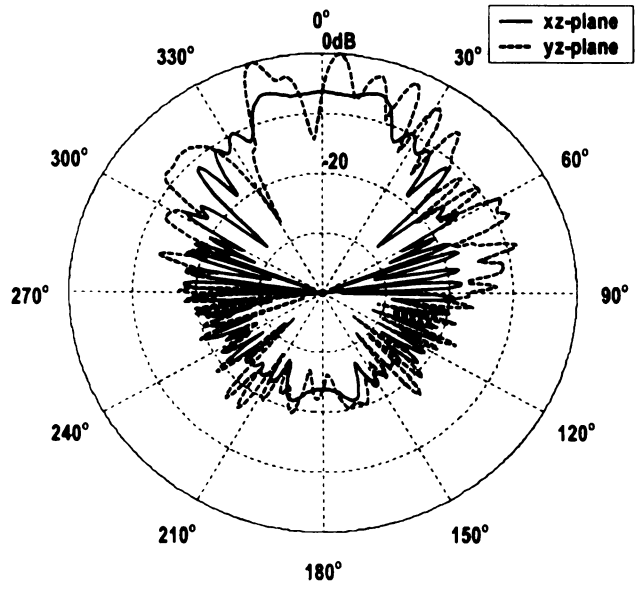

Figure 3.119 E_ϕ (xz-plane) and E_θ (yz-plane) patterns at 1400 MHz

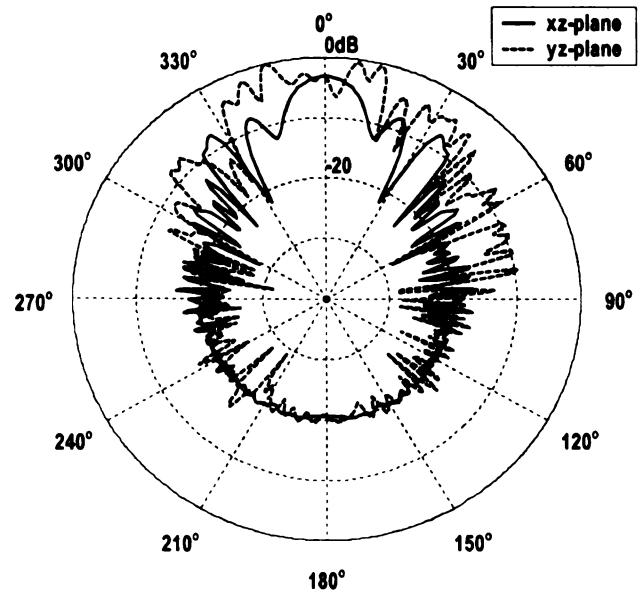

Figure 3.120 E_ϕ (xz-plane) and E_θ (yz-plane) patterns at 2000 MHz

3.3 Conclusions

In this research, twelve different types of antennas are synthesized and discussed. Simulation results show that all the antennas have 100 percent radiation efficiency except the one shown in figure 3.115. It is because of the ohmic loss at a 300 ohms terminating load to the ends. The efficiency starts at 81.5 percent at 200 MHz and go up to 99.7 percent at 2000 MHz.

The VSWR versus frequency curves vary with different shapes and segments radii types. Generally, the ones with varying segment radius have lower VSWR values at higher frequency. As shown in figure 3.3, 3.33, 3.63 and 3.93, the VSWR starts at around 3 at low frequency, and decrease to approximately 1 as the frequency goes higher. In figure 3.13, 3.43, 3.73 and 3.103, the VSWR starts from around 3 and slowly decreases to around 1.1 while it is 1 as frequency increases. With the feed impedance of 150 ohms, the VSWR starts at around 3 and drops to around 1.4 at high frequency as shown in figure 3.23, 3.53, 3.83 and 3.113. The mean value of VSWR is higher than that with feed impedance of 600 and 300 ohms. On the other hand, these antennas with symmetric geometry have smoother impedance versus frequency curves than those of asymmetric geometry. The ones optimized with higher feeding impedance have better VSWR properties.

For the antennas with the feed impedance of 600 ohms, the real parts of the input impedance vary around 600 ohms and the imaginary parts vary around zero. For ones with 300 and 150 ohms feed impedance, the real parts vary down to around 300 and 150 ohms, respectively. The imaginary parts go up close to zero in the 300 ohms case while they approach to -50 ohms in the 150 ohms case at high frequency.

In figure3.4, 3.34 and 3.64, the radiated power varies around $0.8*10^{-3}$ watts. It starts around $0.8*10^{-3}$ watts but increases around $1.1*10^{-3}$ because of the reduced input impedance at higher frequency as shown in figure 3.94. Figure 3.14, 3.44, 3.74 and 3.104 show the averaged radiated power increases as a function of frequency and the average is $1.7*10^{-3}$ approximately. The average radiated power increases as frequency goes higher as shown in figure 3.24, 3.54, 3.84 and 3.114.

Most of the power gains are above 5 dB over the frequency band as shown in figure 3.6, 3.36, 3.46, 3.66, 3.86, 3.96 3.106 and 3.116. There are several minor dips in figure 3.16 and 3.76. Two big dips happen at 300 MHz and 1200 MHz in figure 3.26. Figure 3.56 shows that there are dips at around 400 and 950 MHz; the one at 950 MHz is especially deep.

All these antennas have good directivity along their length even though the maximum radiation may not be along the same direction over all frequencies. The maximum radiation is mostly in the xz-plane (E_φ) at low frequency and in the yz-plane (E_θ) at higher frequency.

Chapter 4

COMPARISONS ON GMC PULSE RESPONSE

In this chapter, a normalized antenna impulse response is introduced to study the wideband properties of the traveling wave antennas in the time domain. A single waveform, $h_N(t)$, describes an antenna's performance in both transmission and reception. It describes the antenna's responses to an impulse function in reception or to a step function in transmission. A number of useful simplifications can be taken in the antenna equations by using this impulse response.

There are several advantages to using the impulse response to describe the antennas. First of all, the transmission coefficients between the feed line and the antennas are eliminated. Secondly, the antenna impedance does not appear in these equations. Thirdly, the normalized impulse response applies to both transmission and reception equations. Fourthly, the expressions are made very simple by introducing the normalized impulse response $h_N(t)$. Finally, by writing the equations in this manner, it is possible to tie the theory back to the measurements that are usually made on transient antennas.

In this study, $h_N(t)$ cannot be obtained directly because the outputs of GA-NEC are in frequency domain. Its impulse response form in the frequency domain, $h_N(\omega)$, can be expressed as a function of input voltage and radiated filed at a certain distance. When $h_N(\omega)$ is available at a certain number of frequency points, a band-limited version of $h_N(t)$ can be obtained with the inverse Fourier transform.

The normalized impulse response is valid for both reception and transmission. Only the response in transmission is studied in this research. The normalized expression for the radiation field is described in [32] as

$$\frac{E_{rad}(t)}{\sqrt{Z_0}} = \frac{1}{2\pi rc} h_{N,TX}(t) * \frac{1}{\sqrt{Z_C}} \frac{dV_{src}(t)}{dt} \tag{4.1}$$

Here $E_{rad}(t)$ is the radiated electric field, Z_0 is the characteristic impedance of free space (377 Ohms), r is the distance away from the antenna and is chosen to be 100 meters in this study, c is the speed of light in free space, $h_{N,TX}(t)$ is the normalized impulse response in transmission with the units of meters per second, Z_C is the characteristic impedance of the feed cable, * is convolution operator, and $V_{src}(t)$ is the source voltage. In this equation, the antenna's transmission characteristic is described completely by $h_{N,TX}(t)$ and there are no antenna impedance or transmission coefficients involved. The above equation refers by default to the direction of the maximum radiation, but it is easily extended to multiple angles. By taking the Fourier transform, the above equation can be expressed in the frequency domain as

$$h_{N,TX}(\omega) = 2\pi rc \frac{\sqrt{Z_C}}{\sqrt{Z_0}} \frac{E_{rad}(\omega)}{j\omega V_{src}(\omega)} \tag{4.2}$$

There are two unknown variables in this equation, $E_{rad}(\omega)$ and $V_{src}(\omega)$. $V_{src}(\omega)$ is set to 1 volt for simplicity and $E_{rad}(\omega)$ can be easily extracted from the NEC2 outputs. $h_{N,TX}(t)$ can be obtained by taking the inverse Fourier Transform of $h_{N,TX}(\omega)$. The radiated energy of the

normalized impulse response can be calculated by integrating the square of $h_{N,TX}(t)$ over the time window. By calculating the energy at multiple circumferential angles the impulse energy radiation pattern can be plotted.

The frequency band of interest is limited from 200 MHz to 2 GHz. An appropriate weighting function is needed to reduce the Gibbs oscillation when performing the FFT on swept frequency data. In this study, a GMC (Gaussian modulated cosine) waveform is used in order to reduce the oscillation and preserve the bandwidth. The GMC spectrum used in this research is given by [33]

$$W_{gc}(f) = \tau(e^{-\pi((f-f_c)\tau)^2} + e^{-\pi((f+f_c)\tau)^2}) \tag{4.3}$$

Here f_c is the center frequency, and τ is width of the pulse. In this study, f_c = 1 GHz, τ =0.002. The waveform of the GMC pulse is shown in figure 4.1

The loaded dipole described by Clayborne D. Taylor in [33], an optimized dipole and the rhombic antenna mentioned in [34] are chosen to compare with the spline antenna. Both the energy radiation patterns and radiation waveforms at certain angles are studied.

4.1 Dipole

The length of the dipole is optimized in GA-NEC for the GMC pulse radiation (described in equation 4.3). The searching space for the optimal length is in the range of 0.1 to 0.8 m. The value to be optimized is the theta component of the electric field at 100 meters away from the origin along $\theta = 90^\circ$. The weighting function is point-based. "Greater than the value of 0.02" is chosen in the constraint file. A total of 37 equally spaced points are weighted over the

frequency band in the fitness function. The weighting values obey the GMC distribution described in equation 4.3. The optimal length is 0.1504 m which is half wavelength long at 1 GHz.

Figure 4.2 shows the GMC pulse energy radiation pattern. It is a Φ-independent pattern and the maximum radiation is in the $\theta = 90^\circ$ plane. The waveforms of the GMC pulse radiated along $\theta = 30^\circ$, $\theta = 60^\circ$ and $\theta = 90^\circ$ are shown in figure 4.3-4.5, respectively. The pulse consists of ringing due to the strong multiple reflections at the ends. The individual reflections can not be recognized in the time domain because of the short length of the dipole. The first arrival and the reflections overlap in a time period of around 0.02 μs. The width of the pulse response is considerably wider than the GMC pulse shown in Figure 4.1.

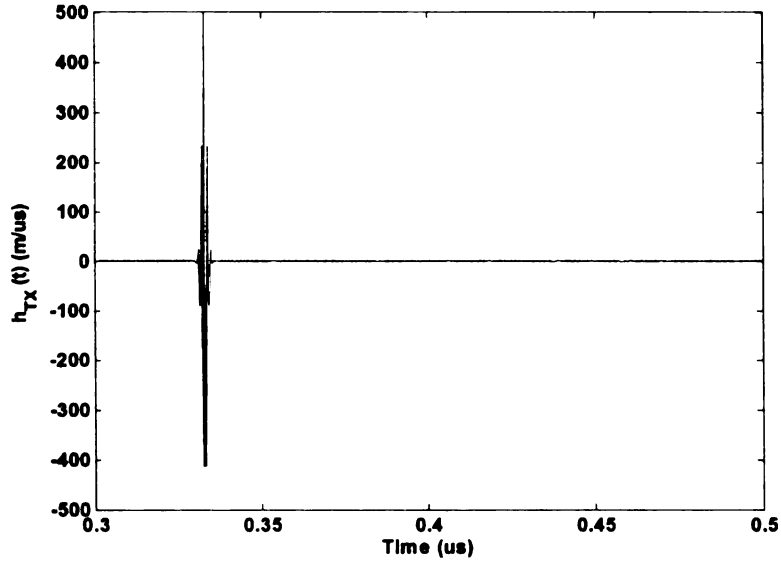

Figure 4.1 Time domain version of the frequency GMC window function

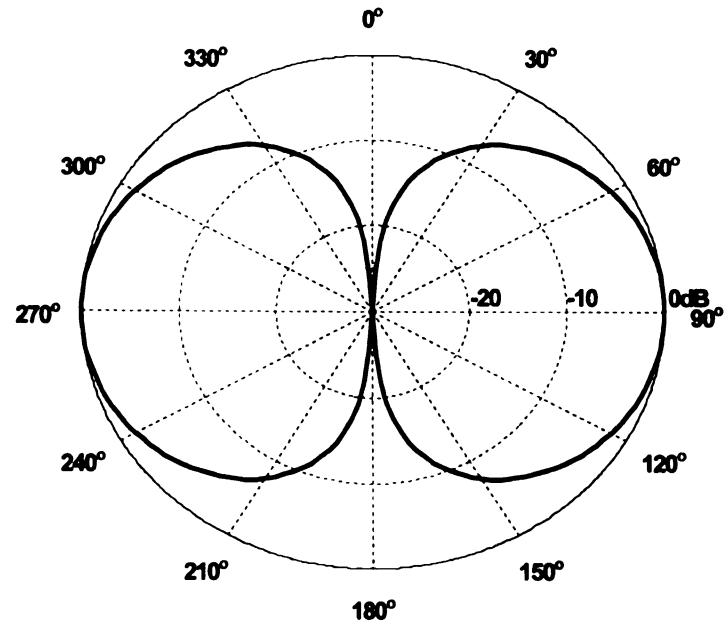

Figure 4.2 Energy in the waveform radiated by the dipole

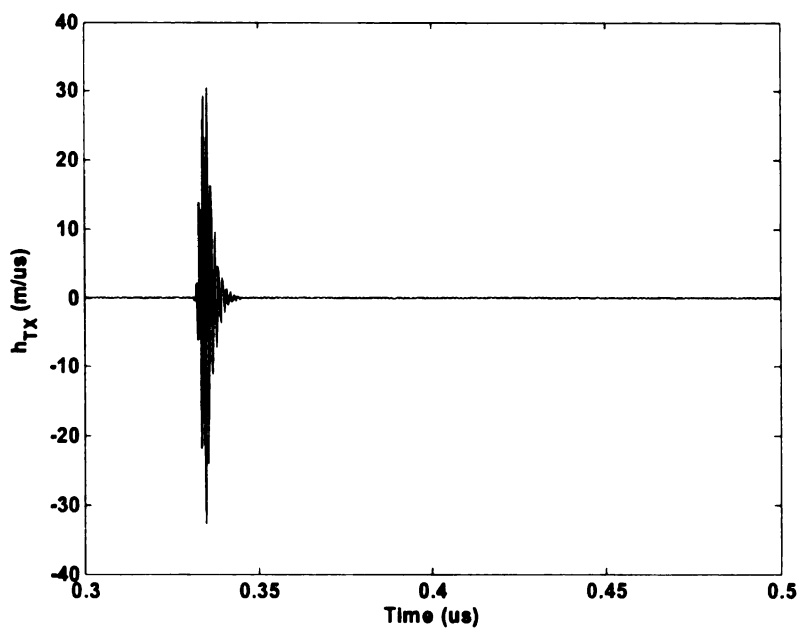

Figure 4.3 Waveform radiated in far-zone field at 30 degrees

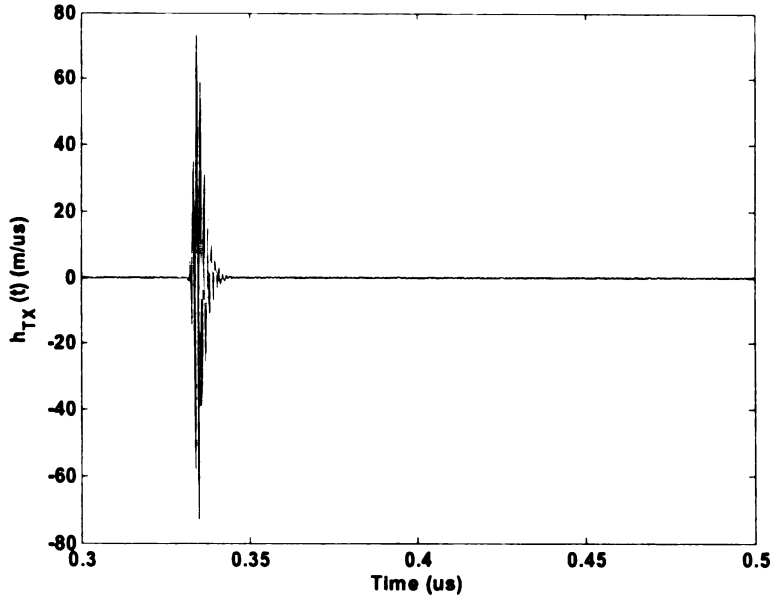

Figure 4.4 Waveform radiated in far-zone field at 60 degrees

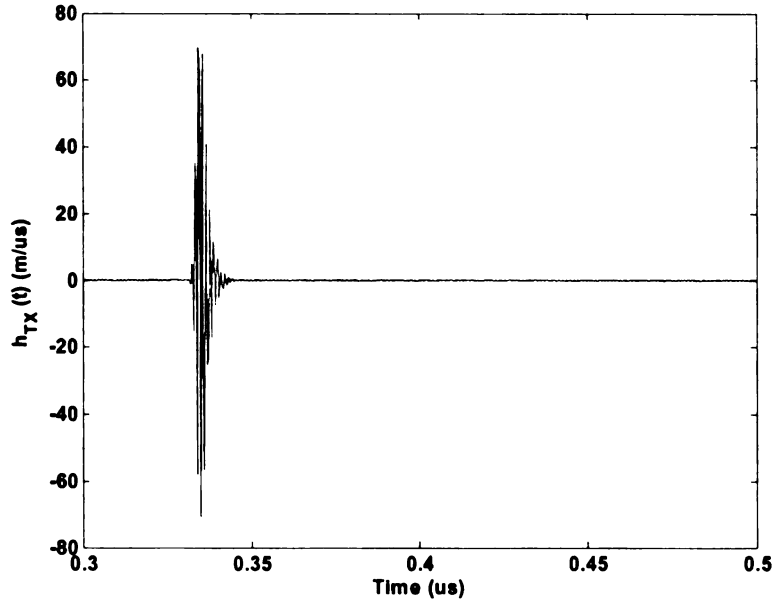

Figure 4.5 Waveform radiated in far-zone field at 90 degrees

4.2 Loaded dipole

The impedance loaded dipole described here is based on the ones that described in [33]. The dipole can be formed to a traveling wave antenna by insert some impedance loads at certain positions along the antenna. Due to the NEC2 limitation on the number of load cards, 24 recalculated impedance loadings are inserted along the wire instead of 48 as listed in [33]. It is simulated in GA-NEC and optimized using the same fitness function as the one for dipole. The searching domain for the loaded dipole length is from 0.1 to 0.8 m. The optimal length of the loaded dipole is 0.453 m.

As with the dipole, waveforms are plotted at 30, 60 and 90 degree as shown in figures 4.7-4.9. There are no reflections seen in these figures, which indicates that the current vanishes at the ends due to the radiation and ohmic loss as the current wave propagates along the wires. The pulse response is a very good reproduction of the GMC pulse shown in figure 4.1. However, the amplitude of $h_{N,TX}(t)$ is much smaller than that of the dipole, due to the resistance of the loading. The normalized energy radiation pattern is obtained over 360 degree with interval of 2 degrees (figure 4.6). There is no radiation at 0 degrees and it increases smoothly as θ goes up. The antenna has maximum radiation along $\theta = 90^{\circ}$ and vanishes to zero at $\theta = 180^{\circ}$. The half energy beam width is slightly wider than that of the dipole.

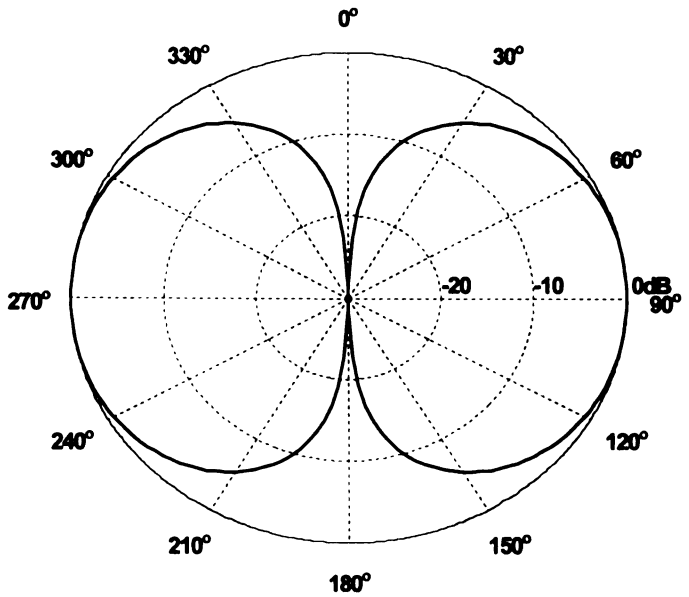

Figure 4.6 Energy in the waveform radiated by loaded dipole

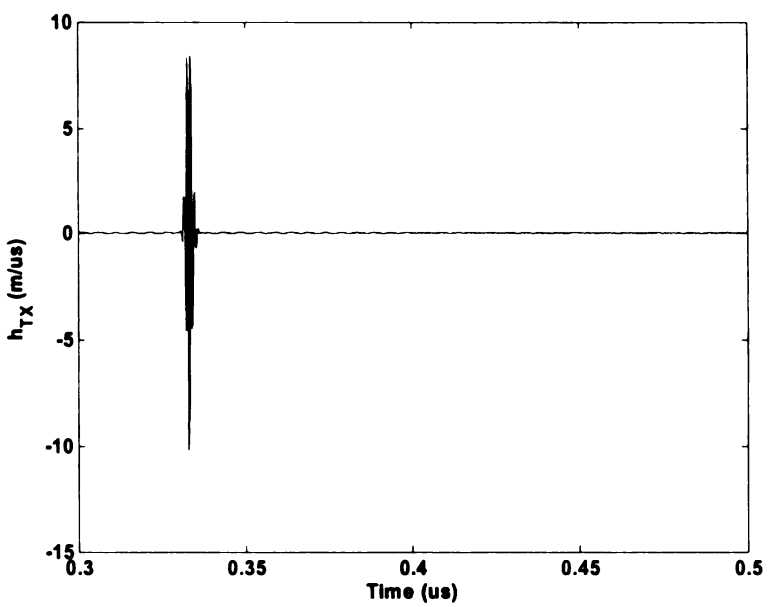

Figure 4.7 Waveform radiated in far-zone field at 30 degrees

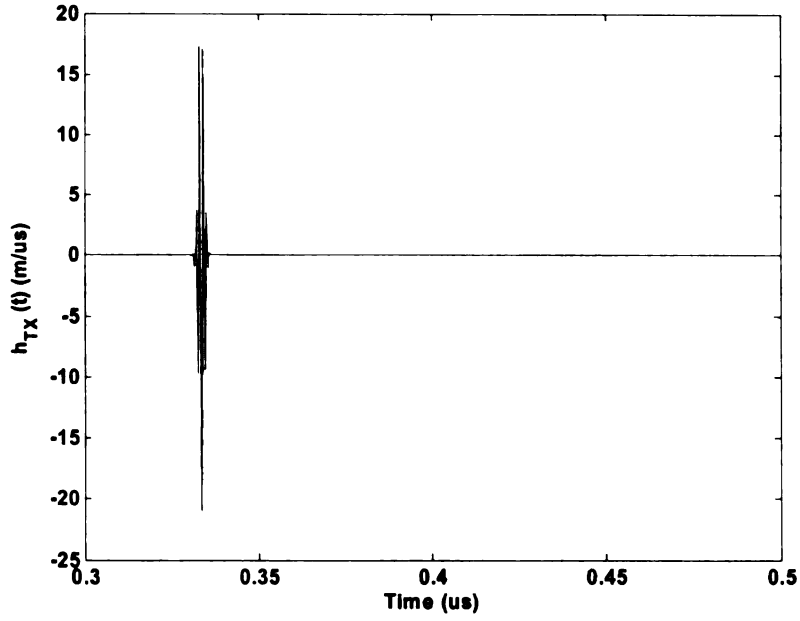

Figure 4.8 Waveform radiated in far-zone field at 60 degrees

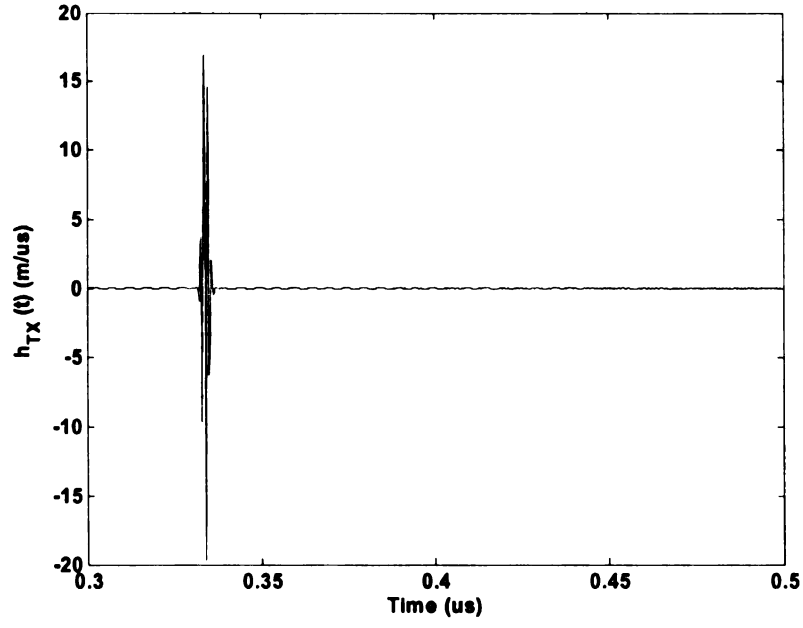

Figure 4.9 Waveform radiated in far-zone field at 90 degrees

4.3 The rhombic antenna

Rhombic antennas are traveling-wave long wire antennas. The wires usually have lengths much greater that one half wavelength long. The rhombic antenna that is simulated here is the one that is described in [35] shown in figure 4.10. The length of each side is set to 1.8 m which corresponding to 6 times the wavelength at 1 GHz and the flare angle $\alpha = 16^{\circ}$.The radius of the wire is 0.001 m and the rhombic terminating impedance is set to 600 Ohms as recommended. The antenna is placed in the y-z plane along +z axis.

The GMC pulse energy radiation is plotted in the y-z plane as a function of azimuth in figure 4.11. It shows that the maximum radiation direction is along z-axis. There are two 10 dB down side lobes located at around 30 degree away from z-axis and one 14 dB down lobe along –z axis. The GMC pulse radiation at different azimuth angles is plotted in figure 4.12-4.18. There are four events observed in figure 4.12. The first event originates when a voltage impulse is induced at the feeding end. compared to figure 4.1, this first event is close to the GMC pulse, but not as close as was the loaded dipole. The second event is significantly smaller, and is due to the current reflecting at the suddenly changing wire direction. The third event is produced by current reflecting from the wire end. The fourth is observed because of the second reflection at the end. The significant different between the amplitudes of first event and the others in figure 4.12 is due to radiation and ohmic loss. The radiation from the two sides of the antenna is out of time synchronization seen from figures 4.13-4.18. The total radiation is the superposition of the distributions of the two sides. The event that is caused by multiple reflections from the ends becomes more apparent as the azimuth angle increases. In

figure 4.18, the dominated event is caused by the reflection from the ends. Figure 4.12 shows that at 0 degrees, $h_{N,TX}(t)$ has much larger amplitude than for a dipole or a loaded dipole.

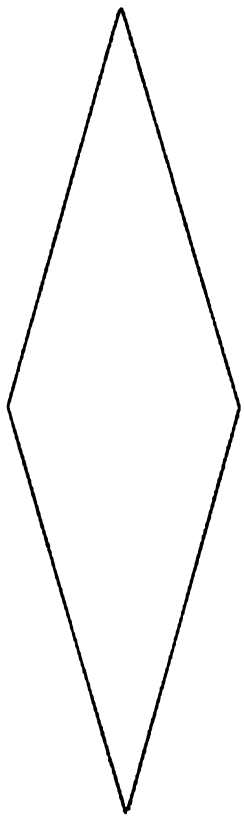

Figure 4.10 The geometry of the rhombic antenna

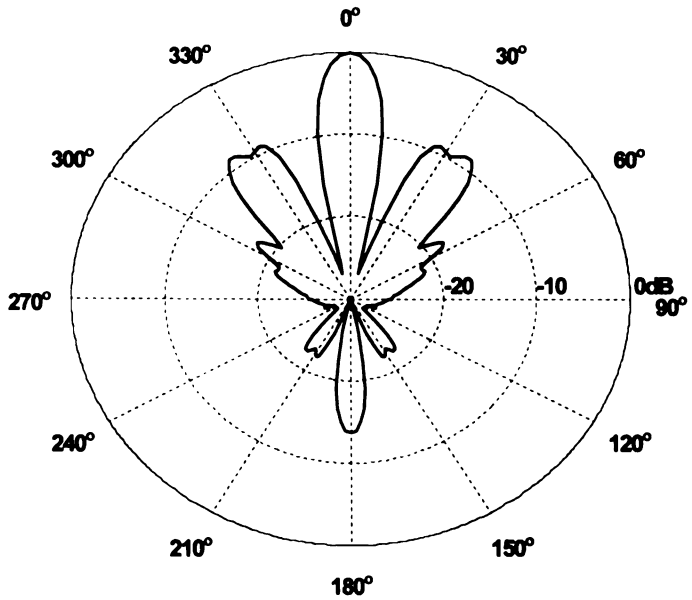

Figure 4.11 Energy in the waveform radiated by the rhombic antenna in y-z plane

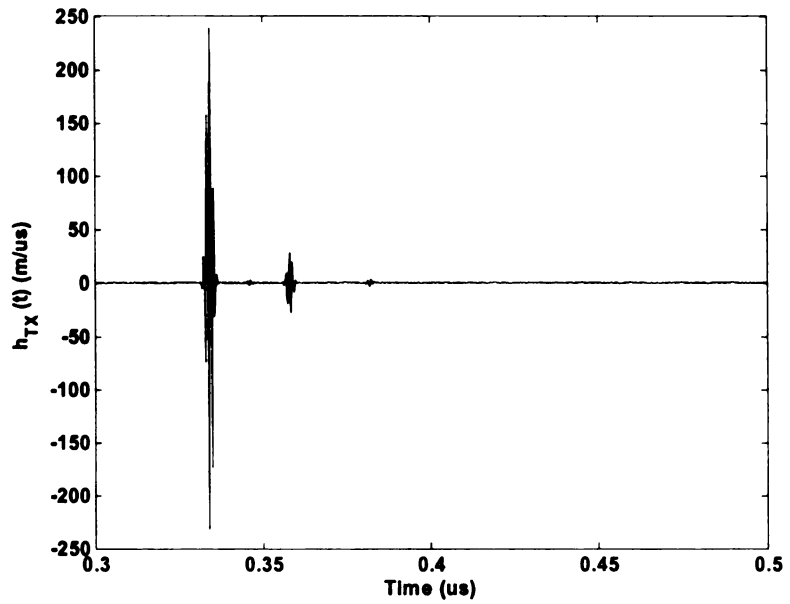

Figure 4.12 Waveform radiated in far-zone field at 0 degrees

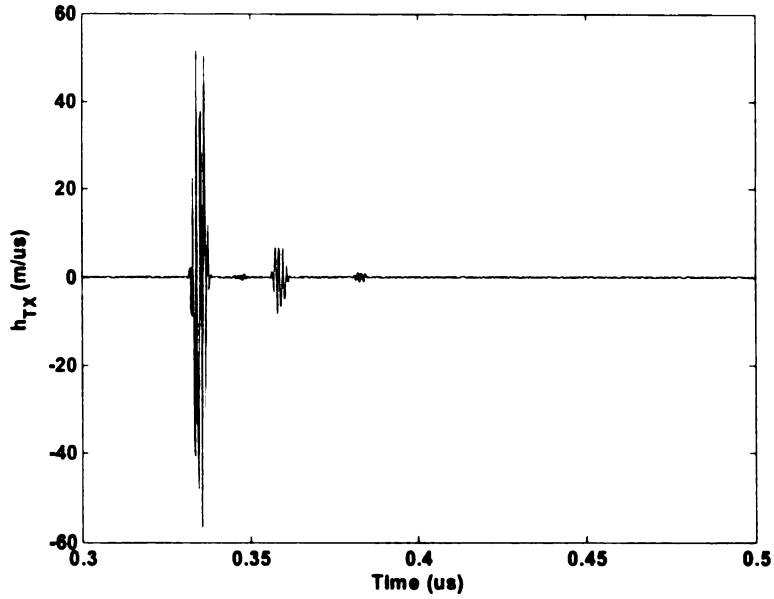

Figure 4.13 Waveform radiated in far-zone field at 30 degrees

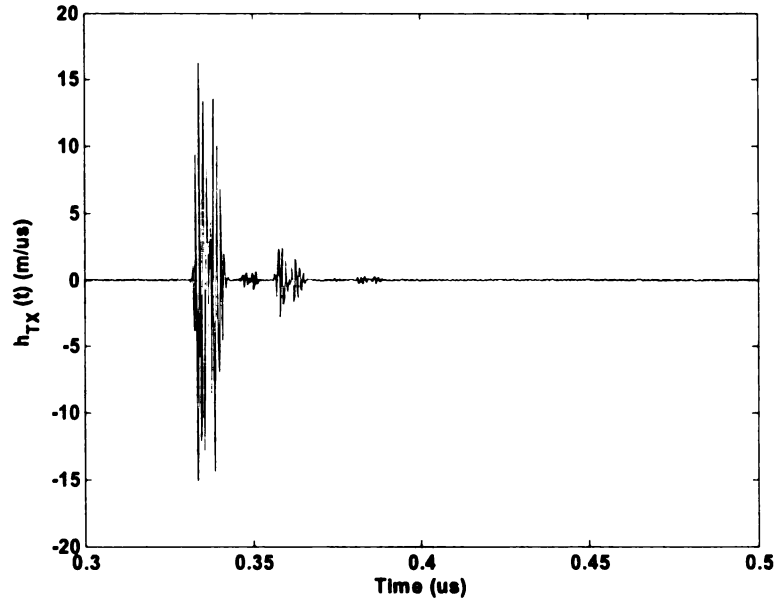

Figure 4.14 Waveform radiated in far-zone field at 60 degrees

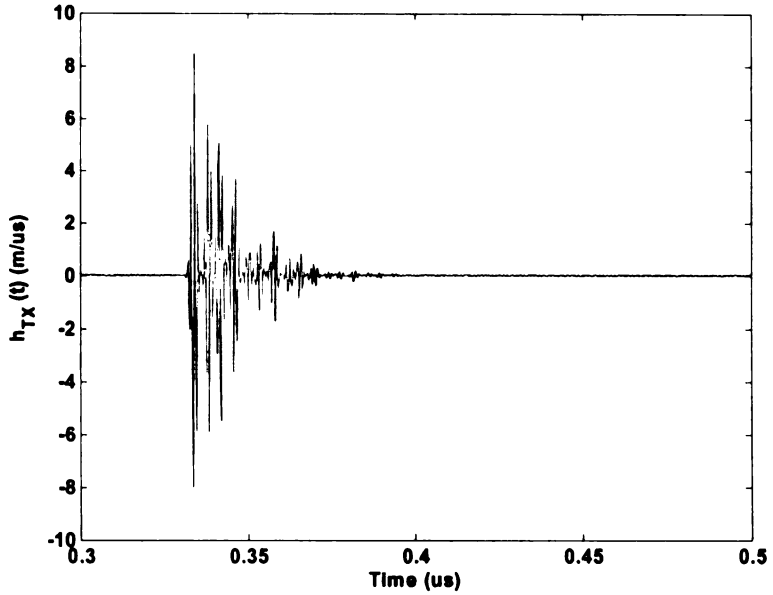

Figure 4.15 Waveform radiated in far-zone field at 90 degrees

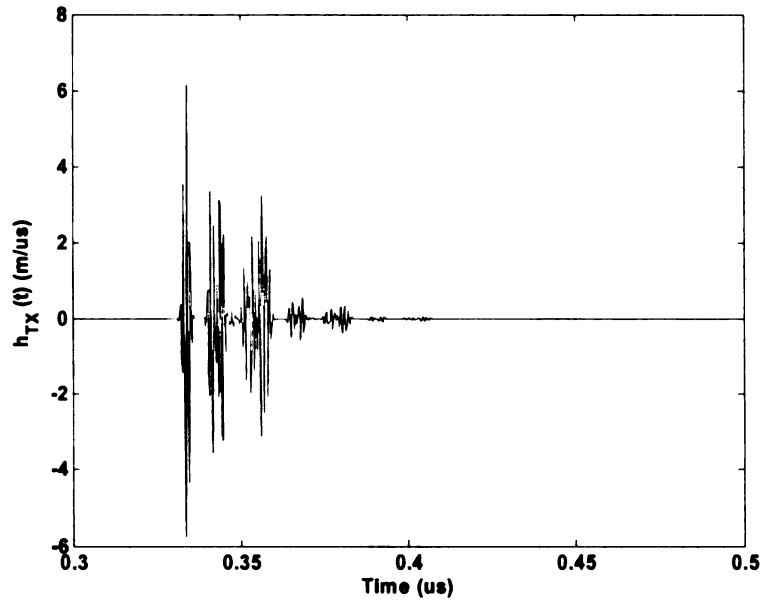

Figure 4.16 Waveform radiated in far-zone field at 120 degrees

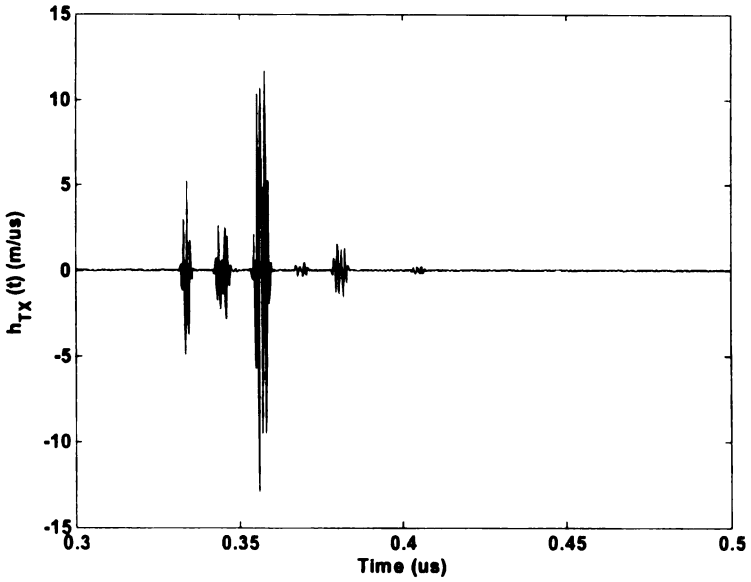

Figure 4.17 Waveform radiated in far-zone field at 150 degrees

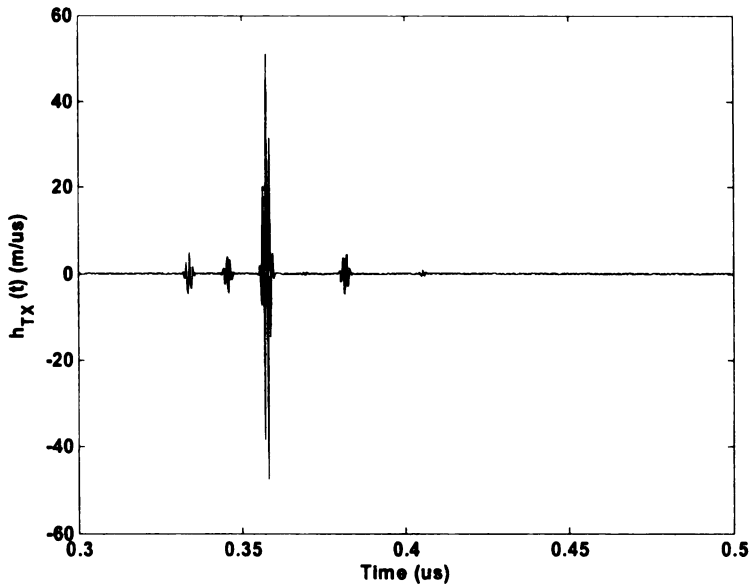

Figure 4.18 Waveform radiated in far-zone field at 180 degrees

4.4 The spline antenna

Figure 4.17 shows the geometry of the spline antenna in the y-z plane. The wires have a constant radius of 0.001 m. The antenna has the same length as the rhombic antenna, 3.46 m. The optimized quantity is the theta component of the electric field 100 meters away along the z-axis. GA-NEC uses the same fitness method as was applied to the loaded dipole including the same fitness file. The optimal impedance load to the ends is 600 ohms.

The GMC pulse energy radiation pattern (figure 4.18 in the y-z plane) reveals that this antenna is directive and radiates most strongly along the z-axis. Two 11 dB down side lobes occur at around 45 degrees away from the maximum radiation direction. There is also a 15 dB down back lobe as with the rhombic antenna. Unlike the rhombic antenna, the second reflection from the wire ends is negligible. Furthermore, the wire shapes are smooth so there is no reflection as with rhombic antenna. The GMC pulse radiation at any angle is the superposition of the contributions from the two wires. Along z-axis, the distributions are in time synchronization. There are only two events that can be seen from figure 4.21. One is from the feed and closely reproduces the GMC pulse and the other is the first reflection from the ends. As shown in figures 4.20-4.25, the distributions from the two wires are out of time synchronization. At 180 degree, the reflection is the main event of the GMC pulse radiation.

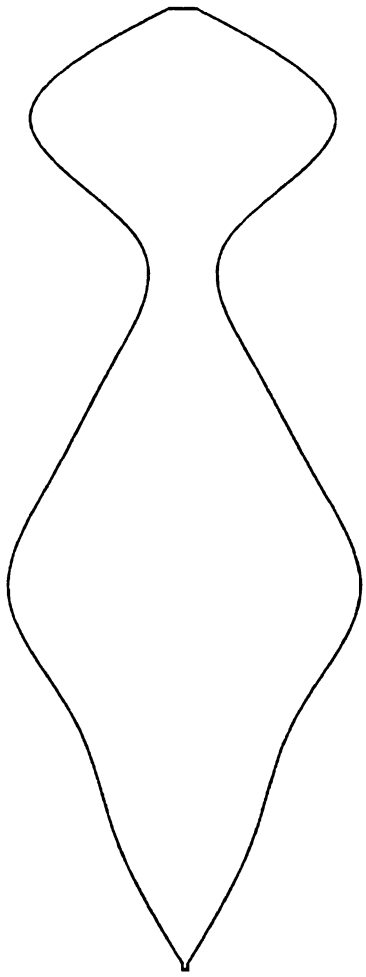

Figure 4.19 The geometry of the spline antenna geometry

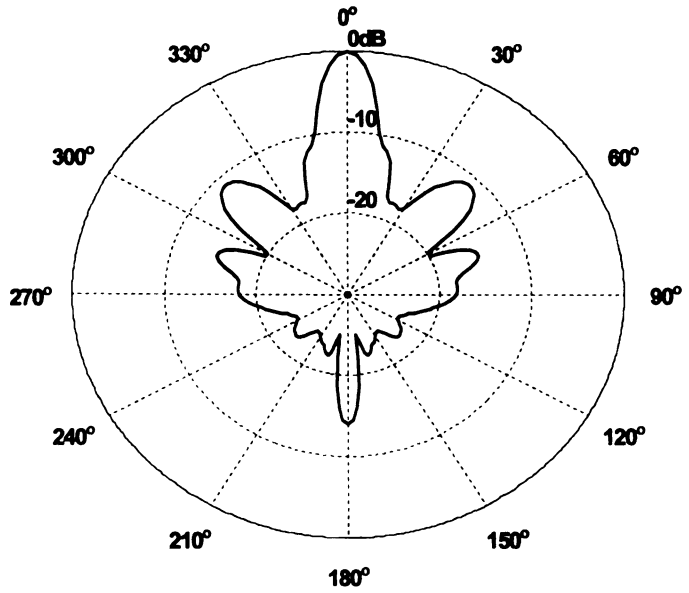

Figure 4.20 Energy in the waveform radiated by the spline antenna in y-z plane

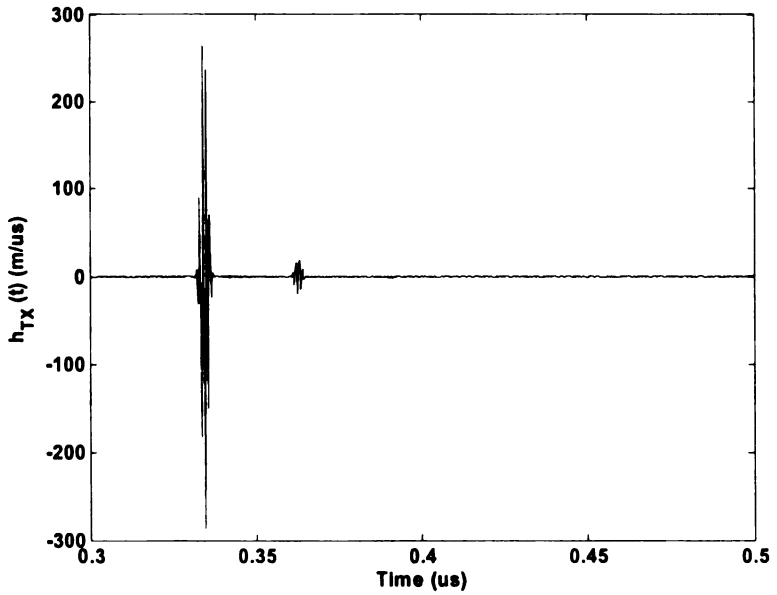

Figure 4.21 Waveform radiated in far-zone field at 0 degrees

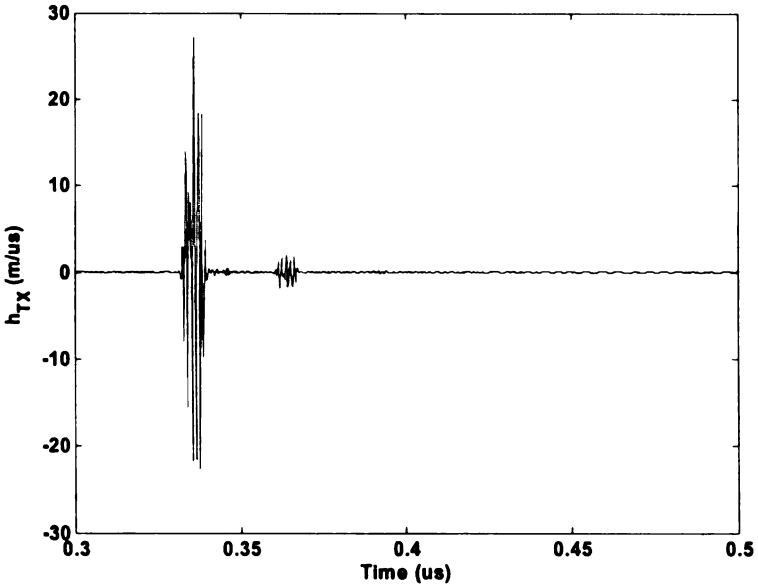

Figure 4.22 Waveform radiated in far-zone field at 30 degrees

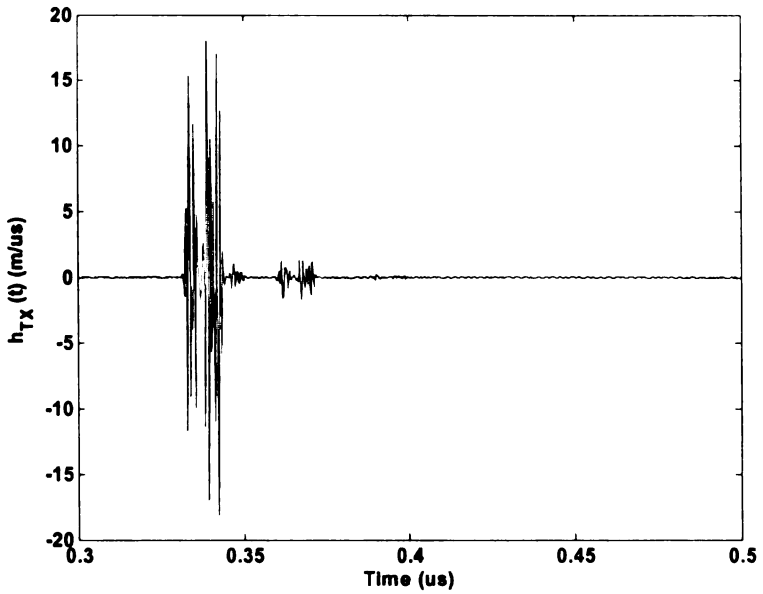

Figure 4.23 Waveform radiated in far-zone field at 60 degrees

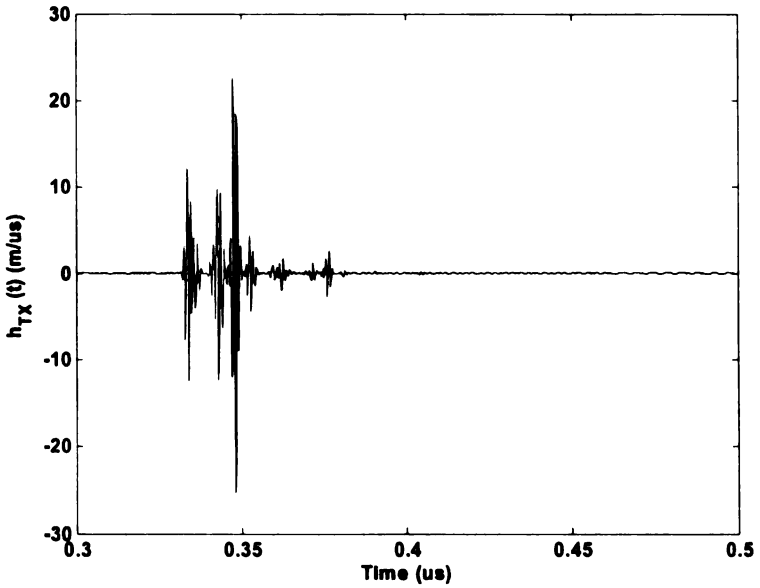

Figure 4.24 Waveform radiated in far-zone field at 90 degrees

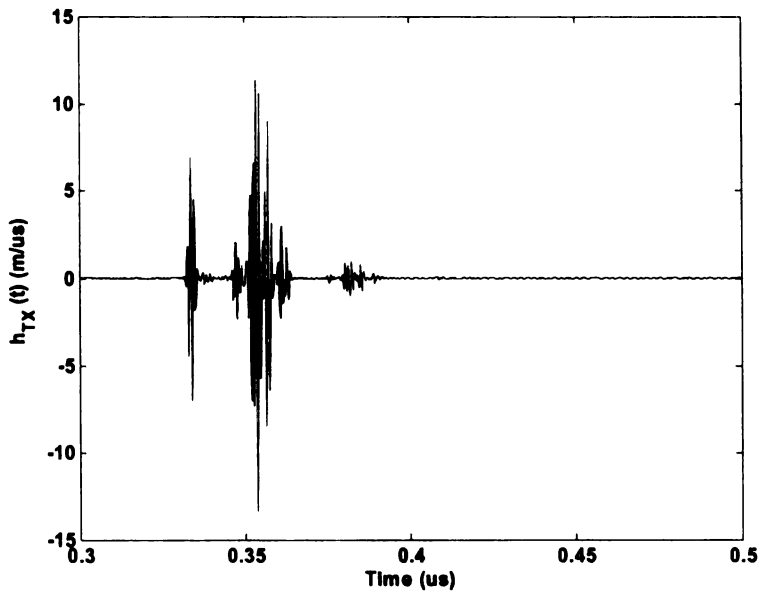

Figure 4.25 Waveform radiated in far-zone field at 120 degrees

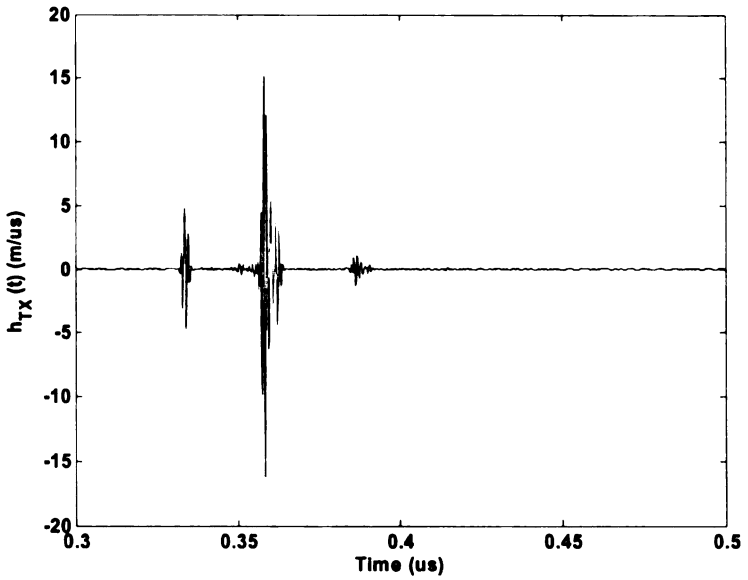

Figure 4.26 Waveform radiated in far-zone field at 150 degrees

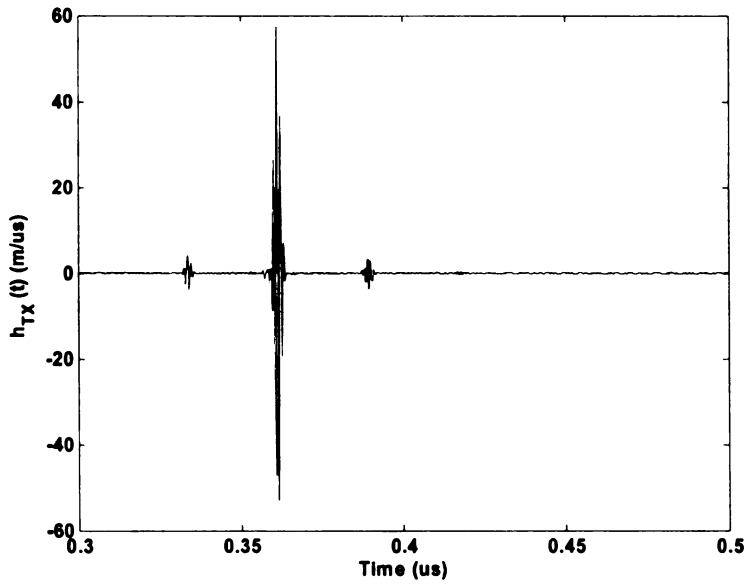

Figure 4.27 Waveform radiated in far-zone field at 180 degrees

4.5 Comparison and Conclusion

Figure 4.28 shows the normalized GMC pulse energy radiation pattern of the dipole, the loaded dipole, the rhombic and the spline antennas. Except for the dipole antenna, the other three are traveling-wave antennas and have wideband properties. The loaded dipole has a azimuthally independent radiation pattern. The maximum radiated energy is nearly 20 dB down to that of the spline antenna and 12 dB down to the dipole. It trades the directivity for wideband radiation. This restricts the loaded dipole for short range signal transmission and reception. The rhombic and the spline antennas have directive radiation abilities. The spline antenna has higher directivity that the rhombic one. There is a 1.6 dB difference along the z-axis. The half energy beam width is 10 degrees for the spline antenna and 12 for the rhombic one. As shown in figures 4.12 and 4.21, the difference between the feed radiation and the reflected radiation is significant. For the spline antenna, there is no reflection from rapidly changing curves as with the rhombic antenna. It is important to have higher directivity and preserve the bandwidth of the impulse radiation.

Figure 4.29 shows the radiation efficiency of the four antennas. It indicates that the radiation efficiency is 100 percent for the dipole and the spline antennas. That means there is no ohmic loss for those two antennas. The radiation efficiency of the rhombic antenna is in the range from 16.8 percent at 200 MHz to 84.9 percent at 2 GHz due to the ohmic loss. The loaded dipole has the even lower radiation efficiency which is in the range from 4.2 to 25.9 percent over the frequency band of interest. Thus, the spline antenna is the choice for the GMC pulse radiation among the four.

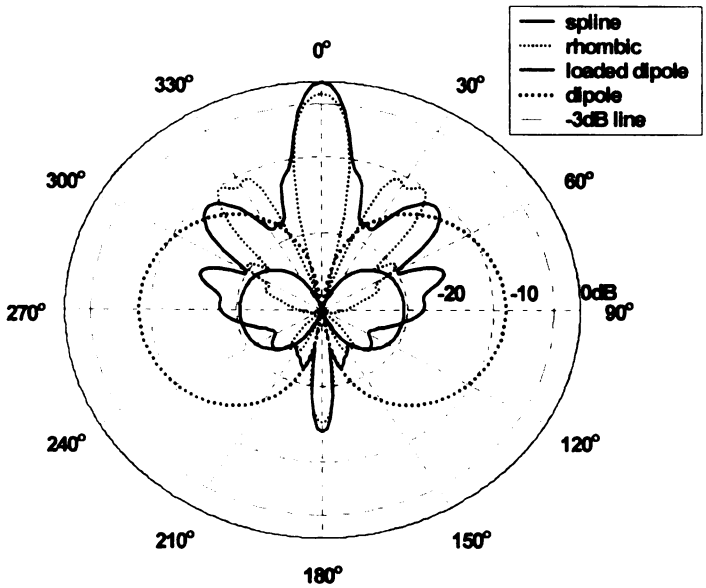

Figure 4.28 Normalized energy radiation patterns (GMC pulse) of the four antennas

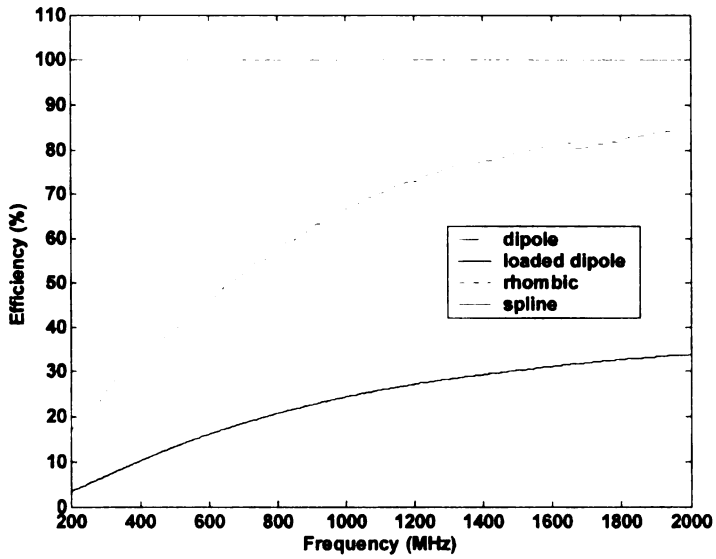

Figure 4.29 Radiation efficiency of the four antennas

Chapter 5

CONCLUSIONS

This thesis has introduced a set of spline traveling-wave antennas that are suitable for the band from 200 MHz to 2 GHz. The EM properties of these antennas such as the input impedance, the radiation efficiency, the VSWR, the radiated power and the power gain were presented and the results are discussed. The responses to a GMC (Gaussian modulated cosine) pulse function were studied and comparisons were made with the loaded dipole and the rhombic antenna.

With the use of GA (Genetic Algorithm), the optimal results were obtained based on the fitness function specified. There were three aspects specified in the fitness function as a goal for GA operations, Gain, efficiency and VSWR. Several types of geometries were optimized, including varying and constant segment radii with symmetric geometry and with asymmetric geometry. These are optimized with varying input impedances. Several runs were made for each case to avoid the GA-NEC optimization process from becoming trapped in a local maximum domain.

Simulation results show that all the optimized spline antennas have 100 percent radiation efficiency except the asymmetric one with 150 ohms feed line, which is from 81.5 to 99.7 percent over the band of interest. The spline antennas show much better efficiency compared with the rhombic antenna with efficiency from 16.8 to 84.9 percent and loaded dipole from 4.2 to 25.9 percent. Most of the VSWRs are in the range from 1 to 3 over the frequency band, except some values exceed 3 at certain low frequencies as shown in figures 3.3 and 3.23. Some of the optimal antennas also yield high power gains (over around 4 dB) over the frequency band as shown in figure 3.6 and figure 3.106. Radiation patterns indicate that the spline antennas are directive along the z-axis.

As a wideband traveling-wave antenna, the spline antenna has better radiation ability for a certain GMC pulse over the loaded dipole and the rhombic antenna as discussed in chapter 4. It can radiate 1.6 dB higher energy than the rhombic antenna and more that 20 dB higher than the loaded dipole along the maximum radiation direction. Also, the spline antenna that was

discussed in chapter 4 is the optimal one for the GMC pulse radiation described by equation 4.3. The antenna should be redesigned for different GMC pulse radiation by changing the weighting value in the fitness file as described in chapter 4.

As an optimizer, GA-NEC searches the best fitted individual in a specified domain. A wider domain and a finer searching step will give GA-NEC more diversity. Thus better results may be found with more powerful computer than used in these studies.

APPENDIX

APPENDIX A

VISUAL BASIC CODE TO GENERATE THE SPLINE ANTENNA WITH SYMMETRIC GEOMETRY

This code is written in Microsoft Visual Basic. It reads the input parameters such as the position of the points and the radius of the segments to generate the spline shape antenna and create an output file as a part of the GA-NEC input file to NEC2.

```
Program: Spline_sy.vbp
Sub Main()
Dim strCommandLineArgs As String
Dim intLocSpace As Integer
Dim strInputFile As String
Dim strOutputFile As String

'get the command line arguments
strCommandLineArgs = LTrim(RTrim(Command))

'there are two arguments separated by one or more spaces
'locate the space
intLocSpace = InStr(1, strCommandLineArgs, " ")

'take apart the string
strInputFile = Left(strCommandLineArgs, intLocSpace)
strOutputFile = Right(strCommandLineArgs, Len(strCommandLineArgs) - intLocSpace)

'call the function used to createt the desired geometry - in this case a splined fit transmission
line
Call SplineTL(strInputFile, strOutputFile)
End Sub


Sub SplineTL(strInputFile As String, strOutputFile As String)
'this subroutine makes a transmission line that is flared
'using a spline fit to several points along the z axis
'segment endpoints
Dim x1 As Single
Dim y1 As Single
Dim z1 As Single
Dim x2 As Single
Dim y2 As Single
Dim z2 As Single

'starting point along z-axis
```

```
Dim zstart As Single

'increment along z-axis
Dim delta As Single

'number of wires
Dim lngWireNumber As Long

'temporary counter
Dim i As Integer

'radius of wires
Dim Radius As Single

'delimiter
Dim strDelimiter As String
strDelimiter = ","

'These variables read from argument file
Dim Length As Single
Dim Separation As Single
Dim z0 As Single
Dim NumberofSegments As Integer
Dim NumberOfTerms As Integer

'open input file and read variables provided by GA-NEC
Open strInputFile For Input As #1
Input #1, Length
Debug.Print "Length = " & Length
Input #1, Separation
Debug.Print "Separation = " & Separation
Input #1, z0
Debug.Print "Impedance = " & z0
Input #1, NumberofSegments
Debug.Print "NumberofSegments = " & NumberofSegments
Input #1, NumberOfTerms
Debug.Print "NumberOfTerms = " & NumberOfTerms

'these variables store the y and z coordinates for each point along the transmission line
ReDim z(NumberOfTerms) As Single
ReDim Y(NumberOfTerms) As Single
ReDim y2a(NumberOfTerms) As Single

'This variable defined below
Dim sglDelta As Single
sglDelta = Length / (NumberOfTerms - 1)
```

```
'counter for segments
Dim intNumSegments As Integer

'read the terms, compute z coordinate for each point along the way
For i = 1 To NumberOfTerms
  z(i) = (i - 1) * sglDelta
  Input #1, Y(i)
  Debug.Print z(i), Y(i)
Next i
Close #1

'open output file and start writing GW commands
Open strOutputFile For Output As #1

'initialize spline function
Call Spline(z(), Y(), NumberOfTerms, 1E+30, 1E+30, y2a())
delta = Length / NumberofSegments

'make excitation segment
lngWireNumber = 1
intNumSegments = 1
x1 = 0
y1 = Separation / 2#
z1 = -1
x2 = 0
y2 = -Separation / 2#
z2 = -1
Radius = Separation / (2# * Cosh(z0 / 120#))
Print #1, "GW " & lngWireNumber & strDelimiter & intNumSegments & strDelimiter & x1
& strDelimiter & y1 & strDelimiter & z1 & strDelimiter & x2 & strDelimiter & y2 &
strDelimiter & z2 & strDelimiter & Radius

'Make Lead in wires
lngWireNumber = 2
intNumSegments = 50
x1 = 0
y1 = Separation / 2#
z1 = -1
x2 = 0
y2 = Separation / 2#
z2 = 0
Radius = Separation / (2# * Cosh(z0 / 120#))
Print #1, "GW " & lngWireNumber & strDelimiter & intNumSegments & strDelimiter & x1
& strDelimiter & y1 & strDelimiter & z1 & strDelimiter & x2 & strDelimiter & y2 &
strDelimiter & z2 & strDelimiter & Radius
```

```
lngWireNumber = 3
intNumSegments = 50
x1 = 0
y1 = -Separation / 2#
z1 = -1
x2 = 0
y2 = -Separation / 2#
z2 = 0
Radius = Separation / (2# * Cosh(z0 / 120#))
Print #1, "GW " & lngWireNumber & strDelimiter & intNumSegments & strDelimiter & x1
& strDelimiter & y1 & strDelimiter & z1 & strDelimiter & x2 & strDelimiter & y2 &
strDelimiter & z2 & strDelimiter & Radius

'make the positive half of the twin wire
lngWireNumber = 99
intNumSegments = 1
zstart = 0
x1 = 0
x2 = 0
z1 = zstart

Call Splint(z(), Y(), y2a(), NumberOfTerms, z1, y1)

y1 = Separation / 2#
For i = 1 To NumberofSegments
 lngWireNumber = lngWireNumber + 1
 z2 = z1 + delta
 Call Splint(z(), Y(), y2a(), NumberOfTerms, z1, y2)
 If y2 < 0 Then y2 = 0
 y2 = y2 + Separation / 2#
 Radius = Abs(2# * y2 / (2# * Cosh(z0 / 120#)))

Print #1, "GW " & lngWireNumber & strDelimiter & intNumSegments & strDelimiter & x1
& strDelimiter & y1 & strDelimiter & z1 & strDelimiter & x2 & strDelimiter & y2 &
strDelimiter & z2 & strDelimiter & Radius
 z1 = z2
 y1 = y2
Next i

Call Splint(z(), Y(), y2a(), NumberOfTerms, z1, y1)
y1 = Separation / 2#
lngWireNumber = lngWireNumber + 1
Print #1, "GW " & lngWireNumber & strDelimiter & intNumSegments & strDelimiter & x1
& strDelimiter & y1 & strDelimiter & z1 & strDelimiter & x2 & strDelimiter & y2 &
strDelimiter & z2 & strDelimiter & Radius
```

```
'Make the negative half of the twin wire
zstart = 0
z1 = zstart

Call Splint(z(), Y(), y2a(), NumberOfTerms, z1, y1)

y1 = -Separation / 2#
For i = 1 To NumberofSegments
 lngWireNumber = lngWireNumber + 1
 z2 = z1 + delta

Call Splint(z(), Y(), y2a(), NumberOfTerms, z1, y2)

 If y2 < 0 Then y2 = 0
 y2 = -y2 - Separation / 2#
 Radius = Abs(2# * y2 / (2# * Cosh(z0 / 120#)))
 Print #1, "GW " & lngWireNumber & strDelimiter & intNumSegments & strDelimiter & x1
& strDelimiter & y1 & strDelimiter & z1 & strDelimiter & x2 & strDelimiter & y2 &
strDelimiter & z2 & strDelimiter & Radius
 z1 = z2
 y1 = y2
Next i

Call Splint(z(), Y(), y2a(), NumberOfTerms, z1, y1)
y1 = -Separation / 2#
lngWireNumber = lngWireNumber + 1
Print #1, "GW " & lngWireNumber & strDelimiter & intNumSegments & strDelimiter & x1
& strDelimiter & y1 & strDelimiter & z1 & strDelimiter & x2 & strDelimiter & y2 &
strDelimiter & z2 & strDelimiter & Radius

'Termination segment
lngWireNumber = 1000
intNumSegments = 1
x1 = 0
y1 = Separation / 2#
x2 = 0
y2 = -Separation / 2#
Radius = Abs(Separation / (2# * Cosh(z0 / 120#)))
Print #1, "GW " & lngWireNumber & strDelimiter & intNumSegments & strDelimiter & x1
& strDelimiter & y1 & strDelimiter & z1 & strDelimiter & x2 & strDelimiter & y2 &
strDelimiter & z2 & strDelimiter & Radius
Close #1
End Sub

Sub Spline(X() As Single, Y() As Single, n As Integer, YP1 As Single, YPN As Single, y2() As
Single)
```

```
'this routine is translated from the one in Numerical Recipes in Fortran
'Given arrays X and Y of length N containing a tabulated function, i.e. Y(i) = f(X(i))
'with X1 < X2 < ... XN, and given values YP1 and YPN for the first derivative of the
'interpolating function at points 1 and N, repectively, this routine returns and
'array Y2 of length N which contains the second derivatives of the interpolating
'function at the tabulated points Xj. If YP1 and/or YP2 are equal to 1x10^30 or
'larger, the routine is signalled to set the corresponding boundary condition for
'a natural spline, with zero second derivative on that boundary.
Dim i As Integer
Dim sig As Single
Dim p As Single
Dim qn As Single
Dim un As Single
Dim K As Integer
ReDim U(n)

If (YP1 > 9.9E+29) Then      'The lower boundary condition is set either to be "natural"
 y2(1) = 0
 U(1) = 0
Else                         'or else to have a specified first derivative
 y2(1) = -0.5
 U(1) = (3# / (X(2) - X(1))) * (Y(2) - Y(1)) / (X(2) - X(1) - YP1)
End If

'this is the decomposition loop of the tridiagonal algorithm.
'Y2 and U are used for temporary storage of the decomposed factors.
For i = 2 To n - 1
 sig = (X(i) - X(i - 1)) / (X(i + 1) - X(i - 1))
 p = sig * y2(i - 1) + 2
 y2(i) = (sig - 1#) / p
 U(i) = (6# * ((Y(i + 1) - Y(i)) / (X(i + 1) - X(i)) - (Y(i) - Y(i - 1)) / (X(i) - X(i - 1))) / (X(i + 1)
- X(i - 1)) - sig * U(i - 1)) / p
Next i
If YPN > 9.9E+29 Then        'The upper boundary condition is set either to be "natural"
 qn = 0
 un = 0
Else                         'or else to have a specified first derivative
 qn = 0.5
 un = (3# / (X(n) - X(n - 1))) * (YPN - (Y(n) - Y(n - 1)) / (X(n) - X(n - 1)))
End If
y2(n) = (un - qn * U(n - 1)) / (qn * y2(n - 1) + 1)
'this is the backsubstitution loop of the tridiagonal algorithm
For K = n - 1 To 1 Step -1
y2(K) = y2(K) * y2(K + 1) + U(K)
Next K
```

```
End Sub

Sub Splint(XA() As Single, YA() As Single, y2a() As Single, n As Integer, X As Single, Y As
Single)

'this routine is translated from Numerical recipes in fortran
'given the arrays xa() and ya() of length N, which tabulate a function
'(with the XAi's in order). adn given the array Y2A(), which is the
'output from the SPLINE routine, and given a value of X, this routine
'returns a cubic-spline interpolated value Y.
Dim klo As Integer
Dim khi As Integer
Dim K As Integer
Dim a As Single
Dim B As Single
Dim H As Single
klo = 1
khi = n

'we will find the right place in the table by means bisection. This is
'optimal if sequential calls to this routine are at random values of
'x. If sequential calls are in order, and closely spaced, on would
'do better to store previous values of Klo and khi and test if they
'remain appropriate on the next call
Splint1:
If (khi - klo > 1) Then
  K = (khi + klo) / 2#
  If (XA(K) > X) Then
    khi = K
  Else
    klo = K
  End If
  GoTo Splint1
End If
'Klo and Khi now bracket the input of x
H = XA(khi) - XA(klo)
'The XA's must be distinct
If H = 0 Then
  MsgBox "Warning! Bad value of XA in Splint!"
End If

'Debug.Print "high, low = ", XA(khi), XA(klo), YA(khi), YA(klo)
'cubic spline is now evaluated
a = (XA(khi) - X) / H
B = (X - XA(klo)) / H
```

```
Y = a * YA(klo) + B * YA(khi) + ((a ^ 3# - a) * y2a(klo) + (B ^ 3# - B) * y2a(khi)) * (H ^ 2#)
/ 6#
End Sub

Function Cosh(X) As Double
'Purpose:
'Compute hyberbolic cosine of X
Cosh = (Exp(X) + Exp(-X)) / 2#
End Function
```

BIBLIOGRAPHY

BIBLIOGRAPHY

[1] H.Schantz, "An Introduction to UWB Antennas", IEEE UWBST 2003 Conference Proceedings.

[2] O.Lodge, "Electric Telegraphy," U.S. Patent 609,154, August 16, 1898

[3] P.S. Carter, "Short Wave Antenna," U.S. Patent 2,175,252, October 10, 1939

[4] P.S. Cater, "Wide Band, Short Wave Antenna and Transmission Line System," U.S. Patent 2,181,870, December 5, 1939

[5] S.A. Schelkunoff, "Ultra Short Wave Radio System," U.S. Patent 2,235,506, March 18, 1941

[6] N.E. Lindenblad, "Wide Band Antenna," U.S. Patent 2,239,724, April 29, 1941

[7] L.N. Brillonin, "Broad Band Antenna," U.S. Patent 2,454,766, November 30 1948

[8] W. Stohr, "Broadband Ellipsoidal Dipole Antenna," U.S. Patent 3,364,491, January 16, 1968

[9] R. H. DuHamel and D. E. Isbell, "Broadband Logarithmically Periodic Antenna Structures National Convention Record, Part 1.

[10] G. Robert-Pierre Marie, "Wide Band Slot Antennas," U.S. Patent 3,031,665, April 24, 1962

[11] F.LALEZARI *et al*, "Broadband Notch Antenna." U.S. Patent 4,843,403, June 27, 1989

[12] M. Thomas *et al*, "Wide Band Arrayable Planar Radiator," U.S. Patent 5,319,377, June 27, 1994

[13] H. Harmuth, "Frequency Independent Shielded Loop Antenna," U.S. Patent 4,506,267, March 19, 1985

[14] M. Barnes, "Ultra-wideband Magnetic Antenna," U.S. Patent 6,091,374, July 18, 2000

[15] M. Barnes, "Ultra-wideband Magnetic Antenna," U.S. Patent 6,400,329, June 2000

[16] H. Schantz, M. Barnes, "The COTAB UWB Magnetic Slot antenna," IEEE International APS Symposium 2001, July 2001

[17] Altshuler, E. E., The traveling-wave linear antenna, IRE Trans. On Antennas and Propagation, vol AP-9, Jul 1961, pp 324-329.

[18] T.T.WU and R.W.P. KING, "The Cylindrical Antenna with Nonreflecting Resistive Loading", IEEE Transactions on Antennas and Propagation, vol. 13, no. 3, 369-373, May 1965.

[19] John Ross and Associates. LLC, "GA-suite with NEC2 analysis"

[20] J.Michael Johnson and Yahya Rahmat-Samii, "Genetic Algorithms in engineering electromagnetics," IEEE Antennas and Propagation Magazine, 7-25, vol.39, no.4, August 1997

[21] Daniel S. Weile and Eric Michielssen, "Genetic Algorithm Optimization Applied to Electromagnetics: A Review" IEEE Transactions on Antennas and Propagation, 343-353, vol. 45, no. 3, March 1997.

[22] K. A. De Jong, "An Analysis of the behavior of a Class of Genetic Adaptive Systems," Doctoral Dissertation, University of Michigan (Dissertation Abstracts International, 36, 10, 5140B, University Microfilms No. 76-9381, (1975)

[23] J. H. Holland, Adaptation in Natural and Artificial System. University of Michigan Press, Ann Arbor, 1975.

[24] Randy L. Haupt, "An introduction to Genetic Algorithms for Electromagnetics" IEEE Antennas and Propagation Magazine, vol.37, no.2, April 1995

[25] Electromagnetic Optimization by Genetic Algorithms, "Chapter 3", Edited by Y. Rahmat-Samii and E. Michielssen 1999 John Wiley & Sons, inc.

[26] E. E. Altshuler and D. S. Linden, "wire-antenna designs using genetic algorithms," IEEE Antennas and Propagation magazine, 33-43, vol39, no.2, April 1997

[27] A. Boag, E. Michielssen, and R. Mittra, "Design of electrically loaded wire antennas using genetic algorithms," IEEE Transactions on Antennas and Propagation, 687-695, vol. 44, no. 5, May 1996.

[28] Z. Altman, R. Mittra, and A. Boag, "New designs of ultra-wideband communication antennas using the genetic algorithm," IEEE Transactions on Antennas and Propagation. 1494-1501, vol 45, no.10, October 1997.

[29] D. Eclercy, A. Reineix, and B. Jecko, "FDTD genetic algorithm for antenna optimization," Microwave Opt. Technol. Lett. 16, 72-74 (1997)

[30] Edward J. Rothwell, Michael J. Cloud, and Ponniah Ilavarasan, "Transient Field Produced by a Traveling-Wave Wire Antenna," IEEE Transactions On Electromagnetic Compatibility, Vol. 33, No. 3, 172-178 August 1991

[31] Constantine A. Balanis, "Antenna Theory Analysis and Design," John Willey & Sons, Inc.

[32] Everett G. Farr, "Time Domain Characterization of Antennas with TEM Feeds," Note 426, Sensor and Simulation Notes, October 1998.

[33] Clayborne D. Taylor *et al*, "Electromagnetic Pulse Generation by an impedance loaded dipole antenna" IEEE Transactions on Antennas and Propagation, vol. 18, no. 1, January 1970.

[34] Warren L. Stutzman, "Antenna theory and design" John Wiley & Sons, inc